The Investigation and Characterization of Redox Enzymes Using Protein Film Electrochemistry

by

Patrick Karchung Kwan

A Dissertation Presented in Partial Fulfillment
Of the Requirements for the Degree
Doctor of Philosophy

Approved November 2014 by the
Graduate Supervisory Committee:

Anne Jones, Chair
Wilson Francisco
Thomas Moore

ARIZONA STATE UNIVERSITY

December 2014

ABSTRACT

Redox reactions are crucial to energy transduction in biology. Protein film electrochemistry (PFE) is a technique for studying redox proteins in which the protein is immobilized at an electrode surface so as to allow direct exchange of electrons. Establishing a direct electronic connection eliminates the need for redox-active mediators, thus allowing for interrogation of the redox protein of interest. PFE has proven a versatile tool that has been used to elucidate the properties of many technologically relevant redox proteins including hydrogenases, laccases, and glucose oxidase.

This dissertation is comprised of two parts: extension of PFE to a novel electrode material and application of PFE to the investigation of a new type of hydrogenase. In the first part, mesoporous antimony-doped tin oxide (ATO) is employed for the first time as an electrode material for protein film electrochemistry. Taking advantage of the excellent optical transparency of ATO, spectroelectrochemistry of cytochrome *c* is demonstrated. The electrochemical and spectroscopic properties of the protein are analogous to those measured for the native protein in solution, and the immobilized protein is stable for weeks at high loadings. In the second part, PFE is used to characterize the catalytic properties of the soluble hydrogenase I from *Pyrococcus furiosus* (*Pf*SHI). Since this protein is highly thermostable, the temperature dependence of catalytic properties was investigated. I show that the preference of the enzyme for reduction of protons (as opposed to oxidation of hydrogen) and the reactions with oxygen are highly dependent on temperature, and the enzyme is tolerant to oxygen during both oxidative and reductive catalysis.

DEDICATION

First, I would like to dedicate this work to my parents, Kai-wan and Jeannie Kwan. For my entire life, they have showered me with love, compassion, and encouragement, and I could not have done any of this without them. They worked tirelessly to provide me with not only a roof over my head and food on the table, but also a relationship of unconditional love and support, even when I did not deserve it. No matter what was happening in my life, I always knew that I could come to them for help. They taught me through their words and also through their actions how to live a life of integrity and kindness, and I hope I can live up to their example. I hope I can make them proud.

I would also like to dedicate this to my older brother and sister. They were both instrumental in shaping me into the person I am today. My brother Willie and I haven't always had the closest relationship, but I always knew that I could count on him to look out for me. And as for my sister Jaime, she has been not only one of my closest friends, but also like a third parent to me. No matter what problems I was facing, I could always turn to her for a sympathetic ear.

I would also like to take this opportunity to thank God, because my faith has been crucial in sustaining me throughout the trials of my life. Although my faith has not been without its challenges, I know in my heart that every stumbling block, every pitfall, and every disappointment I have faced has happened in order to strengthen me and prepare me for whatever lies ahead.

ACKNOWLEDGMENTS

The research presented in this dissertation would not have been possible without scientific collaborations with other research groups. First, I would like to acknowledge Alex Volosin and the rest of Don Seo's lab at Arizona State University for providing the ATO that was used in my research. Second, I would like to acknowledge Mike Adam's group at the University of Georgia for providing the *Pf*SHI that was used in my experiments. Thank you to all of my collaborators for your generosity.

Next, I would like to thank the Science Foundation of Arizona for awarding me with a graduate student fellowship. I would also like to acknowledge the Center for Bio-Inspired Solar Fuel Production, an Energy Frontier Research Center sponsored by the United States Department of Energy. Finally, I need to acknowledge the Department of Chemistry and Biochemistry at Arizona State University for partial financial support of the research presented in this dissertation.

I also need to acknowledge my advisor, Professor Anne K. Jones, for all of her support over the last several years. Thank you for your tireless efforts and for believing in me even when I sometimes did not. Your kindness, insight, and generosity of spirit have made this lab like a second home for me, and I am forever grateful for that. I hope I can make you proud. I would also like to thank all of my colleagues, past and present, who have been invaluable to me during my time here. Thank you to all of you for your encouragement and camaraderie over the years.

TABLE OF CONTENTS

Page

LIST OF FIGURES……... vii

LIST OF TABLES……..... ix

LIST OF ABBREVIATIONS……..x

CHAPTER

1. INTRODUCTION: A PRIMER ON PROTEIN FILM ELECTROCHEMISTRY, TRANSPARENT CONDUCTING OXIDES, HYDROGENASES, AND AN OVERVIEW OF THIS DISSERTATION……...1

Redox Proteins and Protein Film Electrochemistry…….2

Transparent Conducting Oxides……...4

Hydrogenases……...6

The overview and goals of this dissertation……...11

Figures……13

References……..16

2. SPECTROELECTROCHEMISTRY OF CYTOCHROME *C* AND AZURIN IMMOBILIZED IN NANOPOROUS ANTIMONY-DOPED TIN OXIDE…….24

Abstract……..25

Introduction……25

Materials and Methods……...26

Results and Discussion…….. 29

Figures……34

References……..39

CHAPTER Page

3. CATALYTIC BIAS OF THE SOLUBLE HYDROGENASE I FROM *PYROCOCCUS FURIOSUS*…… 43

Abstract……..44

Introduction……44

Materials and Methods……...46

Results……47

Discussion……..49

Figures……51

References……..54

4. THE SOLUBLE [NIFE]-HYDROGENASE I FROM *PYROCOCCUS FURIOSUS* PRODUCES HYDROGEN IN THE PRESENCE OF OXYGEN…..... 57

Abstract……..58

Introduction……58

Materials and Methods……...60

Results……61

Discussion……..64

Figures……68

References……..70

5. INTERACTION OF SOLUBLE, GROUP 3 [NIFE]-HYDROGENASES AND OXYGEN: A NEW TYPE OF OXYGEN-TOLERANCE…..…… 73

Abstract……..74

Introduction……75

CHAPTER Page

Materials and Methods……...79

Results……80

Discussion……..86

Figures……94

References……..97

BIBLIOGRAPHY……....107

APPENDIX

PERMISSION TO REPRODUCE MATERIAL FROM PUBLISHED JOURNALS..... 122

LIST OF FIGURES

Figure Page

1-1 Schematic of Protein Film Electrochemistry and Ideal Voltammetric Response..13

1-2 Schematic of a Typical PFE Electrochemical Cell…….……...13

1-3 The [FeS] Clusters That Form the Electron Relay to the Active Site of the O_2-Tolerant MBH Hyd-1 from *E. coli*……...14

1-4 Schematic of the Catalytic Cycle of [NiFe]-Hydrogenases…..……..14

1-5 Sequence Alignment of Key Regions of the Small Subunits of a Selection of [NiFe]-Hydrogenases……...……..15

2-1 Photograph Demonstrating Optical Transparency of Mesoporous ATO Coating on an FTO Slide……..34

2-2 Cyclic Voltammograms and Trumpet Plot for Adsorbed cyt*C*…… 34

2-3 Cyclic Voltammograms from Control Experiments Demonstrating That cyt*C* Does Not Significantly Adsorb to a Planar (A) ITO or (B) FTO Slide……35

2-4 Cyclic Voltammogram of an ATO Coated Slide with Adsorbed cyt*C* After Storage for Twenty-One Days in pH 7 Buffer (15 mM HEPES, 0.1 M NaCl)….35

2-5 Cyclic Voltammograms of cyt*C* Adsorbed to an ATO Film at Fast Scan Rate… 36

2-6 Reduction of cyt*C* Adsorbed to ATO……...……. 36

2-7 UV-vis Absorbance Spectra from cyt*C* Adsorbed to an ATO Coated Slide…….37

2-8 Cyclic Voltammograms of ATO Coated Slide (Grey Line) and Azurin Adsorbed to Same (Black Line)…..…… 38

3-1 Schematic Representation of *Pf*SHI, Showing the Enzyme's Four Subunits and the Clusters Present in the Enzyme……51

Figure Page

3-2 Cyclic Voltammograms Showing Direct Hydrogen Oxidation and Proton Reduction by *Pf*SHI Adsorbed to a Graphite Electrode at Various pH Values….51

3-3 Chronoamperogram Demonstrating *Pf*SHI Catalysis at 60 ºC……..…… 52

3-4 Temperature Dependence of H^+ Reduction and Hydrogen Oxidation Catalytic Currents from Adsorbed *Pf*SHI…….…… 52

3-5 Dependence of pH of the Mixed Buffer System Used for Electrochemical Experiments on Temperature Within the Range of 15 ºC – 80 ºC….……53

4-1 Catalytic Chronoamperograms Showing H^+ Reduction by *Pf*SHI in the Presence of 1% O_2……...…… 68

4-2 Effect of Temperature on Inhibition of *Pf*SHI H^+-Reduction Activity by H_2 Under Anaerobic Conditions and Aerobic Conditions…… 69

4-3 Aqueous H_2 Concentration Under 1 atm of H_2 vs Temperature…… 69

5-1 *Pf*SHI Reacts With O_2 to Form Two Inactive States That Are Distinguished by the Electrochemical Potential Required to Reactivate Them…….... 94

5-2 Hydrogen Oxidation Activity Under Prolonged O_2 Exposure at 25 ºC, 60 ºC and 80 ºC…….. 95

5-3 Potential Step Experiment at 45 ºC Demonstrating Hydrogen Oxidizing Activity After Transient Oxygen Exposure……. 96

LIST OF TABLES

Table Page

5-1 Reduction Potentials and Proportions of Each Inactive State Formed for All Temperatures Investigated……..95

LIST OF ABBREVIATIONS

ATO	Antimony-Doped Tin Oxide
CHES	2-[*N'*-Cyclohexyl-Amino]Ethane-Sulfonic Acid
cyt*C*	Cytochrome *c*
*Df*Hase	[NiFe]-Hydrogenase from *Desulfovibrio fructosovorans*
FTO	Fluorine-Doped Tin Oxide
HEPES	4-(2-Hydroxyethyl)-1-Piperazineethane-Sulfonic Acid
ITO	Indium Tin Oxide
MBH	Membrane-Bound Hydrogenase
MES	2-[*N'*-Morpholino]Ethane-Sulfonic Acid
PEG	Polyethylene Glycol
PFE	Protein Film Electrochemistry
*Pf*SHI	Soluble Hydrogenase I from *Pyrococcus furiosus*
PGE	Edge Plane of Pyrolytic Graphite
*Re*HoxHY	Soluble Hydrogenase Subcomplex from *Ralstonia eutropha*
*Re*MBH	Membrane-Bound Hydrogenase from *Ralstonia eutropha*
*Re*SH	Soluble Hydrogenase from *Ralstonia eutropha*
SAM	Self-Assembled Monolayer
SH	Soluble Hydrogenase
SHE	Standard Hydrogen Electrode
*Syn*SH	Holoenzyme SH from *Synechocystis* sp. PCC6803
TAPS	*N'*-Tris[Hydroxymethyl]Methyl-3-Amino-Propane-Sulfonic Acid
TCO	Transparent (Semi)Conducting Oxide

Chapter 1

Introduction: A Primer on Protein Film Electrochemistry, Transparent Conducting Oxides, Hydrogenases, and Overview of This Dissertation

Patrick Kwan and Anne K. Jones

Department of Chemistry and Biochemistry,

Arizona State University, Tempe, AZ 85287

Redox Proteins and Protein Film Electrochemistry

Redox reactions and the proteins that perform them are at the heart of the energy harnessing reactions of biology.[1-3] Thus, there is keen interest from both basic and applied perspectives to understand their reactivity and structure/function relationships. Unfortunately, many of the common tools used to study redox proteins do not directly probe redox reactions. Instead, they usually measure spectroscopic properties linked to the redox states of cofactors.

Protein film electrochemistry (PFE) is a technique in which the protein of interest is functionally adsorbed to a suitable electrode surface and then interrogated using electrochemical techniques (Figure 1-1). The primary advantage of adsorption is that it eliminates problems associated with the slow diffusion of either the protein or a small chemical mediator to the electrode surface. In addition, since electron transfer is direct between the protein and the electrode, interpretation of both kinetic and thermodynamic properties is simplified.[1, 2, 4]

In PFE, the potential of the electrode on which the redox protein is adsorbed is controlled via a potentiostat, allowing electrons to move to or from the protein's active site depending on the electrode's potential relative to the reduction potential of the redox-active center. The electron flow is measured as current, and no corresponding spectroscopic change is necessary. This can be an invaluable tool for characterizing the reduction potentials of redox-active proteins, especially when the potential is extremely oxidizing or reducing, or when spectroscopic signals from multiple, distinct cofactors overlap. In short, rather than relying on the flow of mediators to and from the protein of

interest, or spectroscopic signals associated with the protein or mediator, the protein itself can be directly interrogated electrochemically.

Non-catalytic PFE

Figure 1-1B shows ideal cyclic voltammetric responses for a redox protein adsorbed to an electrode surface; a non-catalytic response is shown in black and a catalytic in red. Throughout this dissertation, positive potentials are more oxidizing and positive currents arise from oxidation reactions. The non-catalytic response consists of a pair of symmetric oxidative and reductive peaks centered on the reduction potential of the cofactor giving rise to the signal. The area under the peak corresponds to the amount of charge passed and can be used to determine the electroactive surface coverage of the adsorbed redox species:

$$Peak\ Area = nFA\Gamma v \qquad (1)$$

where n is the number of electrons in the redox process, F is the Faraday constant, A is the electrode surface area, Γ is the electroactive surface coverage, and v is the scan rate.

Catalytic PFE

When an enzyme is directly adsorbed to an electrode surface and its substrate is present in solution, current is directly proportional to the rate of the enzymatic catalysis (k) according to

$$i = nFA\Gamma k \qquad (2)$$

in which n, F, A and Γ have their previously defined meanings.[1, 5] Thus PFE offers a unique opportunity to characterize enzymatic activity as a function of electrochemical

potential. In contrast to non-catalytic voltammetry, in the presence of substrate, the enzyme's active site is continuously regenerated by electron exchange with the electrode, producing sigmoidal "catalytic waves" (red trace in Figure 1-1B). Since most solution assays are performed at high overpotentials, the current measured under such conditions is proportional to the traditional k_{cat} of Michaelis-Menten kinetics.[1]

Practical considerations

PFE has several practical advantages over other common techniques. First, solution-based electrochemical experiments rely on an electron donor/acceptor (mediator) which is mixed with the enzyme of interest in solution. This method usually requires a large quantity of enzyme to be successful, whereas PFE requires very little sample, usually in the picomole range. Moreover, since immobilized protein films often have remarkable stability, the same protein film can be studied for several hours and under a variety of conditions. The electrode can simply be transferred to a different solution which, in effect, results in instantaneous dialysis (Figure 1-2). In this way, a redox protein can be studied under different gas atmospheres, temperatures, or pH in a matter of minutes.

Transparent Conducting Oxides

While PFE is a powerful tool, it has limitations. For PFE to be successful, the protein of interest must interact with the electrode in a stable and functional manner. The most successful electrode surface used for PFE is the edge plane of pyrolytic graphite (PGE) and, to a lesser extent, alkanethiol-modified self-assembled monolayers on gold

(Au-SAM).[2, 6] However, many redox proteins have resisted functional immobilization at either of these surfaces due either to a lack of stabilizing interactions or to denaturation at the electrode surface.[7] Also, while PGE and Au-SAM electrodes are ideal for electrochemical experiments, they are optically opaque, making simultaneous spectroscopic investigation of the system practically impossible. Thus, there is a need to identify new surfaces that can be used for protein immobilization, especially for development of hybrid spectroelectrochemical methods. These needs have spurred the use of transparent (semi)conducting oxides (TCOs) for immobilization of redox-active proteins. The immobilization of redox-active proteins has already been demonstrated on TCOs like indium tin oxide (ITO).[8-10] However, the amount of surface coverage is usually not sufficient for spectroscopic studies. On the other hand, nanoporous materials are able to facilitate higher loadings, thus increasing the optical density for spectroscopic applications.[10-14]

ITO is by far the most commonly investigated TCO,[8, 15, 16] and it has been fabricated to form a mesoporous structure for protein incorporation.[10] Recently, antimony-doped tin oxide (ATO) has emerged as an alternative to ITO due to its lower cost and excellent optical transparency and conductivity.[17] The synthesis of ATO with pores accessible for protein incorporation was recently reported, and it has been shown that DNA nanostructures can be incorporated while retaining their native structure.[17, 18] Use of a mesoporous ATO film electrode for protein spectroelectrochemical investigations will be described in Chapter 2, where we report the stable, functional incorporation of two redox proteins into ATO.

Hydrogenases

Greenhouse gas emissions due to increased use of fossil fuels has led to significant concerns about humanity's impact on climate change.[19, 20] Hydrogen is an energy carrier with negligible environmental impact since its combustion yields only energy and water, but an efficient method for production and utilization of hydrogen without fossil fuels is required before a hydrogen economy can be implemented.[20] To accomplish this, efficient catalysts for the production and utilization of hydrogen are required.

In nature, the interconversion of H_2 and protons is carried out by the enzymes known as hydrogenases. There are three types that are distinguished by the metal content of their catalytic centers: [Fe], [FeFe], or [NiFe]. The buried active site is usually connected to the protein surface via a series of [FeS] clusters to facilitate fast electron exchange with the primary electron acceptor or donor. The [NiFe] active site is composed of a redox active nickel ion coordinated by four cysteinyl thiolates, two of which bridge to the low-spin iron (II) atom. The first coordination sphere of the iron is completed by two cyanides and a carbon monoxide.[21-23] The [FeFe]-hydrogenase active site, also known as the "H-cluster," is composed of a [4Fe4S] cubane bridged by a cysteine thiolate to a diiron subsite. This diiron complex is coordinated by five cyanide and carbon monoxide ligands and a bridging aza-propanedithiolate.[21, 24] The [Fe]-hydrogenase is distinct from its bimetallic counterparts in that it has a mononuclear active site, no [FeS] clusters, and cannot oxidize hydrogen without an obligatory organic cofactor.[21, 25] The rest of this chapter will focus on [NiFe]-hydrogenases since they are the subject of the work presented in this dissertation.

[NiFe]-hydrogenases

[NiFe]-hydrogenases are phylogenetically divided into four groups: (1) membrane-bound uptake hydrogenases, (2) cyanobacterial uptake hydrogenases and H_2-sensors, (3) bidirectional heteromultimeric cytoplasmic hydrogenases (the subject of this dissertation), and (4) H_2-evolving, energy-conserving, membrane-bound hydrogenases.[22] The group 1 membrane-bound uptake hydrogenases have been the most commonly studied [NiFe]-hydrogenases. They perform respiratory H_2-oxidation linked to reduction of electron acceptors such as quinones in the membrane. This stores the energy in the form of a proton-motive force. Some group 1 MBHs are also "oxygen-tolerant," meaning they can sustain H_2-oxidation activity in the presence of trace amounts of oxygen.[26-29] Like other [NiFe]-hydrogenases, the group 1 enzymes consist of a large subunit that harbors the active site as well as a separate small protein subunit containing the [FeS] clusters necessary for electron transfer to the physiological partner. In addition, group 1 hydrogenases contain subunits which anchor the hydrogenase heterodimer to the membrane and connect it to the quinone pool of the respiratory chain; this connection is often via a b-type cytochrome.[22] In contrast, group 2 hydrogenases remain in the cytoplasm of the organism. They are further subdivided into the group 2a uptake hydrogenases and group 2b regulatory hydrogenases. Group 2a uptake hydrogenases are typically found in organisms that also produce nitrogenase, and their physiological role appears to be the oxidation of H_2 produced during nitrogen fixation.[22, 30] Group 2b regulatory hydrogenases function as H_2-sensors in regulating the biosynthesis of some proteobacterial uptake hydrogenases in response to the presence of H_2.[22] The group 3 soluble hydrogenases (SHs), also cytoplasmic, are usually associated with additional

subunits that form a diaphorase capable of oxidation/reduction of NAD(H) or NADP(H). They are also sometimes referred to as "bidirectional" [NiFe]-hydrogenases due to their ability to function reversibly (relative to the group 1 and 2 enzymes). Physiologically they appear to link hydrogen metabolism with oxidation/reduction of the soluble pyridine nucleotide cofactors.[22, 31-36] The group 4 membrane-bound hydrogenases (MBHs) have mostly been found in Archaea, in which their physiological role is likely to reduce protons. This catalytic reaction is often linked to ion pumping such that they are able to couple the production of H_2 with energy conservation; the proton gradient that is generated by the reduction of protons is linked to the synthesis of ATP via ATP synthase.[37, 38]

The enzyme that is the subject of this dissertation is the group 3 soluble hydrogenase I from *Pyrococcus furiosus* (*Pf*SHI). *P. furiosus* produces three hydrogenases: two group 3 H_2-evolving hydrogenases (SHI and SHII) and a group 4 MBH.[37, 38] *Pf*SHI and *Pf*SHII were the first hydrogenases from *P. furiosus* to be characterized, and *Pf*SHI was believed to be the primary hydrogen producer in the organism.[39, 40] However, characterization of the *P. furiosus* group 4 MBH revealed very high levels of hydrogen production, suggesting that the MBH is the organism's primary hydrogen-producer.[38, 41-43] The MBH links oxidation of ferredoxin with proton reduction, with concomitant ion pumping, thus facilitating energy conservation.[37] *Pf*SHI may also contribute to hydrogen production in the organism, but its physiological role is currently unclear. On account of its bidirectionality, it may function as a means of regenerating NADPH using H_2 as the electron donor.[44]

Oxygen tolerance in [NiFe]-hydrogenases

There is growing interest in using [NiFe]-hydrogenases in biotechnological applications[21, 45] since, in contrast to their [FeFe] counterparts, they resist irreversible inactivation by trace amounts of O_2.[45, 46] Thus, there has been keen interest in understanding the mechanisms by which [NiFe]-hydrogenases resist inactivation by O_2. Two hypotheses have emerged: (1) restricted gas diffusion prevents effective entry of oxygen to the active site and (2) an unusual [4Fe-3S] cluster proximal to the active site is able to undergo two-electron reactions providing reducing equivalents on demand to completely reduce attacking oxygen molecules. Evidence for the first hypothesis came from investigation of regulatory, group 2 [NiFe]-hydrogenases. These enzymes are not directly involved in energy metabolism but instead are responsible for controlling regulation of genes. The enzymes found in organisms such as *R. eutropha* and *Rhodobacter capsulatus* are almost completely insensitive to O_2 but also have catalytic activities that are at least two orders of magnitude lower than the metabolic enzymes.[33, 45, 47-50] They can be transformed into O_2-sensitive enzymes by replacing the two bulky amino acids that form a constricted gas diffusion channel with smaller residues; this lends credence to the gas diffusion hypothesis.[47] However, attempts to create oxygen-tolerant enzymes using the inverse strategy have proven less useful.[51, 52]

Initial evidence for the second hypothesis came from X-ray crystal structures of two O_2-tolerant MBHs[29, 53-56] which revealed an unexpected [4Fe-3S] cluster proximal to the active site (Figure 1-3) that is not present in the so-called "standard," O_2-sensitive [NiFe]-hydrogenases. [53, 54] As shown in Figure 1-4, in the presence of oxygen and under oxidizing conditions, O_2 sensitive [NiFe]-hydrogenases form two inactive states which

are called Ni-A and Ni-B (named initially for their Ni EPR signals). The two states are not only spectroscopically but also kinetically distinguishable. While both can be reductively reactivated, Ni-B reactivates much more quickly than Ni-A. Thus, Ni-A and Ni-B are referred to as the "unready" and "ready" states, respectively. Unlike O_2-sensitive [NiFe]-hydrogenases, O_2-tolerant MBHs resist O_2 inactivation, meaning they maintain some hydrogen oxidation activity in the presence of O_2. They also form only the quickly-reactivating Ni-B state upon exposure to O_2.[57] It has been hypothesized that this is made possible by the proximal [4Fe-3S] cluster which supplies multiple electrons for the immediate, complete reduction of attacking O_2 molecules to H_2O.[29, 45, 53, 54, 56, 58] Site-directed mutants of *R. eutropha* MBH and Hyd-1 from *Escherichia coli* in which the [4Fe-3S] cluster is converted to a standard [4Fe-4S] cluster are no longer able to sustain H_2-oxidation in the presence of 1% O_2.[29] Spectroscopic results show that the [4Fe-3S] cluster is able to undergo two sequential redox transitions, which allows it to deliver two electrons to the active site to help reduce attacking O_2 molecules.[56, 59, 60] Furthermore, an unconventional [3Fe-4S] cluster in the medial position of the electron transfer chain leading to the active site of MBHs has also been hypothesized to contribute to O_2-tolerance.[29] Directed mutagenesis experiments targeting this medial cluster resulted in Hyd-1 losing its O_2-tolerance. The medial cluster's importance appears to result from its high reduction potential compared to a standard [4Fe-4S] cluster, which makes it more likely to have an electron bound at any given time, thus making an additional electron available for reduction of attacking O_2 molecules.[29] Thus, the unconventional proximal [4Fe-3S] and the medial [3Fe-4S] clusters appear to contribute to the O_2-tolerance exhibited by MBHs.

Sequence alignments suggest that soluble, bidirectional group 3 SHs do not possess either of these unconventional [FeS] clusters (Figure 1-5).[55] Nonetheless, some O_2-tolerant SHs have been described.[61-63] Until this work, very few SHs have been characterized electrochemically, the most precise method for characterizing potential-dependent reactions and reactions with oxygen. We have found that *Pf*SHI is markedly O_2-tolerant although it does not have the modified [FeS] clusters that are associated with O_2-tolerance in MBHs. Furthermore, inactivation of *Pf*SHI by O_2 results in the formation of two inactive states rather than exclusively Ni-B. This means *Pf*SHI is unique from the prototypical O_2-tolerant MBHs.

Overview and Goals of Dissertation

This dissertation consists of three chapters each describing a different use of PFE for the investigation and characterization of redox-active proteins. Specifically the goals are (1) to evaluate nanoporous antimony-doped tin oxide (ATO) as a substrate for protein immobilization for spectroelectrochemistry experiments; (2) to characterize the catalytic properties of the soluble, group 3 hydrogenase from *Pyrococcus furiosus* (*Pf*SHI) including catalytic bias, reactivity in the presence of oxygen, and states formed by reaction with oxygen; (3) to determine the temperature dependences of the properties of *Pf*SHI; and (4) to compare the properties of *Pf*SHI with other [NiFe]-hydrogenases as a means to determine structure/function relationships.

In **Chapter 2**, we describe the immobilization and spectroelectrochemical characterization of two model redox active proteins, cytochrome *c* and azurin, in transparent, conductive nanoporous ATO. We demonstrate that ATO is capable of high

guest incorporation, and good electrical communication is achieved between the ATO and the immobilized protein. Furthermore, taking advantage of the excellent optical transparency of the material, UV-vis spectroscopic signals can be observed under strict electrode potential control. Thus we show that this is a very promising material for spectroelectrochemical experiments without the use of an intervening chemical mediator.

In **Chapter 3**, we evaluate the temperature dependence of the catalytic bias of *Pf*SHI, *i.e.* the ratio of the rate of proton reduction to that of hydrogen oxidation. We show that the catalytic bias of the enzyme depends on temperature and shifts to favor proton reduction at higher temperatures like those normally found in the native environment of *P. furiosus*.

In **Chapter 4**, we demonstrate the ability of *Pf*SHI to reduce protons in the presence of 1% oxygen. Not only can the enzyme reduce protons under these conditions, it retains nearly all of its proton reduction activity.

In **Chapter 5**, we demonstrate that *Pf*SHI exhibits oxygen-tolerance, *i.e*. it is able to maintain hydrogen oxidation in the presence of low concentrations of oxygen, but this tolerance is temperature dependent. Two inactive states are formed upon reaction with oxygen, and the ratio of the populations of the two states formed depends on both temperature and the duration of oxygen exposure. Although oxygen tolerance has been characterized for MBHs and attributed to a modified [4Fe-3S] cluster near to the active site,[29, 45, 53, 54, 56, 58] SH enzymes do not contain the sequence motif necessary for binding this unusual cluster. Thus, *Pf*SHI must achieve oxygen tolerance via an as yet undescribed mechanism, and our results help to define possible mechanisms.

Figures

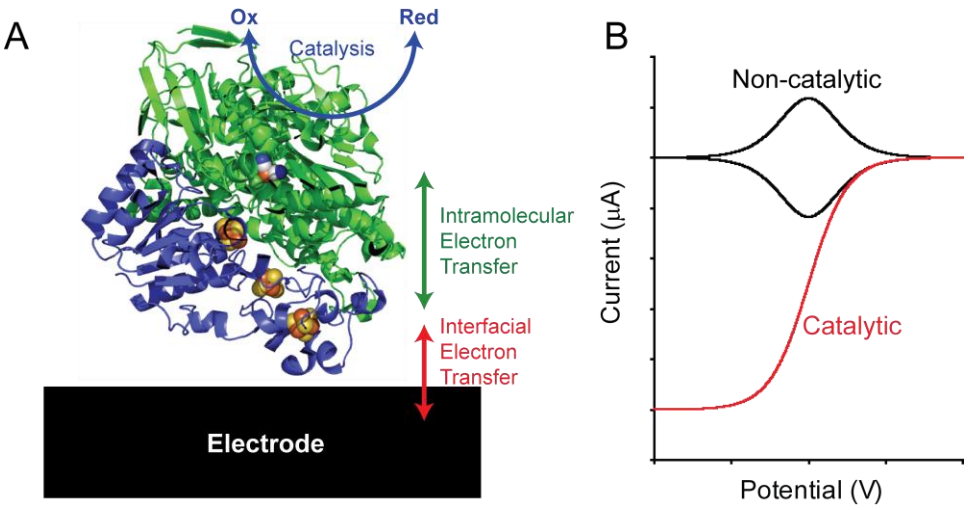


Figure 1-1. Schematic of protein film electrochemistry and ideal voltammetric response. A) Schematic representation of PFE of the membrane extrinsic subunits of the membrane bound hydrogenase from *Ralstonia eutropha* (PDB code: 3RGW). B) Ideal response from a monolayer of adsorbed electroactive species when the electron transfer is reversible and the response is non-catalytic (black) or catalytic (red).

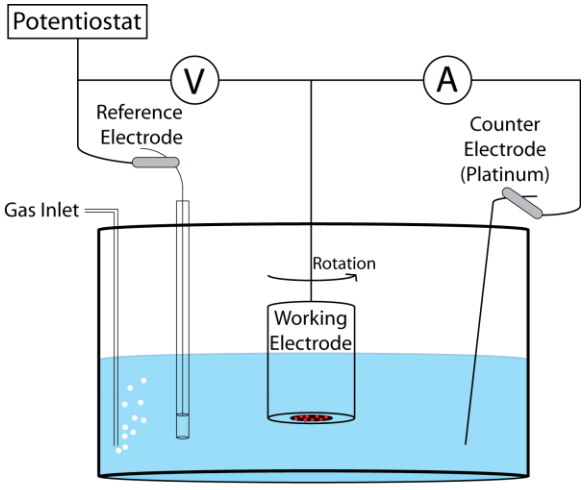


Figure 1-2. Schematic of a typical PFE electrochemical cell. A standard 3-electrode set-up consists of a working electrode, a reference electrode and a counter electrode. A redox enzyme is adsorbed to the working electrode and rotation controls diffusion of substrate to the enzyme and prevents the accumulation of product. A gas inlet is utilized to regulate the gas composition of the electrochemical cell.

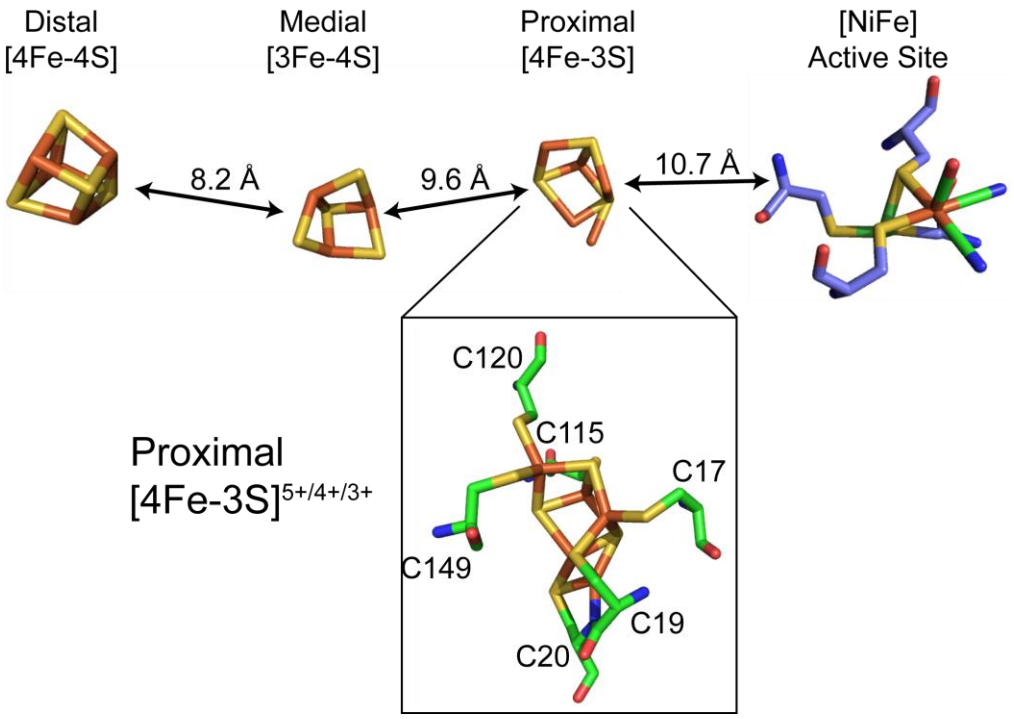


Figure 1-3. The [FeS] clusters that form the electron relay to the active site of the O_2-tolerant MBH Hyd-1 from *E. coli* (PDB code: 3USE). The unconventional proximal [4Fe-3S] cluster is featured in the box. The double-headed arrows indicate the edge-to-edge distances between the redox centers.[29]

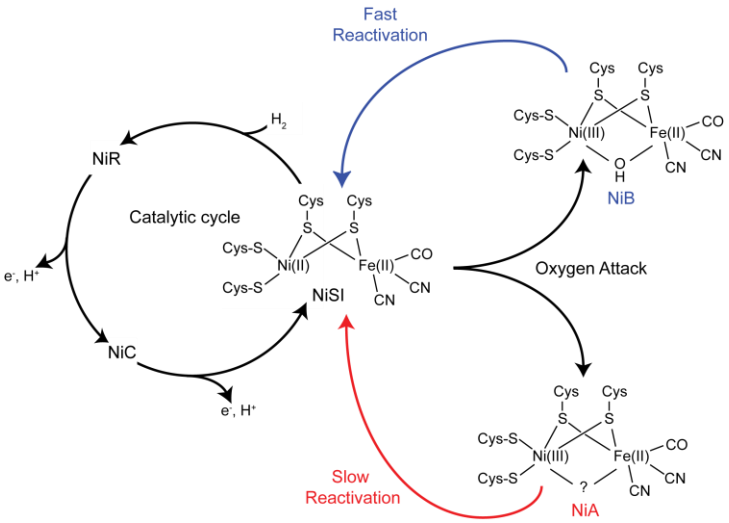


Figure 1-4. Schematic of the catalytic cycle of [NiFe]-hydrogenases. The enzyme is active in the NiSI, NiR, and NiC states. Oxidation converts the enzyme into the Ni-A or Ni-B inactive states. Figure is modified from the article by Abou Hamdan, *et al*.[64]

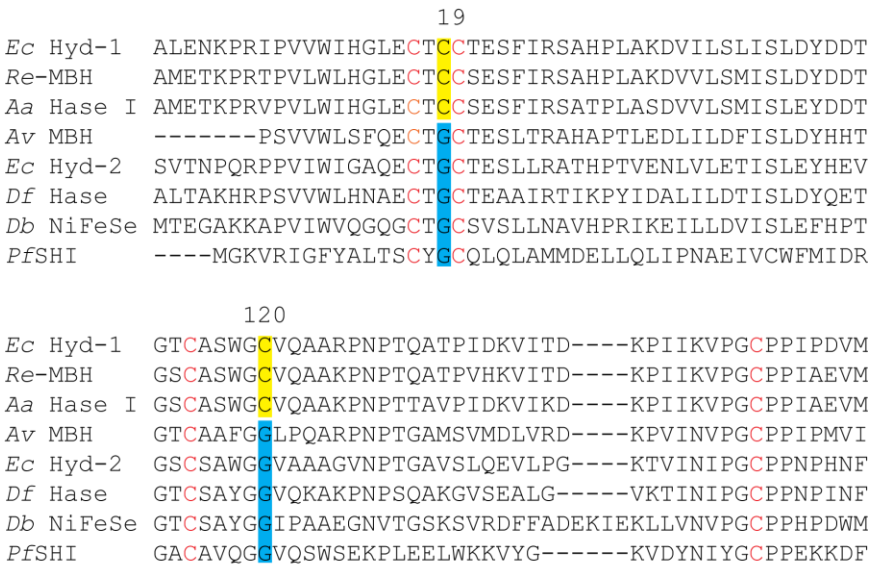


Figure 1-5. Sequence alignment of key regions of the small subunits of a selection of [NiFe]-hydrogenases. *Ec* Hyd-1 = [NiFe]-hydrogenase 1 from *Escherichia coli*, *Re*-MBH = membrane-bound hydrogenase I from *Ralstonia eutropha*, *Aa* Hase I = [NiFe]-hydrogenase I from *Aquifex aeolicus*, *Av* MBH = [NiFe]-hydrogenase from *Allochromatium vinosum*, *Ec* Hyd-2 = [NiFe]-hydrogenase 2 from *E. coli*, *Df* Hase = [NiFe]-hydrogenase from *Desulfovibrio fructosovorans*, *Db* NiFeSe = [NiFe-Se]-hydrogenase from *D. baculatum*, and *Pf*SHI = soluble [NiFe]-hydrogenase I from *P. furiosus.* The four cysteine residues known to coordinate the proximal cluster of *Df*Hase (C17, C20, C115, and C147 in *Ec* Hyd-1 numbering) are shown in red. The two supernumerary cysteine residues (C19 and C120 in *Ec* Hyd-1 numbering) that are found only in O_2-tolerant enzymes are highlighted in yellow, with the corresponding glycines in standard [NiFe]-hydrogenases highlighted in blue. *Pf*SHI sequence was obtained from Pedroni, et al.[64] Figure is modified from the article by Lukey, *et al*, Copyright (2011) American Chemical Society.[55, 65]

References

1. Léger, C. & Bertrand, P. Direct electrochemistry of redox enzymes as a tool for mechanistic studies. *Chem. Rev.* **108**, 2379-2438 (2008).

2. Léger, C., Elliott, S.J., Hoke, K.R., Jeuken, L.J.C., Jones, A.K. & Armstrong, F.A. Enzyme electrokinetics: Using protein film voltammetry to investigate redox enzymes and their mechanisms. *Biochemistry* **42**, 8653-8662 (2003).

3. Buettner, G.R., Wagner, B.A. & Rodgers, V.G.J. Quantitative Redox Biology: An Approach to Understand the Role of Reactive Species in Defining the Cellular Redox Environment. *Cell Biochem. Biophys.* **67**, 477-483 (2013).

4. Armstrong, F.A., Heering, H.A. & Hirst, J. Reactions of complex metalloproteins studied by protein-film voltammetry. *Chem. Soc. Rev.* **26**, 169-179 (1997).

5. Léger, C., Heffron, K., Pershad, H.R., Maklashina, E., Luna-Chavez, C., Cecchini, G., Ackrell, B.A.C. & Armstrong, F.A. Enzyme electrokinetics: Energetics of succinate oxidation by fumarate reductase and succinate dehydrogenase. *Biochemistry* **40**, 11234-11245 (2001).

6. Armstrong, F.A., Camba, R., Heering, H.A., Hirst, J., Jeuken, L.J.C., Jones, A.K., Léger, C. & McEvoy, J.P. Fast voltammetric studies of the kinetics and energetics of coupled electron-transfer reactions in proteins. *Farad. Discuss.* **116**, 191-203 (2000).

7. Wang, S.F., Xie, F. & Liu, G.D. Direct electrochemistry and electrocatalysis of heme proteins on SWCNTs-CTAB modified electrodes. *Talanta* **77**, 1343-1350 (2009).

8. Gordon, R.G. Criteria for choosing transparent conductors. *MRS Bull.* **25**, 52-57 (2000).

9. Collinson, M. & Bowden, E.F. UV-Visible Spectroscopy of Adsorbed Cytochrome-*C* on Tin Oxide Electrodes. *Anal. Chem.* **64**, 1470-1476 (1992).

10. Frasca, S., von Graberg, T., Feng, J.J., Thomas, A., Smarsly, B.M., Weidinger, I.M., Scheller, F.W., Hildebrandt, P. & Wollenberger, U. Mesoporous Indium Tin Oxide as a Novel Platform for Bioelectronics. *ChemCatChem* **2**, 839-845 (2010).

11. Nishiyama, K., Ishida, H. & Taniguchi, I. Aminosilane modified indium oxide electrodes for direct electron transfer of ferredoxin. *J. Electroanal. Chem.* **373**, 255-258 (1994).

12. Topoglidis, E., Cass, A.E., Gilardi, G., Sadeghi, S., Beaumont, N. & Durrant, J.R. Protein Adsorption on Nanocrystalline TiO_2 Films: An Immobilization Strategy for Bioanalytical Devices. *Anal. Chem.* **70**, 5111-5113 (1998).

13. Topoglidis, E., Cass, A.E.G., O'Regan, B. & Durrant, J.R. Immobilisation and bioelectrochemistry of proteins on nanoporous TiO_2 and ZnO films. *J. Electroanal. Chem.* **517**, 20-27 (2001).

14. Topoglidis, E., Astuti, Y., Duriaux, F., Gratzel, M. & Durrant, J.R. Direct Electrochemistry and Nitric Oxide Interaction of Heme Proteins Adsorbed on Nanocrystalline Tin Oxide Electrodes. *Langmuir* **19**, 6894-6900 (2003).

15. Lewis, B.G. & Paine, D.C. Applications and processing of transparent conducting oxides. *MRS Bull.* **25**, 22-27 (2000).

16. Ginley, D.S. & Bright, C. Transparent conducting oxides. *MRS Bull.* **25**, 15-18 (2000).

17. Simmons, C.R., Schmitt, D., Wei, X.X., Han, D.R., Volosin, A.M., Ladd, D.M., Seo, D.K., Liu, Y. & Yan, H. Size-Selective Incorporation of DNA Nanocages into Nanoporous Antimony-Doped Tin Oxide Materials. *ACS Nano* **5**, 6060-6068 (2011).

18. Hou, K., Puzzo, D., Helander, M.G., Lo, S.S., Bonifacio, L.D., Wang, W.D., Lu, Z.H., Scholes, G.D. & Ozin, G.A. Dye-Anchored Mesoporous Antimony-Doped Tin Oxide Electrochemiluminescence Cell. *Adv. Mater.* **21**, 2492-2496 (2009).

19. Murray, J. & King, D. Climate policy: Oil's tipping point has passed. *Nature* **481**, 433-435 (2012).

20. Cipriani, G., Di Dio, V., Genduso, F., La Cascia, D., Liga, R., Miceli, R. & Galluzzo, G.R. Perspective on hydrogen energy carrier and its automotive applications. *Int. J. Hydrogen Energ.* **39**, 8482-8494 (2014).

21. Jones, A.K., Dutta, A., Kwan, P., McIntosh, C.L., Roy, S. & Yang, S. in Enzymatic Fuel Cells 80-108 (John Wiley & Sons, Inc., 2014).

22. Vignais, P.M. & Billoud, B. Occurrence, classification, and biological function of hydrogenases: An overview. *Chem. Rev.* **107**, 4206-4272 (2007).

23. Pierik, A.J., Roseboom, W., Happe, R.P., Bagley, K.A. & Albracht, S.P.J. Carbon monoxide and cyanide as intrinsic ligands to iron in the active site of [NiFe]-hydrogenases - $NiFe(CN)_2CO$, biology's way to activate H_2. *J. Biol. Chem.* **274**, 3331-3337 (1999).

24. Popescu, C.V. & Munck, E. Electronic structure of the H cluster in [Fe]-hydrogenases. *J. Am. Chem. Soc.* **121**, 7877-7884 (1999).

25. Shima, S., Pilak, O., Vogt, S., Schick, M., Stagni, M.S., Meyer-Klaucke, W., Warkentin, E., Thauer, R.K. & Ermler, U. The crystal structure of [Fe]-hydrogenase reveals the geometry of the active site. *Science* **321**, 572-575 (2008).

26. Cracknell, J.A., Wait, A.F., Lenz, O., Friedrich, B. & Armstrong, F.A. A kinetic and thermodynamic understanding of O_2 tolerance in [NiFe]-hydrogenases. *Proc. Natl. Acad. Sci. U.S.A.* **106**, 20681-20686 (2009).

27. Lenz, O., Ludwig, M., Schubert, T., Bürstel, I., Ganskow, S., Goris, T., Schwarze, A. & Friedrich, B. H_2 Conversion in the Presence of O_2 as Performed by the Membrane-Bound [NiFe]-Hydrogenase of *Ralstonia eutropha*. *ChemPhysChem* **11**, 1107-1119 (2010).

28. Vincent, K.A., Cracknell, J.A., Clark, J.R., Ludwig, M., Lenz, O., Friedrich, B. & Armstrong, F.A. Electricity from low-level H_2 in still air - an ultimate test for an oxygen tolerant hydrogenase. *Chem. Commun.* **48**, 5033-5035 (2006).

29. Evans, R.M., Parkin, A., Roessler, M.M., Murphy, B.J., Adamson, H., Lukey, M.J., Sargent, F., Volbeda, A., Fontecilla-Camps, J.C. & Armstrong, F.A. Principles of Sustained Enzymatic Hydrogen Oxidation in the Presence of Oxygen - The Crucial Influence of High Potential Fe-S Clusters in the Electron Relay of [NiFe]-Hydrogenases. *J. Am. Chem. Soc.* **135**, 2694-2707 (2013).

30. Appel, J. & Schulz, R. Hydrogen metabolism in organisms with oxygenic photosynthesis: hydrogenases as important regulatory devices for a proper redox poising? *J. Photoch. Photobio. B* **47**, 1-11 (1998).

31. Ma, K., Hao, Z. & Adams, M.W.W. Hydrogen production from pyruvate by enzymes purified from the hyperthermophilic archaeon, *Pyrococcus furiosus*: A key role for NADPH. *FEMS Microbiol. Lett.* **122**, 245-250 (1994).

32. Burgdorf, T., van der Linden, E., Bernhard, M., Yin, Q.Y., Back, J.W., Hartog, A.F., Muijsers, A.O., de Koster, C.G., Albracht, S.P.J. & Friedrich, B. The soluble NAD^+-reducing [NiFe]-Hydrogenase from *Ralstonia eutropha* H16 consists of six subunits and can be specifically activated by NADPH. *J. Bacteriol.* **187**, 3122-3132 (2005).

33. Friedrich, B., Buhrke, T., Burgdorf, T. & Lenz, O. A hydrogen-sensing multiprotein complex controls aerobic hydrogen metabolism in *Ralstonia eutropha*. *Biochem. Soc. T.* **33**, 97-101 (2005).

34. Appel, J., Phunpruch, S., Steinmuller, K. & Schulz, R. The bidirectional hydrogenase of *Synechocystis* sp PCC 6803 works as an electron valve during photosynthesis. *Arch. Microbiol.* **173**, 333-338 (2000).

35. Cournac, L., Mus, F., Bernard, L., Guedeney, G., Vignais, P. & Peltier, G. Limiting steps of hydrogen production in *Chlamydomonas reinhardtii* and *Synechocystis* PCC 6803 as analysed by light-induced gas exchange transients. *Int. J. Hydrogen Energ.* **27**, 1229-1237 (2002).

36. Cournac, L., Guedeney, G., Peltier, G. & Vignais, P.M. Sustained photoevolution of molecular hydrogen in a mutant of *Synechocystis* sp strain PCC 6803 deficient in the type I NADPH-dehydrogenase complex. *J. Bacteriol.* **186**, 1737-1746 (2004).

37. Schut, G.J., Boyd, E.S., Peters, J.W. & Adams, M.W.W. The modular respiratory complexes involved in hydrogen and sulfur metabolism by heterotrophic hyperthermophilic archaea and their evolutionary implications. *FEMS Microbiol. Rev.* **37**, 182-203 (2013).

38. Jenney, F.E., Jr. & Adams, M.W.W. Hydrogenases of the model hyperthermophiles. *Ann. NY Acad. Sci.* **1125**, 252-266 (2008).

39. Bryant, F.O. & Adams, M.W.W. Characterization of Hydrogenase from the Hyperthermophilic Archaebacterium, *Pyrococcus furiosus*. *J. Biol. Chem.* **264**, 5070-5079 (1989).

40. Ma, K., Schicho, R.N., Kelly, R.M. & Adams, M.W.W. Hydrogenase of the hyperthermophile *Pyrococcus furiosus* is an elemental sulfur reductase or sulfhydrogenase: evidence for a sulfur-reducing hydrogenase ancestor. *Proc. Natl. Acad. Sci. U.S.A.* **90**, 5341-5344 (1993).

41. Sapra, R., Verhagen, M.F. & Adams, M.W.W. Purification and characterization of a membrane-bound hydrogenase from the hyperthermophilic archaeon *Pyrococcus furiosus*. *J. Bacteriol.* **182**, 3423-3428 (2000).

42. McTernan, P.M., Chandrayan, S.K., Wu, C.H., Vaccaro, B.J., Lancaster, W.A., Yang, Q.Y., Fu, D., Hura, G.L., Tainer, J.A. & Adams, M.W.W. Intact Functional Fourteen-subunit Respiratory Membrane-bound [NiFe]-Hydrogenase Complex of the Hyperthermophilic Archaeon *Pyrococcus furiosus*. *J. Biol. Chem.* **289**, 19364-19372 (2014).

43. Schut, G.J., Nixon, W.J., Lipscomb, G.L., Scott, R.A. & Adams, M.W.W. Mutational analyses of the enzymes involved in the metabolism of hydrogen by the hyperthermophilic archaeon *Pyrococcus furiosus*. *Front. Microbiol.* **3**, 1-6 (2013).

44. Ma, K., Adams, M.W.W. & Kelly, R.M. in Methods in Enzymology 208-216 (Academic Press, 2001).

45. Fritsch, J., Lenz, O. & Friedrich, B. Structure, function and biosynthesis of O_2-tolerant hydrogenases. *Nat. Rev. Microbiol.* **11**, 106-114 (2013).

46. De Lacey, A.L., Fernandez, V.M., Rousset, M. & Cammack, R. Activation and inactivation of hydrogenase function and the catalytic cycle: Spectroelectrochemical studies. *Chem. Rev.* **107**, 4304-4330 (2007).

47. Buhrke, T., Lenz, O., Krauss, N. & Friedrich, B. Oxygen tolerance of the H_2-sensing [NiFe]-hydrogenase from *Ralstonia eutropha* H16 is based on limited access of oxygen to the active site. *J. Biol. Chem.* **280**, 23791-23796 (2005).

48. Kleihues, L., Lenz, O., Bernhard, M., Buhrke, T. & Friedrich, B. The H_2 sensor of *Ralstonia eutropha* is a member of the subclass of regulatory [NiFe] hydrogenases. *J. Bacteriol.* **182**, 2716-2724 (2000).

49. Lenz, O., Bernhard, M., Buhrke, T., Schwartz, E. & Friedrich, B. The hydrogen-sensing apparatus in *Ralstonia eutropha*. *J. Mol. Microb. Biotech.* **4**, 255-262 (2002).

50. Haumann, M., Porthun, A., Buhrke, T., Liebisch, P., Meyer-Klaucke, W., Friedrich, B. & Dau, H. Hydrogen-induced structural changes at the nickel site of the regulatory [NiFe] hydrogenase from *Ralstonia eutropha* detected by X-ray absorption spectroscopy. *Biochemistry* **42**, 11004-11015 (2003).

51. Liebgott, P.P., Leroux, F., Burlat, B., Dementin, S., Baffert, C., Lautier, T., Fourmond, V., Ceccaldi, P., Cavazza, C., Meynial-Salles, I., Soucaille, P., Fontecilla-Camps, J.C., Guigliarelli, B., Bertrand, P., Rousset, M. & Léger, C. Relating diffusion along the substrate tunnel and oxygen sensitivity in hydrogenase. *Nat. Chem. Biol.* **6**, 63-70 (2010).

52. Liebgott, P.P., Dementin, S., Léger, C. & Rousset, M. Towards engineering O_2-tolerance in [Ni-Fe] hydrogenases. *Energ. Environ. Sci.* **4**, 33-41 (2011).

53. Fritsch, J., Scheerer, P., Frielingsdorf, S., Kroschinsky, S., Friedrich, B., Lenz, O. & Spahn, C.M. The crystal structure of an oxygen-tolerant hydrogenase uncovers a novel iron-sulphur centre. *Nature* **479**, 249-252 (2011).

54. Goris, T., Wait, A.F., Saggu, M., Fritsch, J., Heidary, N., Stein, M., Zebger, I., Lendzian, F., Armstrong, F.A., Friedrich, B. & Lenz, O. A unique iron-sulfur cluster is crucial for oxygen tolerance of a [NiFe]-hydrogenase. *Nat. Chem. Biol.* **7**, 310-318 (2011).

55. Lukey, M.J., Roessler, M.M., Parkin, A., Evans, R.M., Davies, R.A., Lenz, O., Friedrich, B., Sargent, F. & Armstrong, F.A. Oxygen-Tolerant [NiFe]-Hydrogenases: The Individual and Collective Importance of Supernumerary Cysteines at the Proximal Fe-S Cluster. *J. Am. Chem. Soc.* **133**, 16881-16892 (2011).

56. Pandelia, M.-E., Nitschke, W., Infossi, P., Giudici-Orticoni, M.-T., Bill, E. & Lubitz, W. Characterization of a unique [FeS] cluster in the electron transfer chain

of the oxygen tolerant [NiFe] hydrogenase from *Aquifex aeolicus*. *Proc. Natl. Acad. Sci. U.S.A.* **108**, 6097-6102 (2011).

57. Abou Hamdan, A., Liebgott, P.P., Fourmond, V., Gutierrez-Sanz, O., De Lacey, A.L., Infossi, P., Rousset, M., Dementin, S. & Léger, C. Relation between anaerobic inactivation and oxygen tolerance in a large series of NiFe hydrogenase mutants. *Proc. Natl. Acad. Sci. U.S.A.* **109**, 19916-19921 (2012).

58. Shomura, Y., Yoon, K.S., Nishihara, H. & Higuchi, Y. Structural basis for a [4Fe-3S] cluster in the oxygen-tolerant membrane-bound [NiFe]-hydrogenase. *Nature* **479**, 253-256 (2011).

59. Volbeda, A., Amara, P., Darnault, C., Mouesca, J.M., Parkin, A., Roessler, M.M., Armstrong, F.A. & Fontecilla-Camps, J.C. X-ray crystallographic and computational studies of the O_2-tolerant [NiFe]-hydrogenase 1 from *Escherichia coli*. *Proc. Natl. Acad. Sci. U.S.A.* **109**, 5305-5310 (2012).

60. Roessler, M.M., Evans, R.M., Davies, R.A., Harmer, J. & Armstrong, F.A. EPR spectroscopic studies of the Fe-S clusters in the O_2-tolerant [NiFe]-hydrogenase Hyd-1 from *Escherichia coli* and characterization of the unique [4Fe-3S] cluster by HYSCORE. *J. Am. Chem. Soc.* **137**, 15581-15594 (2012).

61. Herr, N., Ratzka, J., Lauterbach, L., Lenz, O. & Ansorge-Schumacher, M.B. Stability enhancement of an O_2-tolerant NAD^+-reducing [NiFe]-hydrogenase by a combination of immobilisation and chemical modification. *J. Mol. Catal. B: Enzym.* **97**, 169-174 (2013).

62. Lauterbach, L., Lenz, O. & Vincent, K.A. H_2-driven cofactor regeneration with $NAD(P)^+$-reducing hydrogenases. *FEBS J.* **280**, 3058-3068 (2013).

63. Thorgersen, M.P., Stirrett, K., Scott, R.A. & Adams, M.W.W. Mechanism of oxygen detoxification by the surprisingly oxygen-tolerant hyperthermophilic archaeon, *Pyrococcus furiosus*. *Proc. Natl. Acad. Sci. U.S.A.* **109**, 18547-18552 (2012).

64. Abou Hamdan, A., Burlat, B., Gutierrez-Sanz, O., Liebgott, P.P., Baffert, C., De Lacey, A.L., Rousset, M., Guigliarelli, B., Léger, C. & Dementin, S. O_2-independent formation of the inactive states of NiFe hydrogenase. *Nat. Chem. Biol.* **9**, 15-17 (2012).

65. Pedroni, P., Della Volpe, A., Galli, G., Mura, G.M., Pratesi, C. & Grandi, G. Characterization of the locus encoding the [Ni-Fe] sulfhydrogenase from the archaeon *Pyrococcus furiosus*: evidence for a relationship to bacterial sulfite reductases. *Microbiology* **141**, 449-458 (1995).

Chapter 2

Spectroelectrochemistry of Cytochrome *c* and Azurin Immobilized in Nanoporous Antimony-doped Tin Oxide

Patrick Kwan, Dominick Schmitt, Alex M. Volosin, Chelsea L. McIntosh, Dong-Kyun Seo, and Anne K. Jones

Department of Chemistry and Biochemistry,

Arizona State University, Tempe, AZ 85287

Reproduced with permission from [1]:

Kwan, P. et al. Spectroelectrochemistry of cytochrome *c* and azurin immobilized in nanoporous antimony-doped tin oxide. *Chem. Comm.* **47**, 12367-12369 (2011)

–Reproduced by permission of The Royal Society of Chemistry

Abstract

Stable immobilization of two redox proteins, cytochrome *c* and azurin, in a thin film of highly mesoporous antimony tin oxide is demonstrated via UV-vis spectroscopic and electrochemical investigation.

Introduction

Direct electron transfer between redox proteins or enzymes and conductive materials has been demonstrated for a number of proteins and (semi)conductors and has proven useful both in mechanistic studies and development of technologies such as biosensors and fuel cells.[2, 3] Many desirable applications including artificial photosynthetic systems tethered to electrodes benefit from or require either a transparent electrode or a higher loading of protein at the material surface than can be obtained with a planar material.[4-7] Nonetheless, there are very few reported examples of functional interactions between redox proteins and transparent, conductive or porous materials.[8, 9]

Indium tin oxide (ITO) is the most widely investigated transparent, conductive metal oxide, but its high cost limits its application on a large scale.[10-12] Antimony-doped tin oxide (ATO) has emerged as a viable alternative for many applications, and procedures for synthesizing nanoporous powders and films have been reported.[13, 14] With respect to interaction with biomolecules, Simmons and coworkers recently demonstrated that DNA nanostructures can be adsorbed into porous ATO with retention of structure.[14] In this report, we demonstrate that two model redox proteins, the hemoprotein cytochrome *c* (cyt*C*) and the blue copper protein azurin, can be adsorbed in thin films of highly mesoporous ATO with retention of electron transfer functionality.

Materials and Methods

Preparation of Antimony Tin Oxide

In a typical procedure, 0.132 g of $SbCl_3$ (Sigma-Aldrich, 99.9%) was dissolved in 5.5 g of absolute ethanol. 2.80 g of $SnCl_4 \cdot 5H_2O$ (Sigma-Aldrich, 99%) was dissolved in 7 g of deionized water separately and added into the $SbCl_3$ solution while stirring. Polyethylene glycol (PEG) was then added to the solution and stirred for 30 min to achieve homogeneity of the solution. The amount of PEG was ~8% of the total weight of the final precursor solution. In the solution, 1.0 g of resorcinol (Sigma-Aldrich, 99%) and 1.5 g of 37% formaldehyde solution (Sigma-Aldrich, 7 – 8 % methanol as stabilizer) were added while stirring. In the solution, epichlorohydrin (Sigma-Aldrich, 99%) was added to the clear solution in a molar ratio of (Sn + Sb):epichlorohydrin of 1:7 and stirred for 1 min.

Thin film preparation

The thin films were prepared on fluorine-doped tin oxide (FTO) glass slides (Hartford Glass) by employing the doctor-blade method. The FTO glass slides were first rinsed with water, acetone and ethanol in that order. The slides were then covered with transparent Scotch tape except the area (*ca.* 0.3×2 cm^2) where the thin films were to be cast. About 0.1 ml of the precursor solution was dropped on each slide and quickly spread with a glass pipette. Any excess amount of the precursor solution was removed. The slides were then immersed horizontally in a paraffin oil bath in a petri dish, left for 24 hours at room temperature and finally heated in a laboratory oven at 70 °C for 72 hours. The films on the slides remained transparent but became hard and slightly

reddish after the heating. After removal from the oven, the slides were extracted from the oil bath, thoroughly rinsed with hexanes, the transparent Scotch tape was removed from the slides, and they were left in air at room temperature for 24 hours for drying. Finally, the slides were placed in an ashing furnace at 500 °C for 10 hours for calcination of the films.

Cytochrome c spectroelectrochemistry

Bovine heart cytochrome *c* was obtained from Sigma and used without further purification. Biological buffers were of the highest grade commercially available and were also used without further purification. Solutions for electrochemical experiments were prepared using purified water (resistivity 18.2 MΩ cm^{-1}). Electrochemical experiments were routinely conducted in 15 mM 4-(2-hydroxyethyl)-1-piperazineethane-sulfonic acid (HEPES) with 0.1 M NaCl added as supporting electrolyte. Solutions were adjusted to the desired pH by addition of HCl or NaOH.

Routinely the cleanliness of ATO slides used as working electrodes was electrochemically monitored. Adsorbed species were removed by thorough washing with 1 M NaCl solutions. Following cleaning, cytochrome *c* was adsorbed to the ATO by incubation of the slide in a buffered 150 μM protein solution for thirty minutes at room temperature. After incubation, excess protein solution was withdrawn with a pipette, and the electrode surface was thoroughly rinsed with pure water. Electrochemical measurements were made using a CH Instruments Model 1200A series electrochemical analyzer controlled by CHI1200A software. Simultaneous UV-vis spectroscopy was collected by a Perkin-Elmer Lambda 650 UV/Vis spectrophotometer. The

electrochemical cell consisted of a quartz cuvette (5 mm pathlength) in which the ATO coated slide (0.5x 2 cm ATO patch coated on the conductive side of a 3.5x0.75x0.25 cm FTO covered glass slide, Hartford Glass), a 0.5 mm diameter platinum wire counter electrode, and a Ag/AgCl reference electrode (2 mm diameter, Driref-2, World Precision Instruments) were linearly positioned in 500 μL of protein-free buffered electrolyte. Effects of uncompensated cell resistance were minimized by invoking the positive-feedback iR compensation function of the potentiostat, set at a value slightly below that at which current oscillations emerge. All potentials were corrected to the standard hydrogen electrode (SHE) according to the equation $E_{SHE} = E_{Ag/AgCl} + 197$ mV at 25 °C.[15] Electrochemical data were analyzed with SOAS, an electrochemical program freely available for download on the web at http://bip.cnrs-mrs.fr/bip06/software.html.[16] Transmission spectra were recorded through the ATO coated working electrode with the cell potential simultaneously controlled.

Azurin purification and electrochemistry

Purification of azurin followed a previous procedure[17] with the following modifications. The pH of the isolated periplasmic protein solution was adjusted to 4.1 with 20% acetic acid. The first cation exchange column (CM-sepharose, 25 x 20 cm) was equilibrated with 5 mM ammonium acetate buffer at pH 4.1, and the protein was eluted with a pH gradient of 4.1-6.35. The third column, or second cation exchange column, followed the same pH gradient. The gel-filtration column was excluded from the protocol as it was not found to be necessary. Dialysis was used to exchange the buffer following each chromatographic separation. Concentration of the protein was undertaken only after

the final column. Protein purity was verified both by SDS-PAGE and the A_{280}/A_{623} via UV-Vis spectroscopy (0.53). Following electrode cleaning, azurin was adsorbed to the ATO by incubation of the slide in a 50 μM protein solution buffered at pH 4 for thirty minutes at room temperature. After incubation, excess protein solution was withdrawn with a pipette, and the electrode surface was thoroughly rinsed with pure water.

Results and Discussion

Mesoporous ATO films were synthesized on fluorine-doped tin oxide coated glass slides (FTO) using a sol-gel method.[14, 18] As shown in Figure 2-1, the resulting coatings are uniform and transparent. The Brunauer-Emmett-Teller specific surface area was 92 $m^2\ g^{-1}$ with a pore volume of 0.41 $cm^3\ g^{-1}$ and an average pore size of 18 nm. The detailed physical properties and pore characteristics will be published separately.[19] To adsorb protein, ATO-coated slides were incubated in a solution of 150 μM cyt*C* for thirty minutes and then rinsed to remove loosely bound protein. Cyclic voltammetry of the slide revealed a pair of oxidation/ reduction peaks centered at 195 ± 20 mV vs. SHE not present on the slide before exposure to protein (Figure 2-2A). Furthermore, incubation of either a planar ITO or FTO slide with cyt*C, i.e.* a conductive slide without an ATO coating, did not result in detectable Faradaic current, indicating the vast majority of protein adsorption is due to the large surface area presented by the ATO (Figure 2-3). The average potential of the voltammetric peaks is similar to that previously measured for cyt*C* in solution and much higher than the values recorded on electrodes known to partially unfold the protein and induce pentacoordination of the heme iron.[20-22] This suggests the structure of the protein is largely intact on the surface and the heme

hexacoordinate. The peak separation is small (16 mV) and the half height peak width nearly ideal (70 mV), demonstrating that the observed electrochemical signal arises from a fast, fully reversible, adsorbed redox couple. Integration of the areas of the voltammetric peaks can be used to quantify the amount of electroactive protein on the electrode surface as 199 pmol cm^{-2}. The adsorbed protein is also remarkably stable on the electrode surface. After storing slides in buffer for more than three weeks, the protein electrochemical signals were still clearly present (Figure 2-4).

As shown in Figure 2-2B, fast scan voltammetric analysis was used to quantify the rate of electron exchange between the protein and the electrode (Figure 2-5). Using a Butler-Volmer kinetic model to fit the data, a k_0 of 1.35 s^{-1} was determined.[15, 23, 24] Although faster rates have been reported with planar electrodes (18 s^{-1} on ITO)[25], this rate is comparable to that determined for cyt*C* adsorbed to other mesoporous materials like SnO_2 or porous ITO.[9, 26]

Owing to the excellent transparency of the porous ATO films, the characteristic UV-vis spectrum of oxidized cyt*C* including both the Soret band (409 nm) and the Q-band (circa 530 nm) could be easily detected through the coated slide in an ordinary transmission mode experiment without any signal amplification (Figure 2-6A). Additionally, it was possible to reduce the protein directly via potentiostatic control of the electrode without any intervening chemical mediator and observe the expected resolution of the Q-band region into two distinct peaks and shifting of the Soret band to 415 nm (Figure 2-7A and 2-7C). The protein could then also be reversibly reoxidized (Figure 2-7B). The close agreement between the spectra for the adsorbed protein and spectra obtained from protein free in solution provides further evidence that the protein's native

structure is retained within the porous ATO material. The data in the Q-band region were fit with a Nernstian curve to determine a reduction potential of 207 mV for the cyt*C* (Figure 2-6B). This value is within the error of the reduction potential determined electrochemically.

Based on the extinction coefficient for cyt*C*, the spectroscopic surface coverage was determined to be 1650 pmol cm^{-2}.[27, 28] We note that this value is nearly an order of magnitude larger that the electroactive coverage determined under the same conditions. This suggests that as much as 90% of the protein in the ATO pores is not in fast electronic communication with the material. However, on the longer timescale of the spectroelectrochemistry experiment, the protein redox state can be controlled and observed. We consider three possible explanations. First, the pore sizes may be large enough that much of the protein in the pores is not in direct physical contact with the electrode material. However, we are loathe to suggest that protein is freely diffusing within or between pores since the adsorbed protein is stable on the timescale of weeks. If it were so mobile, degradation of signal over this time period would be expected. Second, much of the surface area of the material may have limited conductivity such that protein in contact with these areas may not efficiently exchange electrons. Third, the protein may be very strongly adsorbed to the ATO surface in an orientation that is not ideal for electron transfer and limits motions required to attain an ideal conformation.[29]

As the unique promise of porous materials is the ability to accumulate more material than at a flat surface, it is also important to compare the coverage of cyt*C* on porous ATO to that on ordinary planar surfaces. Based on the X-ray crystallographic structure of cyt*C*, the cross-sectional area of the protein can be estimated to be 7 nm^2 and

a flat monolayer of protein is expected to have a coverage of ~16 pmol cm^{-2}.[30] This number matches well with reported coverages for adsorbed cyt*C* at flat surfaces including ITO or self-assembled monolayer (SAM) covered gold.[25, 31] On the other hand, coverages on the order of 100s of pmols cm^{-2} have been reported for cyt*C* adsorbed to mesoporous ITO.[9] Thus cyt*C* is clearly penetrating the pores of the ATO and both the electrochemistry and the spectroscopy benefit from the ability to accumulate a substantial amount of material in close contact with the conductive surface.

The ATO surface, like that of other metal oxides, carries a substantial negative charge, and the interaction with cyt*C* is expected to be largely electrostatic and mediated by surface lysines. With this in mind, cyt*C* is an ideal protein for interaction with metal oxides, and other redox proteins may not be expected to adsorb stably with retention of functionality. As a second example of adsorption of a redox protein to ATO, we have undertaken experiments with the blue copper protein azurin, a protein known to interact with both pyrolytic graphite and SAM covered gold[32] but not yet demonstrated to have a functional redox interaction with metal oxides. As shown in Figure 2-8, after incubation of an ATO coated slide in 50 μM azurin solution buffered at pH 4 for 30 minutes, reversible oxidation/reduction peaks centered at 275 mV corresponding to the $Cu^{I/II}$ transition were clearly observed via cyclic voltammetry. It is interesting to note that at higher pH values, the signal was greatly attenuated. The isoelectric point of azurin is ~5.6 so that azurin carries a positive charge only at lower pH values. This provides further evidence that the interaction of proteins with the ATO is facilitated largely via electrostatic interactions.

We have demonstrated the functional adsorption of two redox proteins to thin films of mesoporous ATO. It is interesting to note that Marshall and coworkers were able to tune the redox potential of azurin over more than 700 mV via changes at the active site that left the protein surface relatively unchanged, demonstrating the potential versatility of this protein.[33] Furthermore, both rational protein design and directed evolution have been employed to redesign proteins for alternative function.[34] The combination of porous ATO with the azurin scaffold presented in this paper overcomes the challenge of finding a stable protein/ transparent electrode interface and is poised for protein engineering to develop artificial photosynthetic systems.

Figures

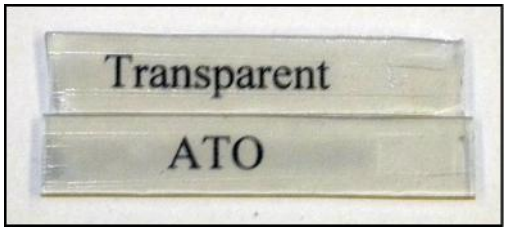


Figure 2-1. Photograph demonstrating optical transparency of mesoporous ATO coating on an FTO slide.

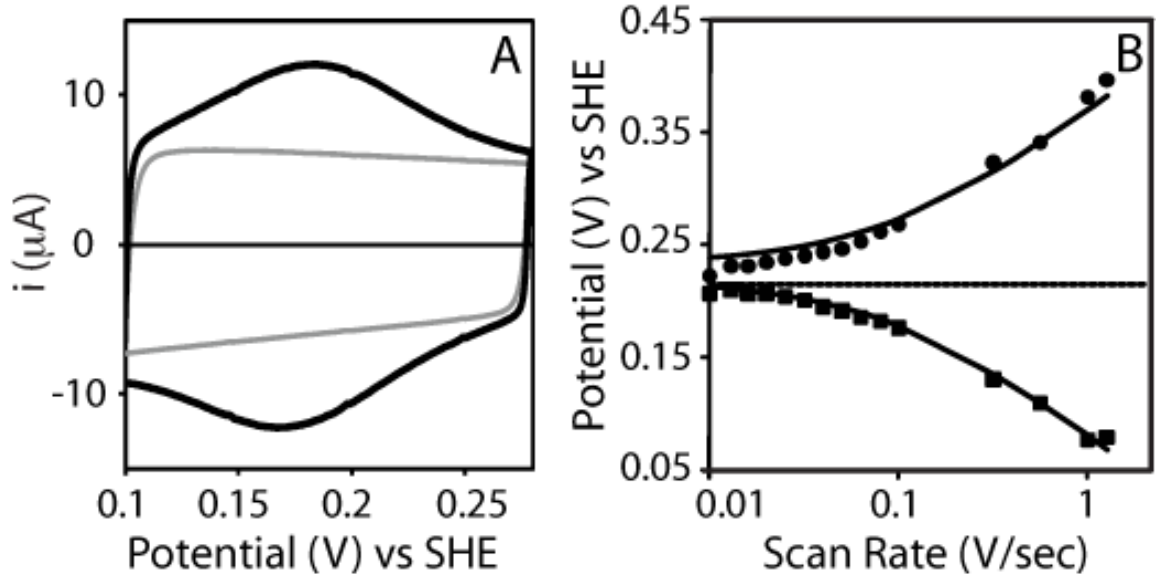


Figure 2-2. Cyclic voltammograms and trumpet plot for adsorbed cyt*C*. (A) Cyclic voltammograms of ATO coated slide (grey line) and cyt*C* adsorbed in an ATO coated slide (black line). Potential was scanned at a rate of 0.01 V/s starting from the reductive limit. (B) Voltammetric peak positions as a function of scan rate for cyt*C* adsorbed to an ATO coated slide. Squares represent the reductive peak positions and circles the oxidative peak positions. The black lines show a fit of the data using the Butler-Volker model with k_0 of 1.35 s^{-1}. The line at 215 mV shows the average reduction potential at a scan rate of 10 mV s^{-1}. The solution was buffered at pH 7 with 15 mM HEPES containing 0.1 M NaCl.

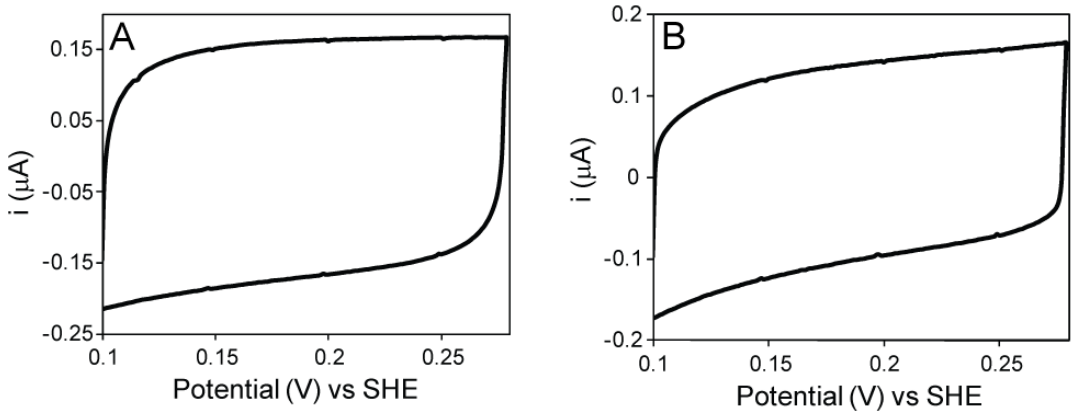


Figure 2-3. Cyclic voltammograms from control experiments demonstrating that cyt*C* does not significantly adsorb to a planar (A) ITO or (B) FTO slide. Experimental conditions are as in Figure 2-2 but slides without ATO coatings were used as working electrodes.

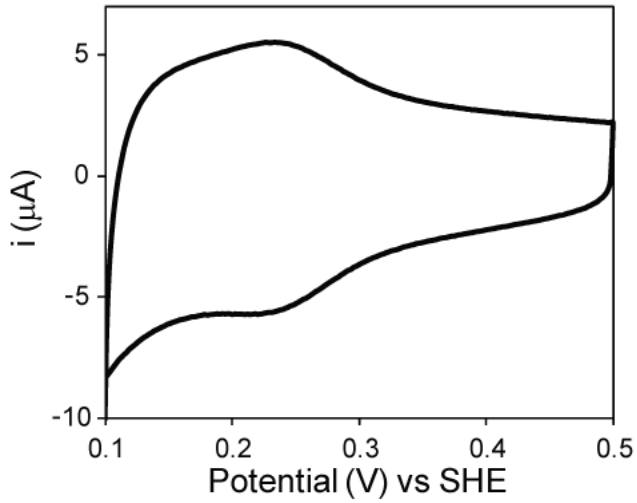


Figure 2-4. Cyclic voltammogram of an ATO coated slide with adsorbed cyt*C* after storage for twenty-one days in pH 7 buffer (15 mM HEPES, 0.1 M NaCl). The voltammogram was obtained in solution of the same composition.

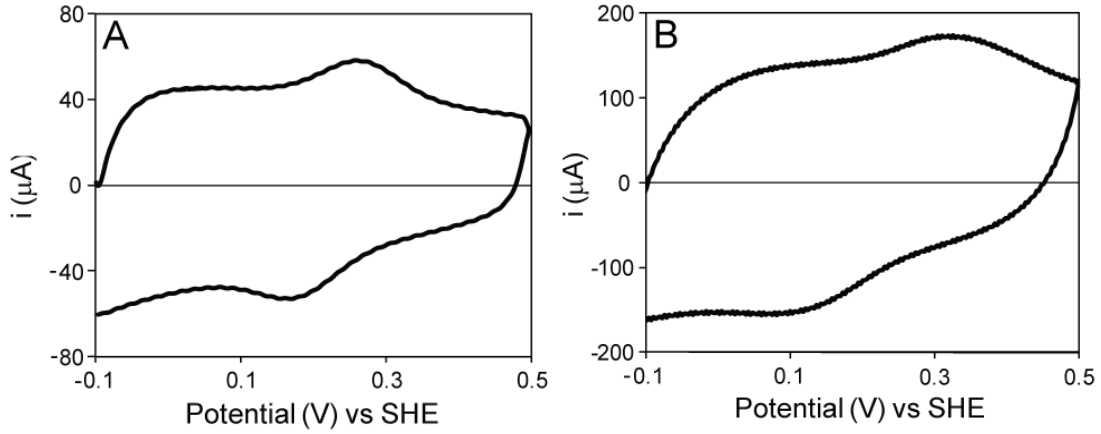


Figure 2-5. Cyclic voltammograms of cyt*C* adsorbed to an ATO film at fast scan rates. (A) 100 mV s^{-1} and (B) 316 mV s^{-1}. Other conditions are as indicated in Figure 2-2.

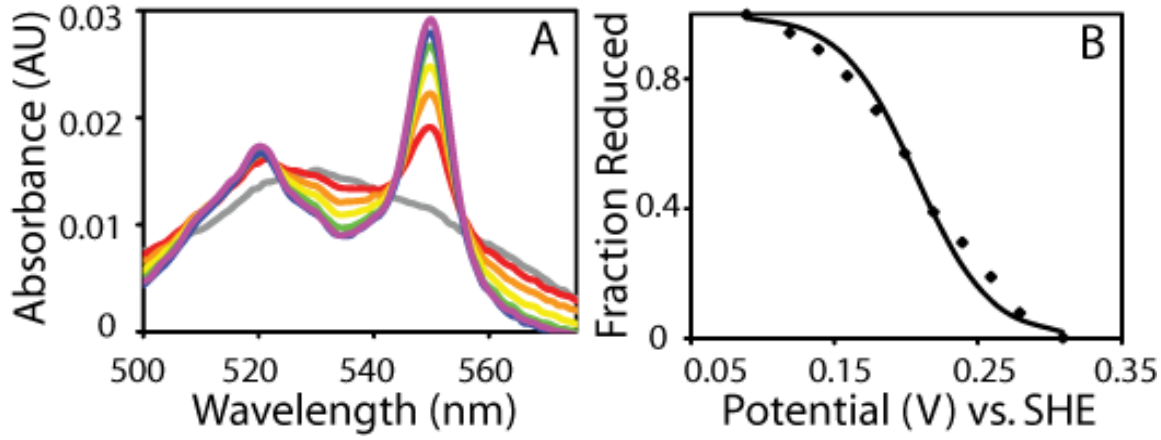


Figure 2-6. Reduction of cyt*C* adsorbed to ATO. (A) UV-vis absorbance spectra in the Q-band region for cyt*C* adsorbed to an ATO coated slide as a function of applied redox potentials as follows: air oxidized (grey), 199 mV (red), 179 mV (orange), 159 mV (yellow), 139 mV (green), 119 mV (blue), 89 mV (violet). Each potential was held for ten minutes before acquisition of spectra. (B) Fraction cyt*C* reduced as a function of reduction potential calculated based on absorbance at 550 nm. The black line shows a fit of the data to a Nernstian curve (n = 1) with E^0 = 207 mV. Experimental conditions are otherwise as indicated in Figure 2-2.

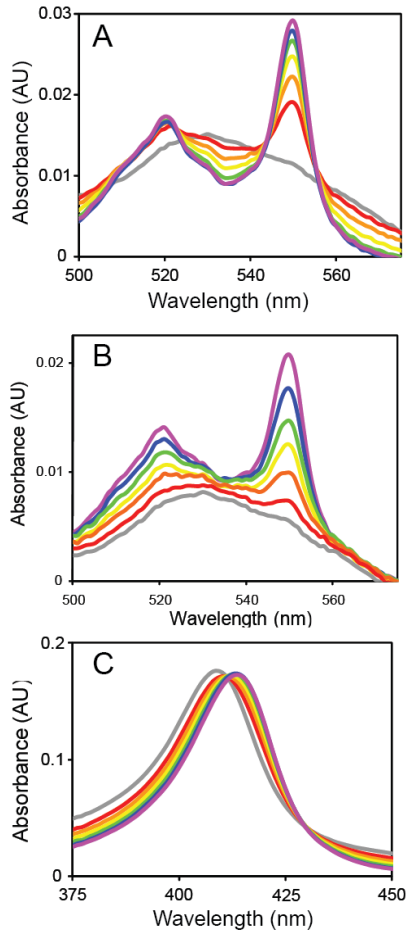


Figure 2-7. UV-vis absorbance spectra from cyt*C* adsorbed to an ATO coated slide. (A) Spectra in the Q-band region as the protein is reduced from the air-oxidized state. Spectra are colored as follows: air oxidized (grey), 199 mV (red), 179 mV (orange), 159 mV (yellow), 139 mV (green), 119 mV (blue), 89 mV (violet). Each potential was held for ten minutes before the acquisition of spectra. (B) Analogous spectra obtained starting from the reduced form of cyt*C.* Spectra are colored as follows: 309 mV (grey), 279 mV (red), 259 mV (orange), 239 mV (yellow), 219 mV (green), 199 mV (blue), 179 mV (violet). (C) UV-vis absorbance spectra in the Soret region as a function of applied redox potentials colored for the same potentials as in panel A. Other experimental conditions are as indicated in the legend of Figure 2-2.

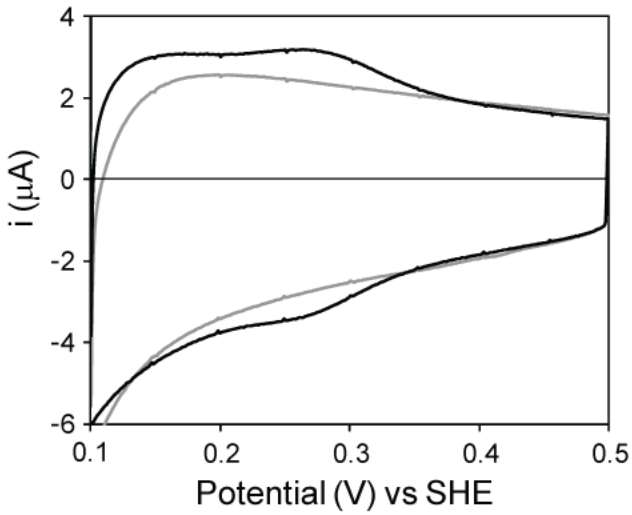


Figure 2-8. Cyclic voltammograms of ATO coated slide (grey line) and azurin adsorbed to same (black line). The solution was buffered at pH 5 with 15 mM HEPES and contained 0.1 M NaCl as electrolyte. Potential was scanned at 0.01 V/s starting from the reductive limit.

References

1. Kwan, P., Schmitt, D., Volosin, A.M., McIntosh, C.L., Seo, D.K. & Jones, A.K. Spectroelectrochemistry of cytochrome *c* and azurin immobilized in nanoporous antimony-doped tin oxide. *Chem. Commun.* **47**, 12367-12369 (2011).

2. Léger, C. & Bertrand, P. Direct electrochemistry of redox enzymes as a tool for mechanistic studies *Chem. Rev.* **108**, 2379-2438 (2008).

3. Cracknell, J.A., Vincent, K.A. & Armstrong, F.A. Enzymes as working of inspirational electrocatalysts for fuel cells and electrolysis. *Chem. Rev.* **108**, 2439-2461 (2008).

4. Kaim, W. & Fiedler, J. Spectroelectrochemistry: the best of two worlds. *Chem. Soc. Rev.* **38**, 3373-3382 (2009).

5. Herrero, C., Quaranta, A., Leibl, W., Rutherford, A.W. & Aukauloo, A. Artificial photosynthetic systems. Using light and water to provide electrons and protons for the synthesis of a fuel. *Energ. Environ. Sci.* **4**, 2353-2365 (2011).

6. MacFarlane, S.L., Day, B.A., McEleney, K., Freund, M.S. & Lewis, N.S. Designing electronic/ionic conducting membranes for artificial photosynthesis. *Energ. Environ. Sci.* **4**, 1700-1703 (2011).

7. Woolerton, T.W., Sheard, S., Pierce, E., Ragsdale, S.W. & Armstrong, F.A. CO_2 photoreduction at enzyme-modified metal oxide nanoparticles. *Energ. Environ. Sci.* **4**, 2393-2399 (2011).

8. Topoglidis, E., Cass, A.E., Gilardi, G., Sadeghi, S., Beaumont, N. & Durrant, J.R. Protein Adsorption on Nanocrystalline TiO_2 Films: An Immobilization Strategy for Bioanalytical Devices. *Anal. Chem.* **70**, 5111-5113 (1998).

9. Frasca, S., von Graberg, T., Feng, J.-J., Thomas, A., Smarsly, B.M., Weidinger, I.M., Scheller, F.W., Hildebrandt, P. & Wollenberger, U. Mesoporous indium tin oxide as a novel platform for bioelectronics. *ChemCatChem* **2**, 839-845 (2010).

10. Ginley, D.S. & Bright, C. Transparent conducting oxides. *MRS Bull.* **25**, 15-18 (2000).

11. Lewis, B.G. & Paine, D.C. Applications and processing of transparent conducting oxides. *MRS Bull.* **25**, 22-27 (2000).

12. Gordon, R.G. Criteria for choosing transparent conductors. *MRS Bull.* **25**, 52-57 (2000).

13. Hou, K., Puzzo, D., Helander, M.G., Lo, S.S., Bonifacio, D., Wang, W., Lu, Z.-H., Scholes, G.D. & Ozin, G.A. Dye-anchored mesoporous antimony-doped tin oxide electrochemiluminescence cell. *Adv. Mater.* **21**, 2492-2496 (2009).

14. Simmons, C.R., Schmitt, D., Wei, X., Han, D., Volosin, A.M., Ladd, D.M., Seo, D.-K., Liu, Y. & Yan, H. Size selective incorporation of DNA nanocages into nanoporous antimony-doped tin oxide materials. *ACS Nano* **5**, 6060-6068 (2011).

15. Bard, A.J. & Faulkner, L.R. Electrochemical Methods: Fundamentals and Applications (John Wiley & Sons, Inc., New York, 2001).

16. Fourmond, V., Hoke, K.R., Heering, H.A., Baffert, C., Leroux, F., Bertrand, P. & Léger, C. SOAS: A free program to analyze electrochemical data and other one-dimensional signals. *Bioelectrochemistry* **76**, 141-147 (2009).

17. Manetto, G.D., Grasso, D.M., Milardi, D., Pappalardo, M., Guzzi, R., Sportelli, L., Verbeet, M.R., Canters, G.W. & Rosa, C. The role played by the cc-helix in the unfolding pathway and stability of azurin: Switching between hierarchic and nonhierarchic folding. *Chembiochem* **8**, 1941-1949 (2007).

18. Sharma, S., Volosin, A.M., Schmitt, D. & Seo, D.-K. Preparation and electrochemical properties of nanoporous transparent antimony-doped tin oxide (ATO) coatings. *J. Mater. Chem.* **1**, 699-706 (2013).

19. Volosin, A.M., Sharma, S., Traverse, C., Newman, N. & Seo, D.-K. One-pot synthesis of highly mesoporous antimony-doped tin oxide from interpenetrating inorganic/organic networks. *J. Mater. Chem.* **21**, 13232-13240 (2011).

20. Collinson, M., Bowden, E.F. & Tarlov, M.J. Voltammetry of Covalently Immobilized Cytochrome-*C* on Self-Assembled Monolayer Electrodes. *Langmuir* **8**, 1247-1250 (1992).

21. Willit, J.L. & Bowden, E.F. Adsorption and redox thermodynamics of strongly adsorbed cytochrome *c* on tin oxide electrodes. *J. Phys. Chem.* **94**, 8241-8246 (1990).

22. Hildebrandt, P. & Stockburger, M. Cytochrome *c* at charged interfaces. 1. Conformation and redox equilibria at the electrode/electrolyte interface probed by surface-enhanced resonance raman spectroscopy. *Biochemistry* **28**, 6710-6721 (1989).

23. Laviron, E. Voltammetric Methods For The Study Of Adsorbed Species. *Electroanal. Chem.* **12**, 53-157 (1982).

24. Jeuken, L.J.C. http://www.mnp.leeds.ac.uk/ljcjeuken/Jellyfit.htm

25. El Kasmi, A., Leopold, M.C., Galligan, R., Robertson, R.T., Saavedra, S.S., El Kacemi, K. & Bowden, E.F. Adsorptive immobilization of cytochrome *c* on indium/tin oxide (ITO): electrochemical evidence for electron transfer-induced conformation changes. *Electrochem. Commun.* **4**, 177-181 (2002).

26. Topoglidis, E., Astuti, Y., Duriaux, F., Gratzel, M. & Durrant, J.R. Direct Electrochemistry and Nitric Oxide Interaction of Heme Proteins Adsorbed on Nanocrystalline Tin Oxide Electrodes. *Langmuir* **19**, 6894-6900 (2003).

27. Collinson, M. & Bowden, E.F. UV-visible spectroscopy of adsorbed cytochrome *c* on tin oxide electrodes. *Anal. Chem.* **64**, 1470-1476 (1992).

28. Heineman, W.R. & Kuwana, T. Spectroelectrochemical Studies of Metal Deposition and Stripping and of Specific Adsorption on Mercury-Platinum Optically Transparent Electrodes. *Anal. Chem.* **44**, 1972-1978 (1972).

29. Kranich, A., Ly, H.K., Hildebrandt, P. & Murgida, D.H. Direct observation of the gating step in protein electron transfer: electric-field-controlled protein dynamics. *J. Am. Chem. Soc.* **130**, 9844-9848 (2008).

30. Takano, T., Kallai, O.B., Swanson, R. & Dickerson, R.E. The structure of ferrocytochrome *c* at 2.45 A resolution. *J. Biol. Chem.* **248**, 5234-5255 (1973).

31. Davis, K.L., Drews, B.J., Yue, H., Waldeck, D.H., Knorr, K. & Clark, R.A. Electron-transfer kinetics of covalently attached cytochrome c/SAM/Au electrode assemblies. *J. Phys. Chem. C* **112**, 6571-6576 (2008).

32. Jeuken, L.J.C. & Armstrong, F.A. Electrochemical origin of hysteresis in the electron-transfer reactions of adsorbed proteins: Contrasting behavior of the "blue" copper protein, azurin, adsorbed on pyrolytic graphite and modified gold electrodes. *J. Phys. Chem. B* **105**, 5271-5282 (2001).

33. Marshall, N.M., Garner, D.K., Wilson, T.D., Gao, Y.G., Robinson, H., Nilges, M.H. & Lu, Y. Rationally tuning the reduction potential of a single cupredoxin beyond the natural range. *Nature* **462**, 113-116 (2009).

34. Lu, Y., Berry, S.M. & Pfister, T.D. Engineering novel metalloproteins: design of metal-binding sites into native protein scaffolds. *Chem. Rev.* **101**, 3047-3080 (2001).

Chapter 3

Catalytic Bias of the Soluble Hydrogenase I from *Pyrococcus furiosus*

Patrick Kwan,[†] Michael W.W. Adams,[‡] and Anne K. Jones,[†]

[†]Department of Chemistry and Biochemistry,

Arizona State University, Tempe, AZ 85287;

[‡]Department of Biochemistry,

The University of Georgia, Athens, GA 30602

Abstract

Electrochemical characterization of the soluble hydrogenase I from *Pyrococcus furiosus* (*Pf*SHI) has revealed that the electrocatalytic bias of the enzyme, *i.e.* the ratio of the maximal rates for hydrogen oxidation and proton reduction, is highly dependent on temperature. Increases in temperature cause a concomitant increase in the rate of proton reduction activity, but hydrogen oxidation activity is relatively unaffected by temperature. This uneven response to temperature results in a dramatic shift in the catalytic bias to favor the proton reduction direction at elevated temperatures. The shift in catalytic bias may arise from different rate determining steps for the forward and reverse reactions that behave differently as a function of temperature.

Introduction

The degree of preference for either reductive or oxidative catalysis, a property that we refer to as catalytic bias, *i.e.* the ratio of the maximal rates in the two directions, is widely various across different classes of redox enzymes. For example, the oxygen-evolving complex of Photosystem II oxidizes water to oxygen but does not catalyze the reverse reaction, making it effectively an irreversible catalyst.[1, 2] On the other hand, both formate oxidation and carbon dioxide reduction are catalyzed by a number of formate dehydrogenases with varying relative efficiencies.[3, 4] Catalytic bias is not only a fundamental mechanistic property of an enzyme. Control and modulation of catalytic bias also come to the fore as important goals in protein and metabolic pathway engineering for technological applications. Nonetheless, there are few enzymes for which the

mechanisms determining catalytic bias have been precisely defined or for which researchers have been able to demonstrate the ability to tune bias via either mutagenesis or control of reaction conditions.

[NiFe]-hydrogenases, a class of enzymes that catalyze hydrogen oxidation and production,[5-7] offer an excellent model to define protein features that can control catalytic reversibility in redox enzymes for several reasons. First, the catalytic reactions they perform require two-electrons, meaning they serve as a tractable model for multi-electron catalysis. Second, the catalysis involves proton-coupled electron transfer, a key feature in the mechanisms of the vast majority of oxidoreductases. Third, the natural distribution of [NiFe]-hydrogenases and their catalytic biases is very broad so that natural primary sequence variation may offer mechanistic clues.[5, 8, 9] For example, membrane-bound hydrogenases, which oxidize hydrogen to provide energy for the organism, typically have a marked preference for hydrogen oxidation *in vitro* and relatively modest proton reduction activity.[10-15] On the other hand, solution assays have shown that the rate of H_2 evolution by the soluble hydrogenase I from *Pyrococcus furiosus* (*Pf*SHI) at 80 ºC is comparable to that of the [FeFe]-hydrogenase I from *Clostridium pasteurianum*, a well-established hydrogen producer.[16] Similarly, electrocatalytic investigation has shown that the hydrogenase from *Synechocystis* sp. PCC6803 has a slight preference for proton reduction.[7] Furthermore, many [NiFe]-hydrogenases are believed to catalyze proton reduction *in vivo*.[17-20]

P. furiosus is a hyperthermophilic, strictly anaerobic archaean that grows optimally at 100 ºC by fermentation of carbohydrates.[21, 22] It contains three [NiFe]-hydrogenases: two soluble group 3 enzymes (SHI and SHII) and a group 4

H_2-evolving MBH.[17, 18, 20, 23] As shown in Figure 3-1, *Pf*SHI is a heterotetrameric enzyme that contains within its α-subunit the [NiFe] binding site and within the δ-subunit a chain of three [4Fe4S] clusters. It is proposed *in vivo* to oxidize the hydrogen produced by the organism's group 4 H^+-reducing MBH.[20, 24] Herein, we exploit the ability of *Pf*SHI to catalyze both hydrogen oxidation and production over an extremely broad temperature range to characterize the temperature dependence of the catalytic bias. We show that at low temperatures, the enzyme is marginally faster in the hydrogen oxidation direction, but at higher, more physiological temperatures, there is a marked increase in the proton reduction rate that dramatically shifts the catalytic bias. To the best of our knowledge, this is the first demonstration of the modulation of the catalytic bias of a wild-type redox enzyme by almost an order of magnitude via manipulation of experimental conditions.

Materials and Methods

Purification of the enzyme was performed as previously described according to Ma, *et al.*[17] Protein film electrochemistry (PFE) was performed in an anaerobic glovebox as described by McIntosh, *et al.*[7] All chemicals were of the highest grade commercially available and were used without further purification. Solutions for electrochemical experiments were prepared using purified water (resistivity 18.2 MΩ cm^{-1}). The mixed buffer consisted of 15 mM each of 4-(2-hydroxyethyl)-1-piperazineethane-sulfonic acid (HEPES), 2-[*N'*-cyclohexyl-amino]ethane-sulfonic acid (CHES), 2-[*N'*-morpholino]ethane-sulfonic acid (MES), *N'*-tris[hydroxymethyl] methyl-3-amino-propane-sulfonic acid (TAPS), and sodium acetate with 0.1 M NaCl as supporting electrolyte (HEPES, MES, CHES, TAPS, and sodium acetate from Sigma and USB, NaCl

from VWR). Solutions were adjusted to the desired experimental pH with either NaOH or HCl. The experimental conditions for each experiment are indicated in the figure legend. Gas mixtures were purchased from Praxair and used as received. Enzyme films were prepared by first abrading the graphite surface with fine emery paper (Norton, P500J) followed by briefly polishing the electrode with a 1 μm aqueous alumina (Buehler) slurry and thorough sonication in water with rinsing. A 25 μL enzyme solution (~0.3 mg/mL) was then pipetted onto the electrode surface and left undisturbed for 120 seconds, followed by removal of the enzyme solution by pipette and rinsing of the electrode surface with water. All electrochemical experiments were conducted using a three-electrode system consisting of a pyrolytic graphite rotating disk working electrode, a platinum wire auxiliary electrode and a Ag/AgCl reference electrode. The electrode rotation rate was 3600 rpm, and, for cyclic voltammetry experiments, the potential scan rate was 10 mV s^{-1}, unless otherwise indicated. Temperature-controlled experiments were conducted using a water-jacketed electrochemical cell connected to a temperature-controlled water bath. The electrochemical data were analyzed with SOAS, an electrochemical program freely available for download on the web at http://bip.cnrs-mrs.fr/bip06/software.html.[25]

Results

Electrocatalysis by Pf*SHI adsorbed to pyrolytic graphite*

Figure 3-2 shows that *Pf*SHI functions as an electrocatalyst when adsorbed to a pyrolytic graphite electrode. Under a nitrogen atmosphere (panel B), proton reduction is observed as a negative current, and the magnitude of the catalytic current, which is

directly proportional to turnover frequency, increases with decreasing pH, *i.e.* increasing substrate concentration. Similarly, upon addition of hydrogen to the experiment (panel A), hydrogen oxidation is observed as a positive current. In this case, the dependence of turnover frequency on pH shows the opposite trend, *i.e.* higher pH results in faster hydrogen oxidation. It is important to note that catalytic activity is only observed when the enzyme is adsorbed to the electrode surface; no catalytic signals are present when a clean graphite electrode is used. Additionally, catalytic current does not require that enzyme be present in the experimental solution, demonstrating that the catalysis arises from enzyme that is adsorbed to the electrode surface.

Temperature dependence of electrocatalytic activity of Pf*SHI*

Solution assays using soluble mediators as electron donors/acceptors have shown that the catalytic activities of *Pf*SHI are strongly dependent on temperature.[16] The influence of temperature on the electrocatalytic activity of adsorbed *Pf*SHI at pH 6.5 was probed via chronoamperometric experiments conducted at temperatures from 25 ºC to 80 ºC, such as that shown in Figure 3-3. In short, the working electrode with adsorbed enzyme was first held at -563 mV to fully reductively activate the *Pf*SHI. Activation was monitored as increasing H^+-reduction current, and i_{Red}, a measure of the rate of H^+-reduction activity, was determined once the current stabilized. Following activation, the gas composition above the electrochemical cell was switched from 100% N_2 to 100% H_2 and the potential of the electrode was stepped to +197 mV to observe H_2 oxidation current. The value i_{Ox} is the current observed 300 s after the jump to oxidizing potential. Figure 3-4 shows that both H^+-reduction and H_2-oxidation activities increased

as a function of temperature, but the rate of proton reduction increased much more dramatically. Between 15 ºC and 80 ºC, H^+-reduction activity increased by a factor of 35, while H_2 oxidation activity increased only by a factor of 2 (Figure 3-4A). The result of this uneven response is a dramatic shift in the catalytic bias of the enzyme towards H^+-reduction at high temperatures such that proton reduction is 0.48 times as fast as H_2 oxidation at 25 ºC and 5.3 times faster than H_2 oxidation at 80 ºC (Figure 3-4B). It is important to note that the pH of the mixed buffer decreases marginally as a function of temperature, as shown in Figure 3-5 (pH decreases from 6.5 to 6.0 when the temperature is increased from 15 ºC to 80 ºC). This change in pH impacts the catalytic bias, but alone it can only account for a small fraction of the observed change.

Discussion

Our electrocatalytic experiments demonstrate that the catalytic bias of *Pf*SHI can be modulated by an order of magnitude simply via variation of the temperature between 25 and 80 ºC. This is consistent with the results of Bryant, *et al.* which demonstrated a similar shift in catalytic bias with temperature. Solution assays revealed that the rate of H^+-reduction catalysis increased 40-fold between 45 and 95 ºC.[16] Similarly, electrochemical experiments using *Pf*SHI revealed a 35-fold increase in H^+-reduction between 25 and 80 ºC, while H_2-oxidation activity only increased by a factor of 2. Thus, remarkably, the shift in catalytic bias arises from a marked temperature dependence only of the reductive but not the oxidative catalysis.

Understanding the temperature dependence of the catalytic bias of *Pf*SHI is complicated by the fact that the underlying mechanisms of the catalytic bias itself are still

unclear. Recent experiments have shown that the catalytic bias of [NiFe]-hydrogenases is not as straightforward as previously thought and is almost certainly not trivially determined by the reduction potential of the [NiFe] active site, *i.e.* by the difference between the potential of the hydrogen couple and the potential of the [NiFe] site. Instead, it is likely that the catalytic bias of these enzymes depends on the rates of steps in the catalytic cycle that may be distant from the active site.[26, 27] In addition to the redox chemistry occurring at the active site, the catalytic cycle of a redox enzyme can involve many additional steps, *e.g.*, substrate binding, product release, intramolecular electron transfers between redox active sites, and proton transfers. The rate-limiting steps in the catalytic cycle may differ depending on the directionality of the reaction, as posited by Hamdan, *et al.*[26] In the case of *Pf*SHI, the presence of different rate-limiting steps for H^+-reduction and H_2-oxidation activity with different temperature dependences may be sufficient to explain the temperature-dependent shift in catalytic bias. It is perhaps worth noting nonetheless that temperature dependent reduction potentials may also play a role in the shift in catalytic bias. Our chronoamperometric experiments designed to probe the reactivation of oxygen inactivated enzyme (Chapter 5) suggest that the apparent reduction potentials of the enzyme's inactive states shift to more positive potentials at higher temperatures, *i.e.* the inactive states of the enzyme become easier to reduce at higher temperatures. It is possible that the reduction potentials of the active site states in the catalytic cycle have a similar temperature dependence. This would favor reduced states of the catalytic cycle and perhaps shift the catalytic bias toward the H^+-reducing direction. Further experiments and carefully designed mutants will be required to disentangle these multiple competing influences.

Figures

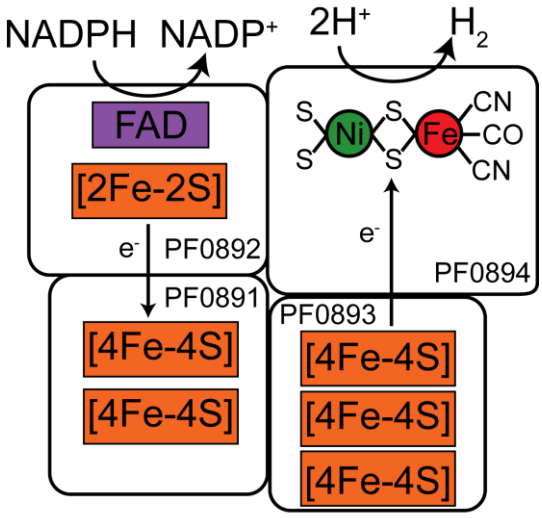


Figure 3-1. Schematic representation of *Pf*SHI, showing the enzyme's four subunits and the clusters present in the enzyme.

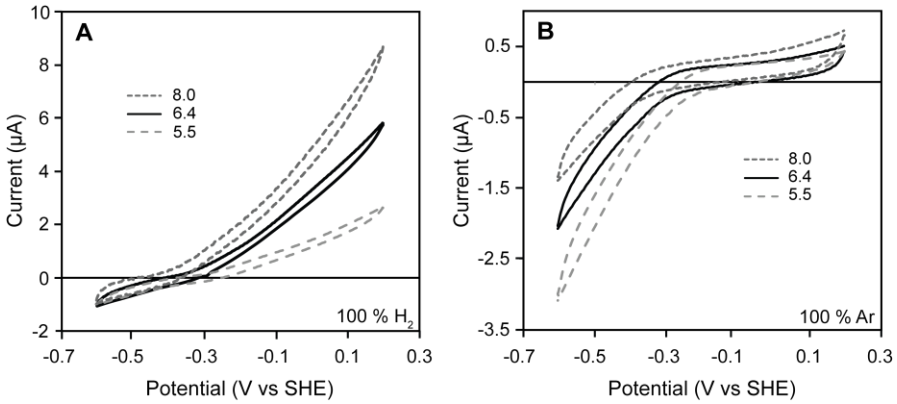


Figure 3-2. Cyclic voltammograms showing direct (A) hydrogen oxidation and (B) proton reduction by *Pf*SHI adsorbed to a graphite electrode at various pH values. Experiments were completed at 25 ºC in a mixed buffer with a potential scan rate of 10 mV s^{-1} and an electrode rotation rate of 2000 rpm. Hydrogen oxidation experiments were performed under 1 atm H_2 and proton reduction experiments under a nitrogen atmosphere.

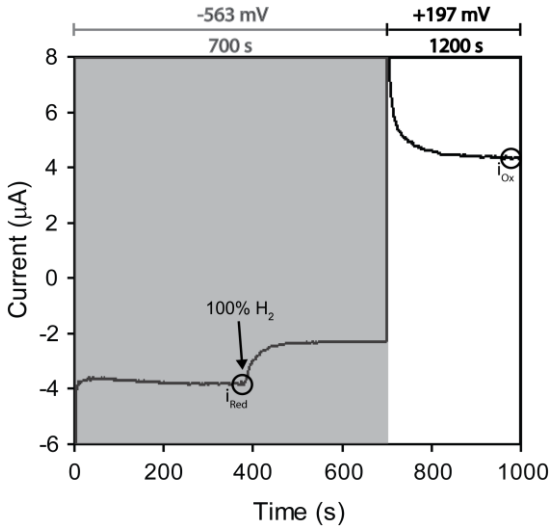


Figure 3-3. Chronoamperogram demonstrating *Pf*SHI catalysis at 60 ºC. Potentials and duration of each step are indicated above the figure. Gray shading indicates that the electrode was held at reductive (-563 mV) potential and white background indicates that the electrode was held at an oxidative (+197 mV) potential. The currents i_{Red} and i_{Ox} indicate H^+ reduction and H_2 oxidation currents, respectively. Hydrogen gas was introduced into the experiment at the point indicated by the arrow.

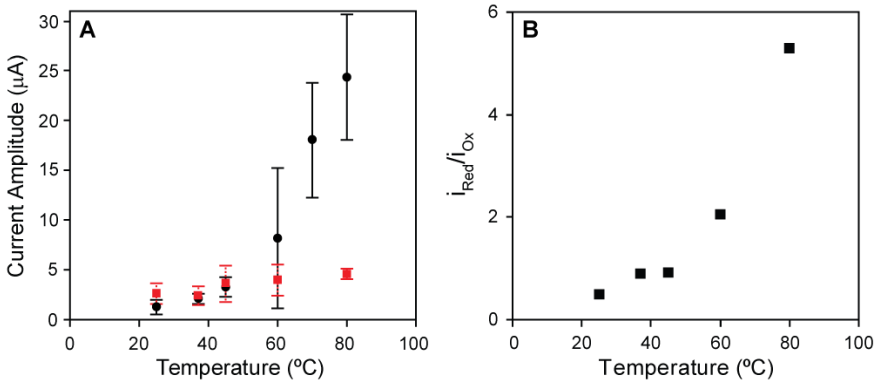


Figure 3-4. Temperature Dependence of (●) H^+ reduction and (●) hydrogen oxidation catalytic currents from adsorbed *Pf*SHI. Each point represents the average value from 3-8 independent chronoamperometry experiments, and the error bars correspond to one standard deviation. In each chronoamperometric experiment, the working electrode with adsorbed *Pf*SHI was first held at -563 mV under 100% N_2 to fully activate the enzyme. The current was monitored throughout this period to assess extent of activation, and the enzyme film was considered "fully activated" when the H^+ reduction current stabilized. This usually required 10-60 minutes. The value i_{Red} is the current observed at E = -563 mV following the activation period. Once the enzyme was completely active, the experimental solution was saturated with 100% H_2 and the electrode potential stepped to +197 mV to observe hydrogen oxidation. The value i_{Ox} is the current 300 s after stepping to the oxidizing potential. Experiments were performed in a mixed buffer with pH = 6.5 at the indicated temperatures.

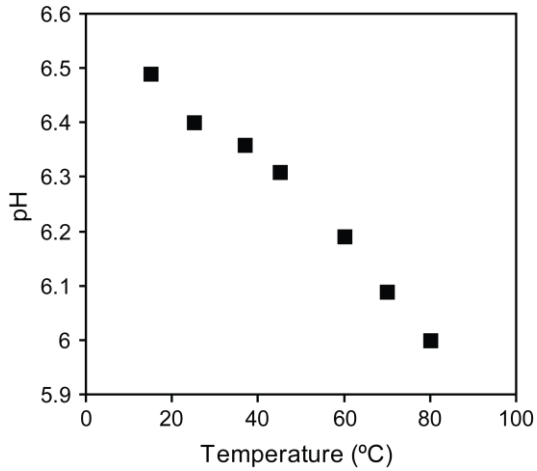


Figure 3-5. Dependence of pH of the mixed buffer system used for electrochemical experiments on temperature within the range of 15 ºC – 80 ºC.

References

1. Dau, H., Zaharieva, I. & Haumann, M. Recent developments in research on water oxidation by photosystem II. *Curr. Opin. Chem. Biol.* **16**, 3-10 (2012).

2. Cox, N., Pantazis, D.A., Neese, F. & Lubitz, W. Biological Water Oxidation. *Accounts Chem. Res.* **46**, 1588-1596 (2013).

3. Reda, T., Plugge, C.M., Abram, N.J. & Hirst, J. Reversible interconversion of carbon dioxide and formate by an electroactive enzyme. *Proc. Natl. Acad. Sci. U.S.A.* **105**, 10654-10658 (2008).

4. Choe, H., Joo, J.C., Cho, D.H., Kim, M.H., Lee, S.H., Jung, K.D. & Kim, Y.H. Efficient CO_2-Reducing Activity of NAD-Dependent Formate Dehydrogenase from *Thiobacillus* sp. KNK65MA for Formate Production from CO_2 Gas. *PLOS One* **9**, e103111 (2014).

5. Vignais, P.M. & Billoud, B. Occurrence, classification, and biological function of hydrogenases: An overview. *Chem. Rev.* **107**, 4206-4272 (2007).

6. Appel, J., Phunpruch, S., Steinmuller, K. & Schulz, R. The bidirectional hydrogenase of *Synechocystis* sp PCC 6803 works as an electron valve during photosynthesis. *Arch. Microbiol.* **173**, 333-338 (2000).

7. McIntosh, C.L., Germer, F., Schulz, R., Appel, J. & Jones, A.K. The [NiFe]-hydrogenase of the cyanobacterium *Synechocystis* sp. PCC 6803 works bidirectionally with a bias to H_2 production. *J. Am. Chem. Soc.* **133**, 11308-11319 (2011).

8. D'Adamo, S., Jinkerson, R.E., Boyd, E.S., Brown, S.L., Baxter, B.K., Peters, J.W. & Posewitz, M.C. Evolutionary and Biotechnological Implications of Robust Hydrogenase Activity in Halophilic Strains of *Tetraselmis*. *PLOS One* **9**, 1-13 (2014).

9. Vignais, P.M., Billoud, B. & Meyer, J. Classification and phylogeny of hydrogenases. *FEMS Microbiol. Rev.* **25**, 455-501 (2001).

10. Cracknell, J.A., Wait, A.F., Lenz, O., Friedrich, B. & Armstrong, F.A. A kinetic and thermodynamic understanding of O_2 tolerance in [NiFe]-hydrogenases. *Proc. Natl. Acad. Sci. U.S.A.* **106**, 20681-20686 (2009).

11. Lenz, O., Ludwig, M., Schubert, T., Bürstel, I., Ganskow, S., Goris, T., Schwarze, A. & Friedrich, B. H_2 Conversion in the Presence of O_2 as Performed by the Membrane-Bound [NiFe]-Hydrogenase of *Ralstonia eutropha*. *ChemPhysChem* **11**, 1107-1119 (2010).

12. Vincent, K.A., Cracknell, J.A., Clark, J.R., Ludwig, M., Lenz, O., Friedrich, B. & Armstrong, F.A. Electricity from low-level H_2 in still air - an ultimate test for an oxygen tolerant hydrogenase. *Chem. Commun.* **48**, 5033-5035 (2006).

13. Evans, R.M., Parkin, A., Roessler, M.M., Murphy, B.J., Adamson, H., Lukey, M.J., Sargent, F., Volbeda, A., Fontecilla-Camps, J.C. & Armstrong, F.A. Principles of Sustained Enzymatic Hydrogen Oxidation in the Presence of Oxygen - The Crucial Influence of High Potential Fe-S Clusters in the Electron Relay of [NiFe]-Hydrogenases. *J. Am. Chem. Soc.* **135**, 2694-2707 (2013).

14. Pandelia, M.-E., Lubitz, W. & Nitschke, W. Evolution and diversification of Group 1 [NiFe] hydrogenases. Is there a phylogenetic marker for O_2-tolerance? *Biochim. Biophys. Acta* **1817**, 1565-1575 (2012).

15. Burgdorf, T., De Lacey, A.L. & Friedrich, B. Functional analysis by site-directed mutagenesis of the NAD^+-reducing hydrogenase from *Ralstonia eutropha*. *J. Bacteriol.* **184**, 6280-6288 (2002).

16. Bryant, F.O. & Adams, M.W.W. Characterization of Hydrogenase from the Hyperthermophilic Archaebacterium, *Pyrococcus furiosus*. *J. Biol. Chem.* **264**, 5070-5079 (1989).

17. Ma, K. & Adams, M.W. Hydrogenases I and II from *Pyrococcus furiosus*. *Methods Enzymol.* **331**, 208-216 (2001).

18. McTernan, P.M., Chandrayan, S.K., Wu, C.H., Vaccaro, B.J., Lancaster, W.A., Yang, Q.Y., Fu, D., Hura, G.L., Tainer, J.A. & Adams, M.W.W. Intact Functional Fourteen-subunit Respiratory Membrane-bound [NiFe]-Hydrogenase Complex of the Hyperthermophilic Archaeon *Pyrococcus furiosus*. *J. Biol. Chem.* **289**, 19364-19372 (2014).

19. Ortega-Ramos, M., Jittawuttipoka, T., Saenkham, P., Czarnecka-Kwasiborski, A., Bottin, H., Cassier-Chauvat, C. & Chauvat, F. Engineering *Synechocystis* PCC6803 for hydrogen production: influence on the tolerance to oxidative and sugar stresses. *PLOS One* **9**, e89372 (2014).

20. Jenney, F.E., Jr. & Adams, M.W.W. Hydrogenases of the model hyperthermophiles. *Ann. NY Acad. Sci.* **1125**, 252-266 (2008).

21. Fiala, G. & Stetter, K.O. *Pyrococcus furiosus* sp. nov. represents a novel genus of marine heterotrophic archaebacteria growing optimally at 100 degrees C. *Arch. Microbiol.* **145**, 56-61 (1986).

22. Schut, G.J., Bridger, S.L. & Adams, M.W.W. Insights into the metabolism of elemental sulfur by the hyperthermophilic archaeon *Pyrococcus furiosus*: Characterization of a coenzyme A-dependent NAD(P)H sulfur oxidoreductase. *J. Bacteriol.* **189**, 4431-4441 (2007).

23. Sapra, R., Verhagen, M.F. & Adams, M.W.W. Purification and characterization of a membrane-bound hydrogenase from the hyperthermophilic archaeon *Pyrococcus furiosus*. *J. Bacteriol.* **182**, 3423-3428 (2000).

24. Schut, G.J., Nixon, W.J., Lipscomb, G.L., Scott, R.A. & Adams, M.W.W. Mutational analyses of the enzymes involved in the metabolism of hydrogen by the hyperthermophilic archaeon *Pyrococcus furiosus*. *Front. Microbiol.* **3**, 1-6 (2013).

25. Fourmond, V., Hoke, K.R., Heering, H.A., Baffert, C., Leroux, F., Bertrand, P. & Léger, C. SOAS: A free program to analyze electrochemical data and other one-dimensional signals. *Bioelectrochemistry* **76**, 141-147 (2009).

26. Abou Hamdan, A., Dementin, S., Liebgott, P.-P., Gutierrez-Sanz, O., Richaud, P., De Lacey, A.L., Rousset, M., Bertrand, P., Cournac, L. & Léger, C. Understanding and Tuning the Catalytic Bias of Hydrogenase. *J. Am. Chem. Soc.* **134**, 8368-8371 (2012).

27. Fourmond, V., Baffert, C., Sybirna, K., Lautier, T., Abou Hamdan, A., Dementin, S., Soucaille, P., Meynial-Salles, I., Bottin, H. & Léger, C. Steady-State Catalytic Wave-Shapes for 2-Electron Reversible Electrocatalysts and Enzymes. *J. Am. Chem. Soc.* **135**, 3926-3938 (2013).

Chapter 4

The Soluble [NiFe]-Hydrogenase I from *Pyrococcus furiosus* Produces Hydrogen in the Presence of Oxygen

Patrick Kwan,[†] Michael W.W. Adams,[‡] and Anne K. Jones,[†]

[†]Department of Chemistry and Biochemistry,

Arizona State University, Tempe, AZ 85287;

[‡]Department of Biochemistry,

The University of Georgia, Athens, GA 30602

Abstract

Soluble hydrogenase I from Pyrococcus furiosus (*Pf*SHI) is an oxygen-tolerant, group 3 [NiFe]-hydrogenase that reduces protons more efficiently than it oxidizes hydrogen. Herein, chronamperometry experiments have been used to characterize the proton reduction activity in the presence of 1% oxygen. For temperatures between 25 and 80 ºC, *Pf*SHI maintains the overwhelming majority of its reductive activity in the presence of 1% oxygen. Furthermore, as a consequence of the design of the chronoamperometry experiment, we also show that hydrogen becomes markedly less effective as an inhibitor of proton reduction at elevated temperatures. Both observations are consistent with a model in which gas diffusion through protein-embedded gas channels is faster at higher temperatures.

Introduction

Due to growing global interest in the use of hydrogen as a carbon-neutral fuel, there is a need for cheap and sustainable hydrogen production catalysts capable of fast turnover at low activation energies. Hydrogenases are a class of enzymes that catalyze the interconversion of H^+ and H_2, and they have proven interesting in this area since they produce hydrogen from protons at rates in excess of 1000 s^{-1} at active sites using only the first row transition metals iron and nickel.[1] Although many hydrogenases are capable of high catalytic turnover at low overpotentials, they are also extremely sensitive to inactivation by oxygen.[2-4] This inactivation has limited their usefulness in both fuel production and fuel cell applications.

Standard [NiFe]-hydrogenases are rapidly inactivated by small amounts of oxygen to form two inactive states. However, an "oxygen-tolerant" subgroup of [NiFe]-hydrogenases, capable of catalytic hydrogen oxidation in the presence of oxygen, has been discovered. These include the membrane-bound enzymes from *Ralstonia eutropha* (*Re*MBH),[5, 6] *Aquifex aeolicus*,[7, 8] *Escherichia coli*,[9, 10] and *Hydrogenovibrio marinus*.[11] Many hypothesize that these enzymes tolerate O_2 exposure by forming exclusively the Ni-B inactive state in the presence of oxygen. The ability to prevent formation of the slowly reactivating Ni-A inactive state is attributed to the enzyme's ability to perform a complete 4-electron reduction of attacking O_2 molecules, preventing the formation of reactive oxygen species and incorporation of partially reduced, oxygen-derived ligands into the enzyme active site.[7, 10, 12, 13] The ability to facilitate this 4-electron reaction appears to be linked to a highly conserved [4Fe-3S] cluster proximal to the active site found in the X-ray structures of two oxygen-tolerance, uptake [NiFe]-hydrogenases.[8, 10, 14, 15] Spectroscopic studies suggest that this nonstandard [4Fe-3S] cluster is stable under physiological conditions in the 3+, 2+, and 1+ oxidation states, and the ability to quickly donate 2 electrons may be crucial to the enzyme's ability to completely reduce attacking oxygen.[8, 11, 14, 15]

Interest in hydrogenases is not limited to their ability to oxidize H_2 in fuel cells; they are also relevant for H_2-producing applications.[16-20] Most investigations of [NiFe]-hydrogenases have involved the group 1 membrane-bound hydrogenases (MBHs), which typically have low H^+-reduction activity. On the other hand, the soluble, or group 3, [NiFe]-hydrogenases often exhibit significant H^+-reduction activity, and many, such as the soluble [NiFe]-hydrogenases (SH) of *R. eutropha* (*Re*SH) and hydrogenase I

from *Pyrococcus furiosus* (*Pf*SHI), also possess some degree of oxygen tolerance. However, these soluble enzymes do not possess the additional cysteine residues found near the proximal FeS cluster in oxygen-tolerant MBHs suggesting that a [4Fe-3S] proximal cluster is not present. Thus it is unclear how these soluble enzymes achieve oxygen tolerance.

In this chapter, we investigate the H^+-reduction ability of *Pf*SHI under aerobic conditions. Since the hyperthermophilic archaean *P. furiosus* grows at temperatures of *ca.* 100 ºC in its native environment, our experiments have been carried out over a range of temperatures. The results are compared to those reported for other [NiFe]-hydrogenases from groups 1 and 3 including HoxEFUYH from *Synechocystis* sp. PCC 6803, the membrane bound hydrogenase from *Ralstonia eutropha* (*Re*MBH), the [NiFeSe]-hydrogenase from *Desulfomicrobium baculatum*, and Hyd-2 from *Escherichia coli*.

Materials and Methods

Purification of the enzyme was performed as previously described by Ma, *et al*.[21] Protein film electrochemistry (PFE) was performed in an anaerobic glovebox as described by McIntosh, *et al*.[1] All chemicals were of the highest grade commercially available and were used without further purification. Solutions for electrochemical experiments were prepared using purified water (resistivity 18.2 MΩ cm^{-1}). The mixed buffer consisted of 15 mM each of 4-(2-hydroxyethyl)-1-piperazineethane-sulfonic acid (HEPES), 2-[*N'*-cyclohexyl-amino]ethane-sulfonic acid (CHES), 2-[*N'*-morpholino]ethane-sulfonic acid (MES), *N'*-tris[hydroxymethyl] methyl-3-amino-propane-sulfonic acid (TAPS), and sodium acetate with 0.1 M NaCl as supporting

electrolyte (HEPES, MES, CHES, TAPS, and sodium acetate from Sigma and USB, NaCl from VWR). Solutions were adjusted to the desired experimental pH with either NaOH or HCl. The experimental conditions for each experiment are indicated in the figure legend. Gas mixtures were purchased from Praxair and used as received. Enzyme films were prepared by first abrading the graphite surface with fine emery paper (Norton, P500J) followed by briefly polishing the electrode with a 1 μm aqueous alumina (Buehler) slurry and thorough sonication in water with rinsing. A 25 μL enzyme solution (~0.3 mg/mL) was then pipetted onto the electrode surface and left undisturbed for 120 s, followed by removal of the enzyme solution by pipette and rinsing of the electrode surface with water. All electrochemical experiments were conducted using a three-electrode system consisting of a pyrolytic graphite rotating disk working electrode, a platinum wire auxiliary electrode and a Ag/AgCl reference electrode. The electrode rotation rate was 3600 rpm and, for cyclic voltammetry experiments, the potential scan rate was 10 mV s^{-1} unless otherwise indicated. Temperature-controlled experiments were conducted using a water-jacketed electrochemical cell connected to a temperature-controlled water bath. The gas composition of the experimental cell was precisely controlled via a gas line placed directly above the electrochemical cell solution.

Results

Oxygen tolerance of proton reduction

Many [NiFe]-hydrogenases possess the ability to reduce H^+ to H_2 in the presence of small amounts of O_2. In fact, this activity may be present in both “oxygen-tolerant” hydrogenases as well as in “standard” hydrogenases which display little or no tolerance

to oxygen during enzymatic H_2-oxidization.[1, 20, 22-24] To evaluate whether *Pf*SHI has this proton reduction activity, an experiment similar to that conducted by McIntosh and co-workers was conducted.[1] As shown in Figure 4-1A, the electrode with a film of adsorbed *Pf*SHI was held at a constant reducing potential (-563 mV vs. SHE) throughout the experiment, and the gas composition of the atmosphere above the cell was changed to vary the proton reduction activity. In the first part of the experiment, the gas composition was 100% N_2, and the negative reduction current observed can be attributed exclusively to enzymatic reduction of H^+ to H_2. Proton reduction by [NiFe]-hydrogenases is ordinarily strongly product inhibited by hydrogen.[1] Figure 4-1A shows that at 25 °C exchanging the nitrogen atmosphere for a hydrogen atmosphere results in a loss of *ca.* 75% of the reductive current, indicating that *Pf*SHI is strongly product inhibited under these conditions. Returning the atmosphere to nitrogen results in an increase in reductive current, demonstrating that the inhibition is reversible. The gas stream was then switched to 1% O_2/99% N_2, and a dramatic increase in reduction current results from direct reduction of O_2 on the PGE electrode surface. To determine the amount of reductive current attributable to enzymatic H^+-reduction by the *Pf*SHI under these conditions, the gas was switched to 1% O_2/99% H_2 to inhibit specifically only enzymatic catalysis. As indicated by the red line in Figure 4-1, the catalytic current decreased by approximately 0.64 μA; this current can be directly attributed to H^+-reduction by *Pf*SHI in 1% O_2. Replacement of the atmosphere with 1% O_2/99% N_2 demonstrates the inhibition is reversible and removal of O_2 by switching back to 100% N_2 shows that the initial activity of the film was still observable. The initial H^+-reduction current is approximately

0.774 μA, so the approximately 0.641 μA of enzymatic H^+-reduction observed in 1% O_2 indicates that *Pf*SHI maintained at least 83% of its reductive activity in 1% O_2.

Proton reduction in 1% O_2 at higher temperatures

Since *Pyrococcus furiosus* is a hyperthermophile, it offers a unique opportunity to evaluate the impact of temperature on catalytic activities, and catalysis by *Pf*SHI at elevated temperatures is of great interest. Experiments analogous to that described above were conducted at 45 and 80 ºC to determine the effect of temperature on the enzyme's ability to catalytically reduce protons in the presence of oxygen (Figures 4-1B and 4-1C). In the first part of each experiment, exchanging the nitrogen atmosphere for a hydrogen atmosphere results in a loss of reductive current indicating that *Pf*SHI is product inhibited under these conditions. However, it is clear that the amount of product inhibition decreases with increasing temperature (Figure 4-2, open squares). While 73% of the proton reduction current from *Pf*SHI was inhibited by a hydrogen atmosphere at 25 ºC, only 48% and 28% of total reductive current was inhibited by hydrogen at 45 ºC and 80 ºC, respectively. To ensure that this decrease in the efficacy of hydrogen as an inhibitor was not due to decreased hydrogen concentration in the solution, we also evaluated the concentration of hydrogen as a function of temperature. As shown in Figure 4-3, the amount of H_2 dissolved in an aqueous solution under 1 atm of pressure does decrease marginally with temperature until approximately 60 ºC above which it levels out and then begins to increase with increasing temperature. Thus, a lower H_2 concentration in solution at higher temperatures cannot explain the decrease in inhibition.

Since product inhibition of the enzyme's H^+-reduction activity is no longer near complete at high temperatures, it is not a reliable direct metric for the amount of enzymatic H^+-reduction occurring in the presence of oxygen. Thus we sought to find an alternative approach to deconvolute current attributable to enzymatic proton reduction from direct electrode reduction of oxygen at higher temperatures. Figure 4-2 shows the effectiveness of hydrogen as an inhibitor in anaerobic conditions (open squares) determined as described above. Additionally, the effectiveness of hydrogen as an inhibitor under *aerobic* conditions was determined (closed diamonds) by assuming that enzymatic proton reduction continued under aerobic conditions at the same rate as anaerobic conditions. Assuming an error in these values of approximately 10%, Figure 4-2 shows that, with the assumption of constant catalytic activity, inhibition by hydrogen is unaffected by the presence of oxygen. Considered from the opposite perspective, assuming that the efficacy of hydrogen as an inhibitor is not impacted by oxygen, the observation that at each temperature the current inhibited by hydrogen is unchanged in anaerobic vs. aerobic conditions suggests that the overall catalytic activity was also unchanged. In short, it is likely that proton reduction by *Pf*SHI is virtually unaffected by 1% oxygen.

Discussion

We have demonstrated herein that *Pf*SHI maintains virtually all of its anaerobic proton reduction activity in the presence of 1% O_2 over the temperature range 25-80 ºC. Several other [NiFe]-hydrogenases have also been shown to produce hydrogen in the presence of oxygen: HoxEFUYH from *Synechocystis* sp. PCC 6803,[1] the membrane

bound hydrogenase from *Ralstonia eutropha* (*Re*MBH),[20] the [NiFeSe]-hydrogenase from *Desulfomicrobium baculatum*,[22] Hyd-2 from *Escherichia coli*, [23] and the standard [NiFe]-hydrogenase from *Desulfovibrio vulgaris* Miyazaki F.[24] Nonetheless, the activity of *Pf*SHI is a remarkable for two reasons. First, *Pf*SHI maintains more of its proton reduction activity, virtually all, in oxygen than the other [NiFe]-hydrogenases described to date. Second, unlike most of the [NiFe]-hydrogenases that have been experimentally characterized, *Pf*SHI is biased towards H^+-reduction rather than H_2 oxidation.[25] In fact, *Pf*SHI evolves H_2 at rates comparable to those of [FeFe]-hydrogenases, which are traditionally considered to be the more efficient H_2 producers.[25] Thus, *Pf*SHI is a viable candidate for use in hydrogen production applications.

The ability of *Pf*SHI to aerobically produce H_2 is likely related to its mechanism for O_2-tolerance. For group 1 [NiFe]-hydrogenases, it has been hypothesized that oxygen-tolerance arises from the ability to completely reduce the attacking O_2 molecule, thus preventing the accumulation of the slowly-reactivating Ni-A inactive state and preferentially forming the quickly-reactivating Ni-B inactive state.[7, 10, 12, 13] In so doing, the enzyme is able to resist long-term inactivation by O_2 attack, and instead is able to quickly recover to its catalytically active state as soon as the enzyme is reduced. This reactivity is thought to be linked to the [4Fe3S] cluster found proximal to the [NiFe]-site. Since H^+-reduction occurs at reducing potentials under which the active site is thought to be reduced, limited "O_2-tolerance" is exhibited by many [NiFe]-hydrogenases during H^+-reduction, despite many of these enzymes not being inherently tolerant to O_2. However, although "standard" [NiFe]-hydrogenases retain a portion of their H^+-reducing activity under O_2, *Pf*SHI is able to maintain virtually all of its H^+-reducing ability in the

presence of O_2. Two hypotheses may explain this observation. First, under reducing conditions, *Pf*SHI may be particularly efficient in complete reduction of oxygen to water or, second, oxygen may simply not bind well to the active site (high K_i). Future work may explore these two new directions.

It is interesting to consider why the inhibition constant for hydrogen seems to be so strongly dependent on temperature. Fourmond and coworkers have hypothesized that inhibition of proton reduction by hydrogen is a result not of active site chemistry but of crowding of the gas channels within the enzyme with hydrogen molecules. If this model is correct, increased temperature might be expected to lead to faster dynamics of the protein structure, faster diffusion, and increased opportunities for these trapped molecules to escape. Thus the inhibition constant (K_i) for hydrogen should become larger with increased temperature. Our observation herein that hydrogen is a less effective inhibitor of *Pf*SHI at elevated temperatures is consistent with this model. Furthermore, if the mechanism is general, then it is likely the case that hydrogen is not a good inhibitor of hydrogenases at the temperatures that are physiologically relevant for thermophiles and hyperthermophiles; this may have relevance for bidirectionality of the enzyme and function within the organism.

Two areas present themselves as obvious future directions for this work. First, although hydrogen is not a good inhibitor, CO or CN^- might prove to be more effective. Experiments analogous to those presented here could be attempted using these or other alternative inhibitors, and more quantitative data may be obtained. Second, since *Pf*SHI is resistant to 1% oxygen, it is natural to ask if it may also function in higher concentrations of oxygen. This may prove a particularly challenging question to address because the

current resulting from direct reduction of oxygen at the electrode surface is expected to increase dramatically at higher oxygen concentrations while hydrogenase activity will stay flat or decrease. Deconvoluting the two contributions under such conditions would likely prove extremely difficult.

Figures

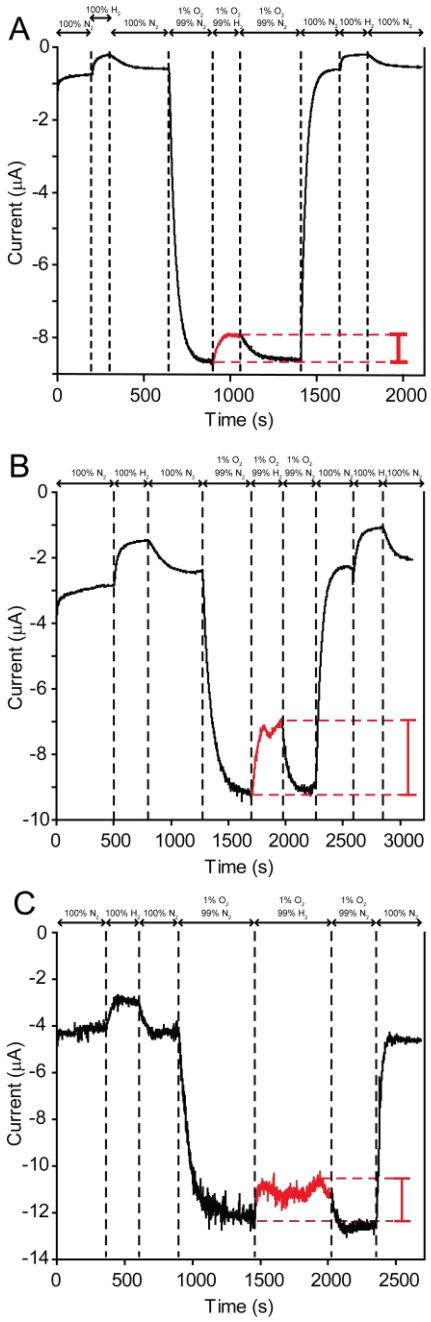


Figure 4-1. Catalytic chronoamperograms showing H^+ reduction by *Pf*SHI in the presence of 1% O_2. Experiments were undertaken at 25 ºC (A), 45 ºC (B), and 80 ºC (C) and pH 6.4. The electrode potential was held at -563 mV vs. SHE and the electrode rotation rate at 3600 rpm. The gas composition above the electrochemical cell was changed as indicated above the graph. The red line in brackets indicates the amount of H^+ reduction current inhibited by introduction of hydrogen in the presence of 1% O_2.

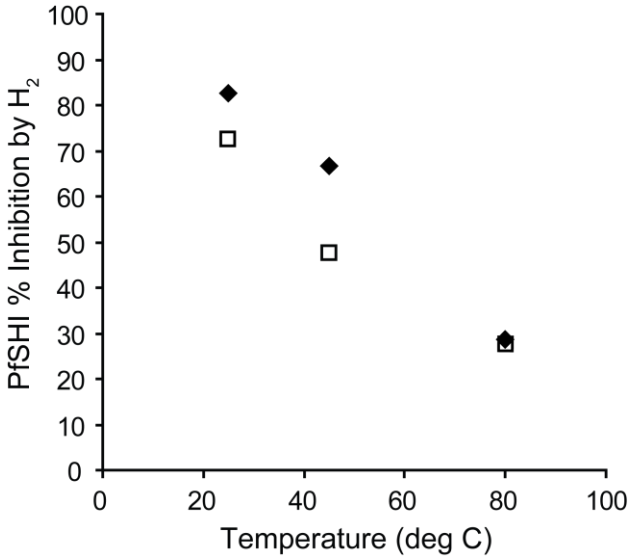


Figure 4-2. Effect of temperature on inhibition of *Pf*SHI H^+-reduction activity by H_2 under anaerobic conditions (□) and aerobic conditions (♦). Data is derived from chronoamperometry experiments shown in Figure 1. For anaerobic conditions, the % inhibition by H_2 is defined as the change in current observed when switching from 100% N_2 to 100% H_2 divided by the initial current magnitude measured under 100% N_2. For aerobic conditions, the % inhibition by H_2 is defined as the change in current observed when switching from 1% O_2/99% N_2 to 1% O_2/99% H_2 (red bracket) divided by the initial current magnitude measured under 100% N_2.

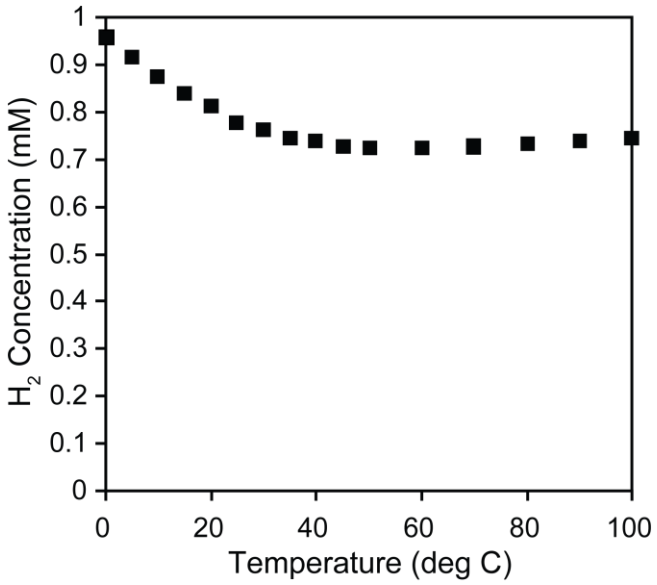


Figure 4-3. Aqueous H_2 concentration under 1 atm of H_2 vs Temperature. H_2 concentrations were determined using Henry's Law, according to Perry's Chemical Engineers' Handbook, Eighth Edition.[26]

References

1. McIntosh, C.L., Germer, F., Schulz, R., Appel, J. & Jones, A.K. The [NiFe]-hydrogenase of the cyanobacterium *Synechocystis* sp. PCC 6803 works bidirectionally with a bias to H_2 production. *J. Am. Chem. Soc.* **133**, 11308-11319 (2011).

2. Jones, A.K., Lamle, S.E., Pershad, H.R., Vincent, K.A., Albracht, S.P.J. & Armstrong, F.A. Enzyme electrokinetics: electrochemical studies of the anaerobic interconversions between active and inactive states of *Allochromatium vinosum* [NiFe]-hydrogenase. *J. Am. Chem. Soc.* **125**, 8505-8514 (2003).

3. Goldet, G., Brandmayr, C., Stripp, S.T., Happe, T., Cavazza, C., Fontecilla-Camps, J.C. & Armstrong, F.A. Electrochemical kinetic investigations of the reactions of [FeFe]-hydrogenase with carbon monoxide and oxygen: comparing the importance of gas tunnels and active-site electronic/redox effects. *J. Am. Chem. Soc.* **131**, 14979-14989 (2009).

4. Lamle, S.E., Albracht, S.P.J. & Armstrong, F.A. Electrochemical potential-step investigations of the aerobic interconversions of [NiFe]-hydrogenase from *Allochromatium vinosum*: Insights into the puzzling difference between unready and ready oxidized inactive states. *J. Am. Chem. Soc.* **126**, 14899-14909 (2004).

5. Lenz, O., Ludwig, M., Schubert, T., Burstel, I., Ganskow, S., Goris, T., Schwarze, A. & Friedrich, B. H_2 Conversion in the Presence of O_2 as Performed by the Membrane-Bound [NiFe]-Hydrogenase of *Ralstonia eutropha*. *ChemPhysChem* **11**, 1107-1119 (2010).

6. Vincent, K.A., Parkin, A., Lenz, O., Albracht, S.P.J., Fontecilla-Camps, J.C., Cammack, R., Friedrich, B. & Armstrong, F.A. Electrochemical definitions of O_2 sensitivity and oxidative inactivation in hydrogenases. *J. Am. Chem. Soc.* **127**, 18179-18189 (2005).

7. Pandelia, M.-E., Fourmond, V., Tron-Infossi, P., Lojou, E., Bertrand, P., Léger, C., Giudici-Orticoni, M. & Lubitz, W. Membrane-bound hydrogenase I from the hyperthermophilic bacterium *Aquifex aelicus*: Enzyme activation, redox intermediates and oxygen tolerance. *J. Am. Chem. Soc.* **132**, 6991-7004 (2010).

8. Pandelia, M.-E., Nitschke, W., Infossi, P., Giudici-Orticoni, M.T., Bill, E. & Lubitz, W. Characterization of a unique [FeS] cluster in the electron transfer chain

of the oxygen tolerant [NiFe] hydrogenase from *Aquifex aeolicus*. *Proc. Nat. Acad. Sci. U.S.A.* **108**, 6097-6102 (2011).

9. Lukey, M.J., Parkin, A., Roessler, M.M., Murphy, B.J., Harmer, J., Palmer, T., Sargent, F. & Armstrong, F.A. How *Escherichia coli* is equipped to oxidize hydrogen under different redox conditions. *J. Biol. Chem.* **285**, 3928-3938 (2010).

10. Lukey, M.J., Roessler, M.M., Parkin, A., Evans, R.M., Davies, R.A., Lenz, O., Friedrich, B., Sargent, F. & Armstrong, F.A. Oxygen-Tolerant [NiFe]-Hydrogenases: The Individual and Collective Importance of Supernumerary Cysteines at the Proximal Fe-S Cluster. *J. Am. Chem. Soc.* **133**, 16881-16892 (2011).

11. Shomura, Y., Yoon, K.S., Nishihara, H. & Higuchi, Y. Structural basis for a [4Fe-3S] cluster in the oxygen-tolerant membrane-bound [NiFe]-hydrogenase. *Nature* **479**, 253-256 (2011).

12. Volbeda, A., Martin, L., Cavazza, C., Matho, M., Faber, B.W., Roseboom, W., Albracht, S.P.J., Garcin, E., Rousset, M. & Fontecilla-Camps, J.C. Structural differences between the ready and unready oxidized states of [NiFe] hydrogenases. *J. Biol. Inorg. Chem.* **10**, 239-249 (2005).

13. Ogata, H., Kellers, P. & Lubitz, W. The crystal structure of the [NiFe] hydrogenase from the photosynthetic bacterium *Allochromatium vinosum:* Characterization of the oxidized enzyme (Ni-A state). *J. Mol. Biol.* **402**, 428-444 (2010).

14. Fritsch, J., Scheerer, P., Frielingsdorf, S., Kroschinsky, S., Friedrich, B., Lenz, O. & Spahn, C.M.T. The crystal structure of an oxygen-tolerant hydrogenase uncovers a novel iron-sulphur centre. *Nature* **479**, 249-252 (2011).

15. Goris, T., Wait, A.F., Saggu, M., Fritsch, J., Heidary, N., Stein, M., Zebger, I., Lendzian, F., Armstrong, F.A., Friedrich, B. & Lenz, O. A unique iron-sulfur cluster is crucial for oxygen tolerance of a [NiFe]-hydrogenase. *Nat. Chem. Biol.* **7**, 310-318 (2011).

16. Gust, D., Moore, T.A. & Moore, A.L. Solar Fuels via Artificial Photosynthesis. *Accounts Chem. Res.* **42**, 1890-1898 (2009).

17. Lubner, C.E., Applegate, A.M., Knorzer, P., Ganago, A., Bryant, D.A., Happe, T. & Golbeck, J.H. Solar hydrogen-producing bionanodevice outperforms natural photosynthesis. *Proc. Natl. Acad. Sci. U.S.A.* **108**, 20988-20991 (2011).

18. Melis, A. & Happe, T. Hydrogen production. Green algae as a source of energy. *Plant Physiol.* **127**, 740-748 (2001).

19. Ghirardi, M., Posewitz, M.C., Maness, P.-C., Dubini, A., Yu, J. & Seibert, M. Hydrogenases and hydrogen photoproduction in oxygenic photosynthetic organisms. *Annu. Rev. Plant Biol.* **58**, 71-91 (2007).

20. Goldet, G., Wait, A.F., Cracknell, J.A., Vincent, K.A., Ludwig, M., Lenz, O., Friedrich, B. & Armstrong, F.A. Hydrogen production under aerobic conditions by membrane-bound hydrogenases from *Ralstonia* species. *J. Am. Chem. Soc.* **130**, 11106-11113 (2008).

21. Ma, K.S. & Adams, M.W.W. Hydrogenase I and II from *Pyrococcus furiosus*. *Method Enzymol.* **331**, 208-216 (2001).

22. Parkin, A., Goldet, G., Cavazza, C., Fontecilla-Camps, J.C. & Armstrong, F.A. The Difference a Se Makes? Oxygen-Tolerant Hydrogen Production by the [NiFeSe]-Hydrogenase from *Desulfomicrobium baculatum*. *J. Am. Chem. Soc.* **130**, 13410-13416 (2008).

23. Lukey, M.J., Parkin, A., Roessler, M.M., Murphy, B.J., Harmer, J., Palmer, T., Sargent, F. & Armstrong, F.A. How *Escherichia coli* Is Equipped to Oxidize Hydrogen under Different Redox Conditions. *J. Biol. Chem.* **285**, 3928-3938 (2010).

24. Shafaat, H.S., Rudiger, O., Ogata, H. & Lubitz, W. [NiFe] hydrogenases: A common active site for hydrogen metabolism under diverse conditions. *Biochim. Biophys. Acta* **1827**, 986-1002 (2013).

25. Bryant, F.O. & Adams, M.W.W. Characterization of Hydrogenase from the Hyperthermophilic Archaebacterium, *Pyrococcus furiosus*. *J. Biol. Chem.* **264**, 5070-5079 (1989).

26. Green, D. & Perry, R. Perry's Chemical Engineers' Handbook, Eighth Edition (McGraw-Hill Education, 2007).

Chapter 5

Interaction of Soluble, Group 3 [NiFe]-hydrogenases and Oxygen: A New Type of Oxygen-tolerance

Patrick Kwan,[†] Michael W.W. Adams[‡], and Anne K. Jones[†]

[†]Department of Chemistry and Biochemistry,

Arizona State University, Tempe, AZ 85287;

[‡]Department of Biochemistry,

The University of Georgia, Athens, GA 30602

Abstract

We report the first direct electrochemical characterization of the impact of oxygen on the hydrogen oxidation activity of an oxygen-tolerant, group 3, soluble [NiFe]-hydrogenase: the soluble hydrogenase I from *Pyrococcus furiosus* (*Pf*SHI). Chronoamperometric experiments were used to probe the sensitivity of *Pf*SHI hydrogen oxidation activity to both brief and prolonged exposure to oxygen. For experiments between 15 and 80 ºC, following short (< 200 s) exposure to 14 μM O_2 under oxidizing conditions, PfSHI always maintains some fraction of its initial hydrogen oxidation activity, *i.e.* it is oxygen-tolerant. Reactivation experiments show that two inactive states are formed by interaction with oxygen and both can be quickly (< 150 s) reactivated. Analogous experiments, in which the interval of oxygen exposure is extended to 900 s show a response that is highly temperature dependent. At 25 ºC, under sustained 1% O_2/ 99% H_2 exposure, the H_2-oxidation activity drops nearly to zero. However, at 80 ºC, up to 32% of the enzyme's oxidation activity is retained. Reactivation of *Pf*SHI following sustained exposure to oxygen occurs on a much longer time scale (10s of minutes), suggesting that a third inactive species predominates under these conditions. These results stand in contrast to the properties of oxygen-tolerant, group 1 [NiFe]-hydrogenases which form a single state upon reaction with oxygen. Furthermore, group 3 [NiFe]-hydrogenases do not possess the proximal [4Fe-3S] cluster associated with the oxygen-tolerance of some group 1 enzymes. Thus a new mechanism is necessary to explain oxygen-tolerance in soluble, group 3 [NiFe]-hydrogenases.

Introduction

Hydrogenases, the enzymes that catalyze H^+/H_2 interconversion, have received widespread attention as models for multielectron redox catalysis at non-precious metal ([FeFe]- or [NiFe]-) active sites.[1-7] Although the high catalytic rates of these enzymes make them technologically appealing,[8-10] the active sites are usually extremely sensitive to redox potential as well as small molecule inhibitors such as oxygen and carbon monoxide, limiting their technological utility.[11-13] In this respect, they are similar to many other energetically important redox metalloenzymes including nitrogenases and some formate dehydrogenases.[14-19]

Compared to the irreversible inactivation of many metalloenzymes by oxygen, [NiFe]-hydrogenases are less sensitive to oxygen since they are reversibly inactivated.[11, 20-22] [NiFe]-hydrogenases are often divided into two categories based on reactivity with oxygen: standard and oxygen-tolerant.[23] Standard [NiFe]-hydrogenases, such as Hyd-2 from *E coli*, *Desulfovibrio fructosovorans* [NiFe]-hydrogenase (*Df*Hase), and the *Allochromatium vinosum* membrane-bound hydrogenase, are reversibly inactivated by exposure to oxygen to form a mixture of two distinct, inactive states referred to as ready and unready, or Ni-B and Ni-A, respectively. Reactivation of Ni-B occurs on a timescale of seconds whereas reactivation of Ni-A requires more prolonged exposure to reductive conditions.[11, 24-30] A second group, called "oxygen-tolerant" [NiFe]-hydrogenases, has been identified based on their ability to maintain some hydrogen oxidation activity for extended periods in the presence of oxygen. This group includes such enzymes as the MBHs from *Ralstonia eutropha* (*Re*MBH),[20, 31] *Aquifex aeolicus*,[32, 33] *Escherichia coli*,[34, 35] and *Hydrogenovibrio marinus*.[36, 37] These hydrogenases are believed to resist

inactivation by oxygen by forming only the Ni-B state of the active site in the presence of oxygen and by having a relatively high reduction potential for reactivation. This resistance to formation of Ni-A has been hypothesized to arise from the ability to reduce attacking oxygen completely with four electrons and prevent formation of any partially reduced blocking species.[27, 28, 32, 35] In support of this hypothesis, *Re*MBH and *E. coli* Hyd-1 have been shown to be able to reduce oxygen to form water.[38, 39]

Although early research suggested that oxygen-tolerance might arise from restricted access of oxygen to the active site,[40-44] more recent evidence has led to the hypothesis that interactions between the active site and the adjacent [FeS] clusters that provide reducing equivalents from external partners are the main factors controlling oxygen-tolerance. X-ray crystal structures determined from three oxygen-tolerant MBHs from different biological sources revealed a [4Fe-3S] cluster proximal to the hydrogen-activating site. This cluster is thought to be stable in the 3+, 2+ and 1+ oxidation states under physiological conditions.[33, 36, 45-51] This capacity to take up two electrons may be key to quickly and simultaneously providing multiple electrons to the active site to reduce oxygen and prevent formation of the "unready" state. Lending further support to this hypothesis, the unusual cluster is coordinated by a six cysteine-containing primary sequence motif that is highly conserved among oxygen-tolerant MBHs.[46, 52, 53] Similarly, based on the decreased oxygen-tolerance of site-directed mutants, the medial [3Fe-4S] cluster of E coli Hyd-1 has also been hypothesized to play a role in oxygen-tolerance.[54] This may be explained by the relatively high reduction potential of the $[3Fe\text{-}4S]^{+/0}$ couple which leaves this cluster reduced, *i.e.* with an electron available to donate to the active site, under most physiologically relevant conditions. Nonetheless, it is difficult to

understand how the [3Fe-4S] cluster can play a defining role since most uptake [NiFe]-hydrogenases, also the oxygen sensitive ones, possess this type of medial cluster. Finally, replacing a non-metal coordinating valine (74) located between the active site and the proximal cluster with a cysteine in the *Df*Hase enzyme created a more oxygen-tolerant enzyme without affecting the reduction potentials of the proximal cluster.[55, 56] This suggests that the protein matrix between the active site and the proximal cluster also plays a crucial role in oxygen-tolerance, perhaps by modulating electronic coupling between the cofactors.

Although [NiFe]-hydrogenases are phylogenetically divided into four diverse groups, the majority of mechanistic studies have utilized enzymes from group 1, enzymes associated physiologically with hydrogen oxidation to provide reducing equivalents to power cellular metabolism.[57] On the other hand, group 3 [NiFe]-hydrogenases, soluble enzymes that are sometimes referred to as bidirectional, couple oxidation of hydrogen to reduction of the pyridine nucleotides NAD^+ or $NADP^+$ at a flavin active site.[58] Unlike group 1 hydrogenases, which are usually isolated as heterodimers consisting of the large hydrogen-activating subunit and the small [FeS]-containing subunit, SHs are heteromultimeric enzymes containing not only the dimeric hydrogenase component but also the multimeric, flavin-containing diaphorase. Previous studies have shown that the soluble [NiFe]-hydrogenases (SH) of *R. eutropha* (*Re*SH) and from *Pyrococcus furiosus* (*Pf*SHI) are, to some extent, oxygen-tolerant, *i.e.* they maintain activity for extended periods in solution assays in the presence of oxygen.[59-61] However, these bidirectional enzymes do not possess the additional cysteine residues near the proximal cluster that have come to be the hallmark of oxygen tolerant group 1 [NiFe]-hydrogenases. This

makes them unlikely to have a modified proximal [FeS] cluster and raises the question of how oxygen tolerance is achieved in SHs.

Protein film electrochemistry (PFE), a technique in which a redox protein is functionally adsorbed to an electrode and electron transfer reactions can be observed without a chemical mediator,[62] has proven invaluable for characterizing the differences in the reactivity of oxygen-sensitive and oxygen-tolerant group 1 [NiFe]-hydrogenases.[11, 13, 63-66] The main advantage of PFE over solution assays is that the need for mediators, redox active molecules that themselves usually react with oxygen, can be eliminated, and the catalytic activity at precisely defined electrochemical potential and solution conditions can be directly monitored as current. Nonetheless, only two SHs have been characterized using PFE: the soluble hydrogenase subcomplex from *Ralstonia eutropha* (*Re*HoxHY) and the holoenzyme SH from *Synechocystis* sp. PCC6803 (*Syn*SH).[60, 67] Both of these enzymes proved oxygen-sensitive. Thus, the reactions of an oxygen-tolerant SH have not yet been characterized using this technique.

In this chapter, we present the first investigation via PFE of the reactions of oxygen with an oxygen-tolerant, soluble, group 3 [NiFe]-hydrogenase, *Pf*SHI. The hyperthermophilic *P. furiosus* grows at temperatures *ca.* 100 ºC in its native environment, and, as such, the electrocatalytic characteristics of *Pf*SHI have been investigated at both high and low temperatures. Experiments wherein the enzyme is subjected to both short- and long-term O_2 exposure have also been conducted to study the kinetics of inactivation and reactivation in the enzyme. We show that, unlike oxygen-tolerant, group 1 [NiFe]-hydrogenases that inactivate to form a single state, following transient exposure to oxygen, *Pf*SHI reacts with oxygen to form two distinct states that are distinguished by the

electrochemical potential required to reactivate them. This is the first demonstration that oxygen tolerance and formation of a single inactive state are not mutually inclusive. Furthermore, prolonged exposure to oxygen, especially at high temperature, forms an additional, slowly reactivating state not previously described. The properties of *Pf*SHI are compared to both oxygen-tolerant and oxygen-sensitive group 1 [NiFe]-hydrogenases as well as *Syn*SH, and possible mechanisms for oxygen tolerance in SHs are considered.

Materials and Methods

Purification of the enzyme was performed as previously described according to Ma, *et al*.[68] Protein film electrochemistry (PFE) was performed in an anaerobic glovebox as described by McIntosh, *et al*.[67] All chemicals were of the highest grade commercially available and were used without further purification. Solutions for electrochemical experiments were prepared using purified water (resistivity 18.2 MΩ cm^{-1}). The mixed buffer consisted of 15 mM each of 4-(2-hydroxyethyl)-1-piperazineethane-sulfonic acid (HEPES), 2-[*N'*-cyclohexyl-amino]ethane-sulfonic acid (CHES), 2-[*N'*-morpholino]ethane-sulfonic acid (MES), *N'*-tris[hydroxymethyl] methyl-3-amino-propane-sulfonic acid (TAPS), and sodium acetate with 0.1 M NaCl as supporting electrolyte (HEPES, MES, CHES, TAPS, and sodium acetate from Sigma and USB, NaCl from VWR). Solutions were adjusted to the desired experimental pH with either NaOH or HCl. The experimental conditions for each experiment are indicated in the figure legend. Gas mixtures were purchased from Praxair and used as received. Enzyme films were prepared by first abrading the graphite surface with fine emery paper (Norton, P500J) followed by briefly polishing the electrode with a 1 μm aqueous alumina (Buehler) slurry

and thorough sonication in water with rinsing. A 25 μL enzyme solution (~0.3 mg/mL) was then pipetted onto the electrode surface and left undisturbed for 120 seconds, followed by removal of the enzyme solution by pipette and rinsing of the electrode surface with water. All electrochemical experiments were conducted using a three-electrode system consisting of a pyrolytic graphite rotating disk working electrode, a platinum wire auxiliary electrode and a Ag/AgCl reference electrode. The electrode rotation rate was 3600 rpm and for cyclic voltammetry experiments, the potential scan rate was 10 mV s^{-1} unless otherwise indicated. Temperature-controlled experiments were conducted using a water-jacketed electrochemical cell connected to a temperature-controlled water bath. The electrochemical data were analyzed with SOAS, an electrochemical program freely available for download on the web at http://bip.cnrs-mrs.fr/bip06/software.html.[69]

Results

Hydrogen oxidation by PfSHI displays oxygen-tolerance

Prototypical, oxygen-sensitive [NiFe]-hydrogenases are known to be inactivated by both oxidative anaerobic and aerobic conditions. In contrast, oxygen-tolerant [NiFe]-hydrogenases distinguish themselves from the standard enzymes by maintaining, albeit often at a lower rate, hydrogen oxidizing activity, even in the presence of oxygen.[32, 54, 70] Chronoamperometry experiments (Figure 5-1A) were used to probe the effects of oxygen on the hydrogen-oxidation activity of *Pf*SHI and the dependence of reactivation from an inactive, oxidized state on electrochemical potential. Figure 5-1A shows that exposure of a *Pf*SHI film oxidizing H_2 at +197 mV to oxygen results in an immediate

decrease in the catalytic current. Importantly, although the catalytic current drops dramatically, it does not reach zero. Instead it decreases to a stable lower value and then slowly increases as the oxygen diffuses out of the electrochemical cell, indicating spontaneous regeneration of catalytic activity. This behavior is in stark contrast to that of standard [NiFe]-hydrogenases which exhibit a sharp drop to zero without any subsequent increase in activity (see, for example, Figure 5 in Ref [67]).

Reactivation following brief exposure to oxygen reveals two inactive states

Standard [NiFe]-hydrogenases are oxidatively inactivated to two distinct states that are distinguished by their kinetics of reactivation: Ni-A and Ni-B. Although Ni-B is reactivated on the timescale of seconds to minutes following a return to reductive conditions, Ni-A requires reduction for tens of minutes before regaining activity.[11, 24-30] On the other hand, oxygen-tolerant enzymes have been shown to form only one inactive state, akin to Ni-B. We have shown previously that the oxygen-sensitive *Syn*SH inactivates to form two states, both of which can be *quickly* reactivated.[67] To probe the inactive states formed by *Pf*SHI, we explored its ability to be reductively reactivated following exposure to oxygen.

As shown in Figure 5-1A, following brief exposure of the enzyme to 14 μM oxygen, the potential of the electrochemical experiment was dropped to more reducing values for 150 s to initiate reactivation. The potential was then returned to +197 mV to observe the resulting hydrogen oxidizing activity. Figure 5-1B shows that at 15 ºC the extent of reactivation (i_2/i_1, where i_2 is the current 300 s after reactivation and i_1 is the current preceding exposure to O_2) of the enzyme depends on the potential of the reductive

pulse in a Nernstian fashion. At less reducing reactivation potentials, less catalytic activity was regenerated. At more reductive potentials, more activity was regained. This suggests that reactivation is a reduction process.

The reactivation data shown in Figure 5-1B could be fit to a linear combination of two one-electron Nernstian processes. Due to the oxygen tolerance of *Pf*SHI, even at the highest reactivation potentials, some H_2 oxidation activity remained. Thus, to facilitate fitting the data, each data set was normalized into the range 0-1, *i.e.* the lowest value is zero and highest value is 1, according to the following formula:

$$NV = \frac{(V - V_{min})}{(V_{max} - V_{min})} \quad \textbf{[1]}$$

where NV is the normalized value, V is the unnormalized fraction reactivated value, V_{min} is the minimum measured fraction reactivated value (at high potentials) and V_{max} is the maximum measured fraction reactivated value (at low potentials). The data were then fit to a linear combination of two, one-electron Nernstian processes according to the following equation:

$$NV = PfSHI_{low}\left(\frac{1}{1+e^{\left(\frac{nF}{RT}(E-E_{low})\right)}}\right) + PfSHI_{high}\left(\frac{1}{1+e^{\left(\frac{nF}{RT}(E-E_{high})\right)}}\right) \quad \textbf{[2]}$$

where $PfSHI_{low}$ is the percentage (expressed as a decimal) of the adsorbed enzyme present in the low potential reactivating state, $PfSHI_{high}$ is the percentage (expressed as a decimal) of the adsorbed enzyme present in the high potential reactivating state, E_{low} is the apparent reduction potential of the low potential reactivating state, E_{high} is the apparent reduction potential of the high potential reactivating state, n is the number of electrons in the redox process and was fixed at 1, F is the Faraday constant, R is the ideal

gas constant, and T is the temperature in Kelvin. We note that this model ostensibly has four variable parameters, but since we have normalized the data set in the range 0-1, the percentage of enzyme in each of the two states must sum to 1. Thus, these two variables are not independent, and the data was fit using only three variables. The best fit at 15 ºC yields apparent reduction potentials of -366 mV and -116 mV with 83.4% and 16.6% of the inactive enzyme in each state, respectively.

Temperature dependence of reactivation

Since the electrocatalytic activity of *Pf*SHI is very sensitive to temperature (see Chapter 3), experiments were conducted at various temperatures between 15 ºC and 80 ºC to investigate the effect of temperature on the inactivation/reactivation of *Pf*SHI. Figure 5-1C shows representative data obtained at 80 ºC. At all temperatures, like at low temperature, the extent of reactivation depends on the potential of the reductive pulse in a Nernstian fashion. However, fits reveal a shift in the apparent reduction potentials of reactivation towards less reducing values at higher temperature. In fact, at temperatures $\geq$ 37 ºC, E_{high} is shifted outside the range of potentials conveniently probed in this experiment (Table 5-1 lists the reduction potentials and proportions of each state formed for all temperatures investigated).

Although E_{high} could not be determined over the entire temperature range of these experiments, Figure 5-1D shows the dependence of E_{low} on temperature. It is immediately clear that there is a particularly large shift to more positive potentials between 60 ºC and 80 ºC. Essentially, above 60 ºC, significantly less negative potentials are required to reactivate aerobically inactivated *Pf*SHI. Quantitatively, the apparent reactivation

potentials as a function of temperature can be fit by a sigmoidal equation with the following form:

$$E_{low}(T) = E_{low,l} + \frac{(E_{low,h} - E_{low,l})}{\left(1 + e^{-\frac{(T-T_0)}{w}}\right)} \quad \textbf{[3]}$$

$E_{low}(T)$ corresponds to the value of E_{low} at the temperature T in Kelvin. Four variable parameters were used to fit the data: (1) $E_{low,h}$, the value in mV *vs.* SHE that E_{low} approaches at high temperature; (2) $E_{low,l}$, the value in mV *vs.* SHE that E_{low} approaches at low temperatures; (3) T_0, the temperature in Kelvin at which $E_{low}(T)$ is the average of $E_{low,h}$ and $E_{low,l}$ and (4) w, a dimensionless width parameter describing how quickly the values shift between the two limits. The data are best fit with $E_{low,h}$ of 35 mV, $E_{low,l}$ of -355 mV, T_0 of 64 ºC, and w of 2.4.

H_2 oxidation during prolonged oxygen exposure

In addition to probing the response of *Pf*SHI to *transient* exposure to oxygen, we have also investigated the ability of the enzyme to perform catalysis in response to *prolonged* exposure to oxygen. Figure 5-2A shows a chronoamperometric trace demonstrating the impact of constant exposure to 1% oxygen for fifteen minutes on electrocatalytic hydrogen oxidation by *Pf*SHI at 25 ºC. Initially, the hydrogen oxidation activity was monitored at +197 mV under an atmosphere of 100% H_2. After establishing the level of catalytic activity, the gas in the experiment was switched to 1% O_2 in 99% N_2, and air-saturated buffer was simultaneously injected into the cell to achieve a final oxygen concentration of 14 μM. Exposure to 1% O_2 was continued for 900 s at which time the atmosphere was returned to 100% hydrogen. In addition to being exposed to

oxygen for a longer period in this experiment, the enzyme is also exposed to oxidizing conditions for a longer interval than during the transient exposure experiments. At the point at which oxygen was introduced into the experiment, the catalytic activity dropped quickly (~ 250 s) to zero, and the immobilized enzyme remained inactive until the experiment was returned to anaerobic conditions. Following the return to anaerobic conditions, a small (1.56 %) amount of catalytic activity was spontaneously regained without exposing the enzyme to more reducing conditions. To characterize the properties of the inactive states formed, the inactive enzyme film was then reduced at -563 mV, and the recovered hydrogen oxidation activity at +197 mV was subsequently monitored. As already described for the transiently aerobic experiments in the previous section, only a brief (150 s) excursion to reducing conditions was necessary to recover a large proportion (48.9 %) of the catalytic activity observed prior to exposure to oxygen.

Since the redox transitions of the active site of *Pf*SHI and its activity are relatively sensitive to temperature, experiments in the continuous presence of oxygen were also undertaken at 60 and 80 ºC. Figure 5-2C shows a representative chronoamperometric trace obtained at 80 ºC. Like the experiment at 25 ºC, at higher temperature, prolonged exposure to oxygen results in a rapid decrease in catalytic activity. However, the decrease in activity at high temperatures occurs over a longer time scale, and, most importantly, the final activity after 900 s of exposure to oxygen is not zero. Essentially, a lower, steady state catalytic activity is attained during the prolonged exposure to oxygen; the enzyme is not completely inactivated. For a collection of three independent experiments at 80 ºC, the final activity after exposure to oxygen was in the range of 6.5-32.2 % of the initial activity under anaerobic conditions (Figure 5-2C).

Similarly, at 60 ºC, up to 8% of the enzyme's initial activity was retained after 900 s of exposure to 1 % oxygen (Figure 5-2B). Thus we conclude that the proportion of *Pf*SHI that remains active after prolonged exposure to oxygen is directly related to the temperature of the experiment. More experiments will be necessary, however, to quantify this correlation. A second notable difference was uncovered by considering the reactivation of the enzyme. At 80 ºC, short (seconds or minutes) excursions to reducing potential resulted in only minimal reactivation. Instead, maximal reactivation, *circa* 30-35% of the pre-oxygen exposure activity level, was observed after 37.5 min of low-potential reactivation. This behavior is in contrast to both experiments in the sustained presence of oxygen at low temperature and experiments with transient exposure to oxygen at high temperatures. For example, at 25 ºC, only 2.5 minutes were required for maximal reactivation, resulting in approximately 50 % recovery of initial activity. Similarly, at 80 ºC, following transient exposure to 14 μM oxygen, maximal reactivation was observed after only a 150 s excursion to -563 mV. Thus the ratio of slowly reactivating inactive state formed at high temperature appears to also require prolonged exposure to oxygen or highly oxidizing conditions to induce formation.

Discussion

While both oxygen-tolerant and oxygen-sensitive group 1 [NiFe]-hydrogenases have been extensively studied using electrochemical methods, this is the first electrochemical characterization of the reactions with oxygen of an intact, *i.e.* containing both hydrogenase and diaphorase, oxygen-tolerant group 3 [NiFe]-hydrogenase (SH). Complete, heteromultimeric SH complexes have proven difficult to isolate, with

heterogeneous preparations often plagued by variable activities or instability.[60, 71-78] *Pf*SHI is a particularly appealing enzyme to use for these studies both because it comes from a hyperthermophilic organism, making it more stable than most SHs, and because it has been successfully heterologously expressed, allowing future access to site-directed mutant enzymes.[79] Herein, we compare the properties of *Pf*SHI with both group 1 [NiFe]-hydrogenases and the two other SHs that have been electrochemically characterized.

We have shown that *Pf*SHI adsorbed at a graphite electrode is oxygen-tolerant, *i.e.* it maintains a non-zero fraction of its hydrogen-oxidizing activity in the presence of oxygen. Furthermore, even without exposing the sample to reducing conditions, a small fraction of the lost activity is spontaneously regained upon removal of oxygen from the electrochemical experiment. By comparison, oxygen-sensitive, standard hydrogenases such as *Df*Hase rapidly lose all activity upon exposure to oxygen (see Figure 3 in Ref. [80]) and do not regain catalytic activity without exposure of the enzyme to reducing conditions. Similarly, *Syn*SH also loses all activity nearly instantaneously upon exposure to oxygen (see Figure 5 in Ref. [67]). The complete, bifunctional, oxygen-tolerant *Re*SH has not been electrochemically characterized, but its hydrogenase subdimer, *Re*HoxHY, was also shown to be quickly and completely inactivated by oxygen (see Figure 7 in Ref. [60]). The response of *Pf*SHI to exposure to oxygen is not only different from oxygen-sensitive enzymes but also from that of prototypical, oxygen-tolerant group 1 [NiFe]-hydrogenases. For example, both *E. coli* Hyd-1 (see Figure 5 in Ref. [54]) and Hase I from *Aquifex aeolicus* (see Figure 6 in Ref. [32]) maintain a significantly higher fraction of their

oxidizing activity upon exposure to oxygen than *Pf*SHI *and* spontaneously regain most of their activity upon removal of the oxygen from the experiment.

The effect of oxygen on the hydrogen oxidation activity of *Pf*SHI is most similar not to another wild-type hydrogenase but to oxygen-tolerant mutants of *Df*Hase.[56, 80, 81] Wild-type *Df*Hase is completely unable to recover from transient oxygen exposure at oxidizing potentials, but mutations of V74 confer the ability to oxidatively regenerate up to 60% of H_2-oxidation activity at 40 ºC.[56] Electrochemical experiments conducted with *Pf*SHI under similar conditions, *i.e.* 45 ºC, pH 6.4, (Figure 5-3), demonstrate recovery of 25% of its H_2-oxidation activity at oxidizing potential, which closely resembles the O_2-tolerance behavior of the V74P mutant. The *D. fructosovorans* results are important primarily for two reasons. First, they demonstrate that an oxygen-sensitive enzyme can be made oxygen-tolerant. Second, they show that a *range* of oxygen-tolerance can be established via mutagenesis. The *Pf*SHI results expand these conclusions by showing that a similar spectrum of oxygen-tolerance already exists for wild-type [NiFe]-hydrogenases; *Pf*SHI is somewhere in the middle of this natural spectrum. Thus oxygen-tolerance should not be thought of as a dichotomous, but rather a continuous, property.

Current models suggest that oxygen-tolerance in group 1 [NiFe]-hydrogenases is achieved by exclusive formation of the Ni-B state upon reaction of the active site with oxygen,[33, 35, 54, 82] but our studies of the reactivation of oxygen-inactivated *Pf*SHI show that it is oxygen-tolerant *and* forms two, distinct oxygen-inactivated states. These states have different reactivation kinetics or thermodynamics, or perhaps even both. Initially, this result may not appear to be surprising since [NiFe]-hydrogenases have long been known to be oxidized to two inactive states: Ni-B (also known as Ni-ready) and Ni-A

(also known as Ni-unready). Furthermore, previous work with the oxygen-sensitive *Df*Hase showed that both of these states can be formed by exposure to either anaerobic or aerobic oxidizing conditions.[25] However, the properties of Ni-A and Ni-B do not correspond to those of the *Pf*SHI inactive states detected in our experiments. Ni-A is defined not only by a characteristic EPR signal but also by a requirement for exposure of the inactivated enzyme to reducing conditions for extended periods of time (often tens of minutes, see Ref [83] and [84]) before catalytic activity is regained. On the other hand, inactivation of *Pf*SHI by transient exposure to oxygen creates two states, both of which can be reactivated on the time scale of seconds. Furthermore, Ni(III) based EPR signals have not been detected for the oxidized, inactive states of *Pf*SHI or any other SH. Thus the nature of these oxygen-inactivated states of SHs is still very much an open question, and we will return to it after discussing also the states formed following sustained exposure of *Pf*SHI to oxygen. Here, we note only that our previous electrochemical characterization of *Syn*SH also showed that two inactive states formed following oxidation and that both could be quickly reactivated by reduction, *i.e.* neither was similar to Ni-A.[67] Furthermore, Abou Hamdan and coworkers showed that reduction and reoxidation of the V74H mutant of *Df*Hase, the mutant enzyme which has been reported to be the most oxygen-tolerant, resulted in an inactive sample with FTIR signals suggesting a mixture of states: Ni-B and a second, unprecedented state.

In addition to studies at room temperature, as a result of the excellent thermostability of *Pf*SHI, we have been able to evaluate the reactions of *Pf*SHI with oxygen over the range 15-80 ºC. At higher temperatures, the apparent reactivation potential is less negative (Figure 5-1D), *i.e.* the active site is easier to reduce. This is an

"apparent" reduction potential because we have not demonstrated that it is a thermodynamic parameter via simultaneous fitting of the data using a defined physical model. Nonetheless, we can conclude that it is easier to reactivate *Pf*SHI at higher temperatures either because the reduction potential of the reactivation transition is less negative or because the kinetics of reactivation are markedly faster (or both). The latter suggests that the rate-limiting step of reactivation is strongly temperature-dependent. One possible explanation is that reactivation relies on a rate-limiting, large-scale protein motion and is not simply an electron transfer reaction. With that in mind, other [NiFe]-hydrogenases might also be more oxygen-tolerant if they could be studied at higher temperatures, and it may be interesting to establish the properties of other [NiFe]-hydrogenases from (hyper)thermophilic sources.

Exposure of *Pf*SHI to oxygen for 15 minutes results in the loss of more catalytic activity than transient oxygen exposure, and the inactive states formed require more time to reactivate. Complete reactivation of the inactive states formed by transient exposure to oxygen occurs within 150 s over the entire temperature range studied, but enzyme inactivated by 15 minutes of exposure to oxygen requires up to 30 minutes to reactivate. Thus we conclude that a third, slowly reactivating, inactive state forms under these conditions, *i.e.* long exposure to oxygen at high temperature. We note that the enzyme is exposed not only to oxygen for a longer period in this experiment but also to oxidizing conditions. Thus, oxidizing conditions, not oxygen itself, may be the trigger required for formation of the slowly reactivating state. It is likely that this slowly reactivating state is formed by reaction of one of the more quickly reactivating states. We hypothesize that this could be an oxidation since it requires prolonged exposure to oxygen or oxidizing

conditions. This hypothesis is being further probed via variation of the inactivation potential which will also help identify whether oxygen is a necessary reactant. The results may lead to a more precise description of the inactive states of *Pf*SHI and their relationships to one another.

Little is known spectroscopically about *Pf*SHI, but the spectroscopic properties of other [NiFe]-hydrogenases may offer clues to the identities of the *Pf*SHI inactivate states and the possible mechanisms of its oxygen-tolerance. Based on EPR spectroscopy, three distinct Ni(III) states of oxygen-tolerant group 1 [NiFe]-hydrogenases have been described: Ni-A, Ni-B and Ni-C. As mentioned previously, Ni-A and Ni-B are both inactive states, but the kinetics of reactivation of Ni-A do not match those for *Pf*SHI following transient exposure to oxygen. Furthermore, although a Ni-C signal has been detected for some SHs,[59] neither Ni-A nor Ni-B has been observed in EPR experiments. Additionally, Ni-A has not been observed for oxygen-tolerant group 1 [NiFe]-hydrogenases. Thus we think it unlikely that the two states formed by transient exposure to oxygen correspond to the classic Ni-A and Ni-B states of group1 [NiFe]-hydrogenases. It is possible that they correspond to states in which the active site is electronically analogous to Ni-A and Ni-B but the paramagnetic Ni center is coupled to some other paramagnet in the enzyme complex. However, this also seems implausible since it would require a new mechanism to explain why the Ni-A-like state is quickly reactivated.

Turning to FTIR-defined states offers a complementary picture. No FTIR characterization of the active site of *Pf*SHI has been reported, but two other SHs have been characterized: the oxygen-sensitive *Syn*SH and the oxygen-tolerant SH from *Re*SH.[59, 60, 85] Only one oxidized, inactive state of *Syn*SH was detected in FTIR

experiments. That state has signals attributable to the CO and CN ligands of the active site at 1957, 2076 and 2088 cm^{-1}. Since these frequencies are most similar to the Ni-B state of group 1 [NiFe]-hydrogenases, this *Syn*SH state has been referred to as Ni_r-B-like.[85] Similarly, only one oxidized, inactive state was observed for the oxygen-tolerant enzyme ReSH characterized *in situ* using soluble extracts. These signals occur at 1957, 2079 and 2089 cm^{-1} and the signal was again called "Ni_r-B-like". Since these two quite phylogenetically distinct SHs share this hitherto unknown state, it is likely that *Pf*SHI also forms an analogous Ni_r-B-like state and that state is one of the ones detected electrochemically. The *Re*HoxHY hydrogenase subdimer of *Re*SH has also been characterized by FTIR spectroscopy.[60] It was isolated in two states: one with FTIR signals at 1956, 2087 and 2096 cm^{-1}, referred to as Ni-Ox, and the other with signals at 1938, 2065 and 2079 cm^{-1}, referred to as Ni-Ox_2. The Ni-Ox_2 state could be generated by reduction of the Ni-Ox state, and reoxidation of sample in the Ni-Ox_2 state by oxygen partially recovered Ni-Ox. The electrochemical data from *Pf*SHI can be explained by hypothesizing that *Pf*SHI has similar oxidized states. In such a scenario, transient exposure to oxygen generates the Ni_r-B-like state in combination with Ni-Ox_2. Then, prolonged oxidation transforms Ni-Ox_2 to Ni-Ox, a more slowly reactivating state.

Finally, we turn to the question of the mechanism of oxygen-tolerance in *Pf*SHI. The primary sequence of the hydrogenase small subunit does not contain the additional cysteine residues associated with formation of the [4Fe-3S] cluster of oxygen-tolerant group 1 [NiFe]-hydrogenases, making the presence of such a cluster improbable. Similarly, the electrocatalytic properties of *Pf*SHI are different from the classical, oxygen-tolerant group 1 [NiFe]-hydrogenases. On the other hand, the properties of *Pf*SHI

are very similar to those described for oxygen-tolerant mutants of *Df*Hase. For that enzyme, oxygen-tolerance was achieved by replacing the valine at position 74 with hydrophilic residues, but the physical mechanism of the oxygen-tolerance is still unclear. For *Pf*SHI, it may also be relevant that no Ni(III) EPR signal has been detected for inactivated enzyme. This may indicate that the inactive states do not include Ni(III) or that Ni(III) is present but coupled to another paramagnetic center elsewhere in the enzyme complex. The latter is an interesting possibility since the lack of EPR signals is general for SHs and such a coupling could be symptomatic of unique pathways that facilitate intramolecular electron transfer and oxygen-tolerance.

Figures

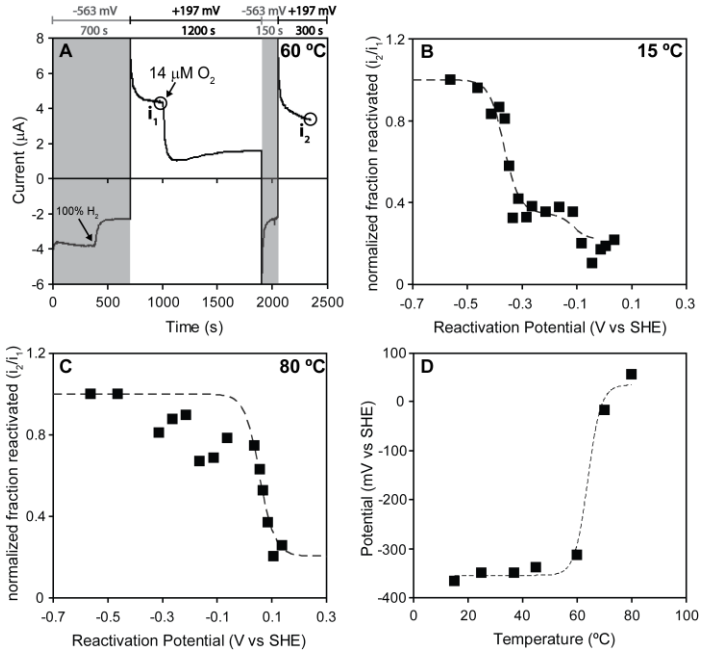


Figure 5-1. *Pf*SHI reacts with O_2 to form two inactive states that are distinguished by the electrochemical potential required to reactivate them. These reactivation profiles shift to less reducing potentials with increasing temperature. (A) Current-time trace for a chronoamperometry experiment evaluating the catalytic activity of *Pf*SHI in the presence of different gases and at different reduction potentials. The potentials and durations of the various electrochemical steps are noted above the figure. Grey or white background denotes portions of the experiment in which the potential was more reducing or more oxidizing than the hydrogen couple, respectively. To ensure complete activation of the enzyme film, the experiment began at reducing conditions under an atmosphere of N_2. Changes in the gas composition in the experimental apparatus are indicated by arrows in Panel A. The times at which the currents in later panels were evaluated are indicated by circles. Introduction of H_2 is continuous, but O_2 was introduced via injection so that it is only transiently present in solution. Control experiments indicate that after injection, 200 s are required for the O_2 concentration to decrease to an undetectable level. The experimental temperature is 60 ºC, and the electrode rotation rate is 3600 rpm. To probe the thermodynamics of reductive reactivation of aerobically inactivated enzyme, the potential of the 150 s reductive pulse was varied. (B) and (C) show the fraction of the H_2 oxidation activity immediately preceding initial exposure to O_2 that was recovered following the reactivation (i_2/i_1) as a function of this reducing potential at 15 ºC (B) and 80 ºC (C). The data are normalized such that the most highly active sample after reactivation, *i.e.* that exposed to the most reducing potentials, has a fraction reactivated value of 1. The dotted lines (B and C) correspond to a fit of the data to a linear combination of two Nernstian processes as described in the text. Panel D shows the dependence of the lower of these two reduction potentials on temperature. The dotted line shows the best fit to a sigmoidal model as described in the text.

Table 5-1. Reduction potentials and proportions of each inactive state formed for all temperatures investigated.

Temperature (º C)	Potential of Low-Potential Inactive State (mV)	Proportion of Enzyme in Low-Potential Inactive State (%)	Potential of High-Potential Inactive State (mV)	Proportion of Enzyme in High-Potential Inactive State
15	-366	83.4	-116	16.6
25	-350	82.4	-105	17.6
37	-350	N/A	N/A	N/A
45	-339	N/A	N/A	N/A
60	-313	N/A	N/A	N/A
70	-18	N/A	N/A	N/A
80	+55	N/A	N/A	N/A

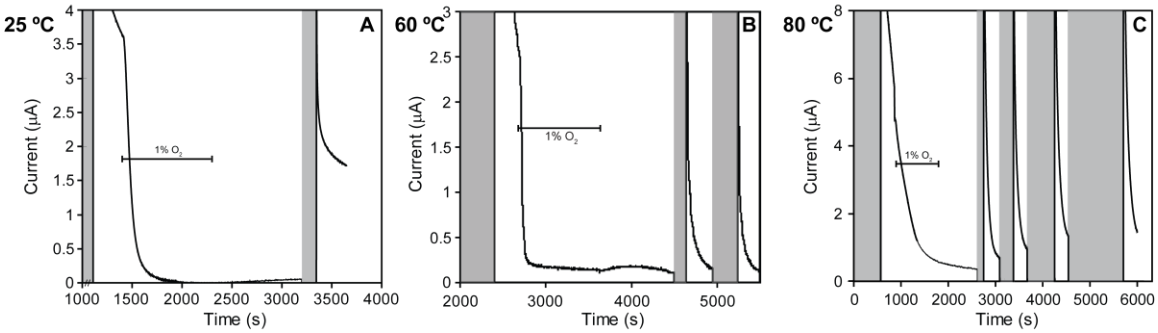


Figure 5-2. Hydrogen oxidation activity under prolonged O_2 exposure at 25 ºC (A), 60 ºC (B) and 80 ºC (C). Gray panels indicate periods where the electrode was held at reducing (-563 mV) potential and white panels indicate periods where the electrode was held at oxidizing (+197 mV) potentials. Unless otherwise indicated, the electrochemical cell is under 100% H_2. At time indicated by the bracketed line, the gas in the electrochemical cell was switched to 1% O_2 in 99% H_2 while simultaneously injecting an air-saturated buffer into the electrochemical cell for a final O_2 concentration of 14 μM. Aerobic inactivation of the enzyme was observed in the form of decreasing H_2-oxidation current.

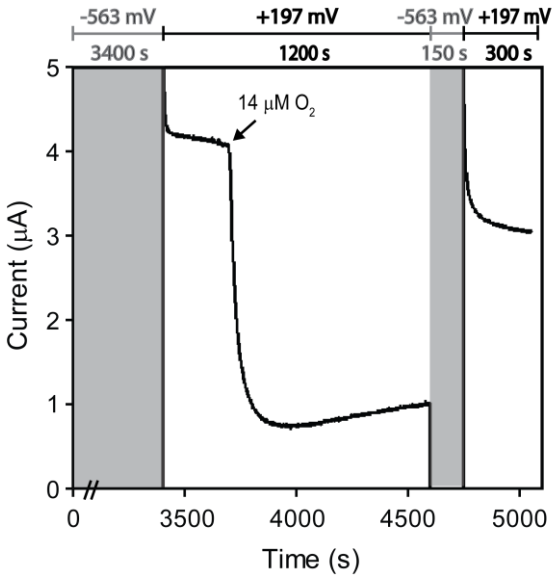


Figure 5-3. Potential step experiment at 45 ºC demonstrating hydrogen oxidizing activity after transient oxygen exposure. Experiment performed at 45 ºC under 100% H_2 in a 75 mM mixed buffer at pH 6.4 with an electrode rotation rate of 3600 rpm. Potentials and duration of each step are indicated above the figure. At t = 3700 s, an aliquot of air-saturated buffer was injected into the cell for an initial O_2 concentration of 14 μM, as indicated by the arrow. The oxygen then spontaneously diffuses out of the cell.

References

1. Cammack, R., Frey, M. & Robson, R. (eds.) Hydrogen as a fuel, learning from Nature (Taylor and Francis, London, 2001).

2. Fontecilla-Camps, J.C., Volbeda, A., Cavazza, C. & Nicolet, Y. Structure/Function Relationships of [NiFe]- and [FeFe]-hydrogenases. *Chem. Rev.* **107**, 4273-4303 (2007).

3. Barton, B.E., Olsen, M.T. & Rauchfuss, T.B. Artificial hydrogenases. *Curr. Opin. Biotechnol.* **21**, 292-297 (2010).

4. Simmons, T.R., Berggren, G., Bacchi, M., Fontecave, M. & Artero, V. Mimicking hydrogenases: From biomimetics to artificial enzymes. *Coord. Chem. Rev.* **270**, 127-150 (2014).

5. Lubitz, W., Ogata, H., Rudiger, O. & Reijerse, E. Hydrogenases. *Chem. Rev.* **114**, 4081-4148 (2014).

6. Shafaat, H.S., Rudiger, O., Ogata, H. & Lubitz, W. [NiFe] hydrogenases: A common active site for hydrogen metabolism under diverse conditions. *Biochim. Biophys. Acta* **1827**, 986-1002 (2013).

7. Gordon, J.C. & Kubas, G.J. Perspectives on How Nature Employs the Principles of Organometallic Chemistry in Dihydrogen Activation in Hydrogenases. *Organometallics* **29**, 4682-4701 (2010).

8. Friedrich, B., Fritsch, J. & Lenz, O. Oxygen-tolerant hydrogenases in hydrogen-based technologies. *Curr. Opin. Biotech.* **22**, 358-364 (2011).

9. Woolerton, T.W., Sheard, S., Chaudhary, Y.S. & Armstrong, F.A. Enzymes and bio-inspired electrocatalysts in solar fuel devices. *Energ. Environ. Sci.* **5**, 7470-7490 (2012).

10. Lubner, C.E., Applegate, A.M., Knorzer, P., Ganago, A., Bryant, D.A., Happe, T. & Golbeck, J.H. Solar hydrogen-producing bionanodevice outperforms natural photosynthesis. *Proc. Natl. Acad. Sci. U.S.A.* **108**, 20988-20991 (2011).

11. Jones, A.K., Lamle, S.E., Pershad, H.R., Vincent, K.A., Albracht, S.P.J. & Armstrong, F.A. Enzyme electrokinetics: electrochemical studies of the anaerobic interconversions between active and inactive states of *Allochromatium vinosum* [NiFe]-hydrogenase. *J. Am. Chem. Soc.* **125**, 8505-8514 (2003).

12. Goldet, G., Brandmayr, C., Stripp, S.T., Happe, T., Cavazza, C., Fontecilla-Camps, J.C. & Armstrong, F.A. Electrochemical kinetic investigations of the reactions of [FeFe]-hydrogenase with carbon monoxide and oxygen: comparing the importance of gas tunnels and active-site electronic/redox effects. *J. Am. Chem. Soc.* **131**, 14979-14989 (2009).

13. Lamle, S.E., Albracht, S.P.J. & Armstrong, F.A. Electrochemical potential-step investigations of the aerobic interconversions of [NiFe]-hydrogenase from *Allochromatium vinosum*: Insights into the puzzling difference between unready and ready oxidized inactive states. *J. Am. Chem. Soc.* **126**, 14899-14909 (2004).

14. Reda, T., Plugge, C.M., Abram, N.J. & Hirst, J. Reversible interconversion of carbon dioxide and formate by an electroactive enzyme. *Proc. Natl. Acad. Sci. U.S.A.* **105**, 10654-10658 (2008).

15. Yang, K.Y., Haynes, C.A., Spatzal, T., Rees, D.C. & Howard, J.B. Turnover-Dependent Inactivation of the Nitrogenase MoFe-Protein at High pH. *Biochemistry* **53**, 333-343 (2014).

16. Hoffmann, M.C., Muller, A., Fehringer, M., Pfander, Y., Narberhaus, F. & Masepohl, B. Coordinated Expression of *fdxD* and Molybdenum Nitrogenase Genes Promotes Nitrogen Fixation by *Rhodobacter capsulatus* in the Presence of Oxygen. *J. Bacteriol.* **196**, 633-640 (2014).

17. Zhang, X., Sherman, D.M. & Sherman, L.A. The uptake hydrogenase in the unicellular diazotrophic cyanobacterium *Cyanothece* sp. strain PCC 7822 protects nitrogenase from oxygen toxicity. *J. Bacteriol.* **196**, 840-849 (2014).

18. Gallon, J.R. The Oxygen Sensitivity of Nitrogenase - A Problem for Biochemists and Microorganisms. *Trends Biochem. Sci.* **6**, 19-23 (1981).

19. Hille, R., Hall, J. & Basu, P. The Mononuclear Molybdenum Enzymes. *Chem. Rev.* **114**, 3963-4038 (2014).

20. Vincent, K.A., Parkin, A., Lenz, O., Albracht, S.P.J., Fontecilla-Camps, J.C., Cammack, R., Friedrich, B. & Armstrong, F.A. Electrochemical definitions of O_2 sensitivity and oxidative inactivation in hydrogenases. *J. Am. Chem. Soc.* **127**, 18179-18189 (2005).

21. Bleijlevens, B., van Broekhuizen, F.A., De Lacey, A.L., Roseboom, W., Fernandez, V.M. & Albracht, S.P.J. The activation of the [NiFe]-hydrogenase from *Allochromatium vinosum*. An infrared spectro-electrochemical study. *J. Biol. Inorg. Chem.* **9**, 743-752 (2004).

22. Schneider, K. & Schlegel, H.G. Purification and Properties of Soluble Hydrogenase from *Alcaligenes eutrophus* H16. *Biochim. Biophys. Acta* **452**, 66-80 (1976).

23. Parkin, A. & Sargent, F. The hows and whys of aerobic H_2 metabolism. *Curr. Opin. Chem. Biol.* **16**, 26-34 (2012).

24. Pinske, C., Jaroschinsky, M., Sargent, F. & Sawers, G. Zymographic differentiation of [NiFe]-Hydrogenases 1, 2 and 3 of *Escherichia coli* K-12. *BMC Microbiol.* **12**, 134-145 (2012).

25. Abou Hamdan, A., Burlat, B., Gutierrez-Sanz, O., Liebgott, P.P., Baffert, C., De Lacey, A.L., Rousset, M., Guigliarelli, B., Léger, C. & Dementin, S. O_2-independent formation of the inactive states of NiFe hydrogenase. *Nat. Chem. Biol.* **9**, 15-17 (2012).

26. Albracht, S.P.J., Kalkman, M.L. & Slater, E.C. Magnetic Interaction of Nickel(III) and the Iron-Sulfur Cluster in Hydrogenase from *Chromatium vinosum*. *Biochim. Biophys. Acta* **724**, 309-316 (1983).

27. Ogata, H., Kellers, P. & Lubitz, W. The crystal structure of the [NiFe] hydrogenase from the photosynthetic bacterium *Allochromatium vinosum:* Characterization of the oxidized enzyme (Ni-A state). *J. Mol. Biol.* **402**, 428-444 (2010).

28. Volbeda, A., Martin, L., Cavazza, C., Matho, M., Faber, B.W., Roseboom, W., Albracht, S.P.J., Garcin, E., Rousset, M. & Fontecilla-Camps, J.C. Structural differences between the ready and unready oxidized states of [NiFe] hydrogenases. *J. Biol. Inorg. Chem.* **10**, 239-249 (2005).

29. Teixeira, M., Moura, I., Xavier, A.V., Moura, J.J.G., Legall, J., Dervartanian, D.V., Peck, H.D. & Huynh, B.H. Redox Intermediates of *Desulfovibrio gigas* [NiFe] Hydrogenase Generated Under Hydrogenase - Mossbauer and EPR Characterization of the Metal Centers. *J. Biol. Chem.* **264**, 16435-16450 (1989).

30. Asso, M., Guigliarelli, B., Yagi, T. & Bertrand, P. EPR and Redox Properties of *Desulfovibrio vulgaris* Miyazaki Hydrogenase - Comparison with the NiFe enzyme from *Desulfovibrio gigas*. *Biochim. Biophys. Acta.* **1122**, 50-56 (1992).

31. Lenz, O., Ludwig, M., Schubert, T., Burstel, I., Ganskow, S., Goris, T., Schwarze, A. & Friedrich, B. H_2 Conversion in the Presence of O_2 as Performed by the Membrane-Bound [NiFe]-Hydrogenase of *Ralstonia eutropha*. *ChemPhysChem* **11**, 1107-1119 (2010).

32. Pandelia, M.-E., Fourmond, V., Tron-Infossi, P., Lojou, E., Bertrand, P., Léger, C., Giudici-Orticoni, M. & Lubitz, W. Membrane-bound hydrogenase I from the hyperthermophilic bacterium *Aquifex aelicus*: Enzyme activation, redox intermediates and oxygen tolerance. *J. Am. Chem. Soc.* **132**, 6991-7004 (2010).

33. Pandelia, M.-E., Nitschke, W., Infossi, P., Giudici-Orticoni, M.T., Bill, E. & Lubitz, W. Characterization of a unique [FeS] cluster in the electron transfer chain of the oxygen tolerant [NiFe] hydrogenase from *Aquifex aeolicus*. *Proc. Nat. Acad. Sci. U.S.A.* **108**, 6097-6102 (2011).

34. Lukey, M.J., Parkin, A., Roessler, M.M., Murphy, B.J., Harmer, J., Palmer, T., Sargent, F. & Armstrong, F.A. How *Escherichia coli* is equipped to oxidize hydrogen under different redox conditions. *J. Biol. Chem.* **285**, 3928-3938 (2010).

35. Lukey, M.J., Roessler, M.M., Parkin, A., Evans, R.M., Davies, R.A., Lenz, O., Friedrich, B., Sargent, F. & Armstrong, F.A. Oxygen-Tolerant [NiFe]-Hydrogenases: The Individual and Collective Importance of Supernumerary Cysteines at the Proximal Fe-S Cluster. *J. Am. Chem. Soc.* **133**, 16881-16892 (2011).

36. Shomura, Y., Yoon, K.S., Nishihara, H. & Higuchi, Y. Structural basis for a [4Fe-3S] cluster in the oxygen-tolerant membrane-bound [NiFe]-hydrogenase. *Nature* **479**, 253-256 (2011).

37. Jo, B.H., Hwang, B.H. & Cha, H.J. Draft genome sequence of *Hydrogenovibrio marinus* MH-110, a model organism for aerobic H_2 metabolism. *J. Biotechnol.* **185**, 37-38 (2014).

38. Lauterbach, L. & Lenz, O. Catalytic Production of Hydrogen Peroxide and Water by Oxygen-Tolerant [NiFe]-Hydrogenase during H_2 Cycling in the Presence of O_2. *J. Am. Chem. Soc.* **135**, 17897-17905 (2013).

39. Wulff, P., Day, C.C., Sargent, F. & Armstrong, F.A. How oxygen reacts with oxygen-tolerant respiratory [NiFe]-hydrogenases. *Proc. Natl. Acad. Sci. U.S.A.* **111**, 6606-6611 (2014).

40. Buhrke, T., Lenz, O., Krauss, N., & Friedrich, B. Oxygen tolerance of the H_2-sensing [NiFe]-hydrogenase from *Ralstonia eutropha* H16 is based on limited access of oxygen to the active site. *J. Biol. Chem.* **280**, 23791-23796 (2005).

41. Kleihues, L., Lenz, O., Bernhard, M., Buhrke, T. & Friedrich, B. The H_2 sensor of *Ralstonia eutropha* is a member of the subclass of regulatory [NiFe] hydrogenases. *J. Bacteriol.* **182**, 2716-2724 (2000).

42. Lenz, O., Bernhard, M., Buhrke, T., Schwartz, E. & Friedrich, B. The hydrogen-sensing apparatus in *Ralstonia eutropha*. *J. Mol. Microb. Biotechn.* **4**, 255-262 (2002).

43. Haumann, M., Porthun, A., Buhrke, T., Liebisch, P., Meyer-Klaucke, W., Friedrich, B. & Dau, H. Hydrogen-induced structural changes at the nickel site of the regulatory [NiFe] hydrogenase from *Ralstonia eutropha* detected by X-ray absorption spectroscopy. *Biochemistry* **42**, 11004-11015 (2003).

44. Friedrich, B., Buhrke, T., Burgdorf, T. & Lenz, O. A hydrogen-sensing multiprotein complex controls aerobic hydrogen metabolism in *Ralstonia eutropha*. *Biochem. Soc. T.* **33**, 97-101 (2005).

45. Fritsch, J., Scheerer, P., Frielingsdorf, S., Kroschinsky, S., Friedrich, B., Lenz, O. & Spahn, C.M.T. The crystal structure of an oxygen-tolerant hydrogenase uncovers a novel iron-sulphur centre. *Nature* **479**, 249-252 (2011).

46. Goris, T., Wait, A.F., Saggu, M., Fritsch, J., Heidary, N., Stein, M., Zebger, I., Lendzian, F., Armstrong, F.A., Friedrich, B. & Lenz, O. A unique iron-sulfur

cluster is crucial for oxygen tolerance of a [NiFe]-hydrogenase. *Nat. Chem. Biol.* **7**, 310-318 (2011).

47. Frielingsdorf, S., Fritsch, J., Schmidt, A., Hammer, M., Lowenstein, J., Siebert, E., Pelmenschikov, V., Jaenicke, T., Kalms, J., Rippers, Y., Lendzian, F., Zebger, I., Teutloff, C., Kaupp, M., Bittl, R., Hildebrandt, P., Friedrich, B., Lenz, O. & Scheerer, P. Reversible [4Fe-3S] cluster morphing in an O_2-tolerant [NiFe] hydrogenase. *Nat. Chem. Biol.* **10**, 378-387 (2014).

48. Pelmenschikov, V. & Kaupp, M. Redox-Dependent Structural Transformations of the [4Fe-3S] Proximal Cluster in O_2-Tolerant Membrane-Bound [NiFe]-Hydrogenase: A DFT Study. *J. Am. Chem. Soc.* **135**, 11809-11823 (2013).

49. Pandelia, M.-E., Bykov, D., Izsak, R., Infossi, P., Giudici-Orticoni, M.T., Bill, E., Neese, F. & Lubitz, W. Electronic structure of the unique [4Fe-3S] cluster in O_2-tolerant hydrogenases characterized by Fe-57 Mossbauer and EPR spectroscopy. *Proc. Natl. Acad. Sci. U.S.A.* **110**, 483-488 (2013).

50. Mouesca, J.M., Fontecilla-Camps, J.C. & Amara, P. The Structural Plasticity of the Proximal [4Fe3S] Cluster is Responsible for the O_2 Tolerance of Membrane-Bound [NiFe] Hydrogenases. *Angew. Chem. Int. Edit.* **52**, 2002-2006 (2013).

51. Roessler, M.M., Evans, R.M., Davies, R.A., Harmer, J. & Armstrong, F.A. EPR spectroscopic studies of the Fe-S clusters in the O_2-tolerant [NiFe]-hydrogenase Hyd-1 from *Escherichia coli* and characterization of the unique [4Fe-3S] cluster by HYSCORE. *J. Am. Chem. Soc.* **137**, 15581-15594 (2012).

52. Fritsch, J., Scheerer, P., Frielingsdorf, S., Kroschinsky, S., Friedrich, B., Lenz, O. & Spahn, C.M. The crystal structure of an oxygen-tolerant hydrogenase uncovers a novel iron-sulphur centre. *Nature* **479**, 249-252 (2011).

53. Pandelia, M.-E., Lubitz, W. & Nitschke, W. Evolution and diversification of Group 1 [NiFe] hydrogenases. Is there a phylogenetic marker for O_2-tolerance? *Biochim. Biophys. Acta* **1817**, 1565-1575 (2012).

54. Evans, R.M., Parkin, A., Roessler, M.M., Murphy, B.J., Adamson, H., Lukey, M.J., Sargent, F., Volbeda, A., Fontecilla-Camps, J.C. & Armstrong, F.A. Principles of Sustained Enzymatic Hydrogen Oxidation in the Presence of Oxygen - The Crucial Influence of High Potential Fe-S Clusters in the Electron Relay of [NiFe]-Hydrogenases. *J. Am. Chem. Soc.* **135**, 2694-2707 (2013).

55. Liebgott, P.-P., de Lacey, A.L., Burlat, B., Cournac, L., Richaud, P., Brugna, M., Fernandez, V.M., Guigliarelli, B., Rousset, M., Léger, C. & Dementin, S. Original design of an oxygen-tolerant [NiFe] hydrogenase: Major effect of a valine-to-cysteine mutation near the active site. *J. Am. Chem. Soc.* **133**, 986-997 (2011).

56. Abou Hamdan, A., Liebgott, P.P., Fourmond, V., Gutierrez-Sanz, O., De Lacey, A.L., Infossi, P., Rousset, M., Dementin, S. & Léger, C. Relation between anaerobic inactivation and oxygen tolerance in a large series of NiFe hydrogenase mutants. *Proc. Natl. Acad. Sci. U.S.A.* **109**, 19916-19921 (2012).

57. Vignais, P.M., Billoud, B. & Meyer, J. Classification and phylogeny of hydrogenases. *FEMS Microbiol. Rev.* **25**, 455-501 (2001).

58. Tamagnini, P., Leitao, E., Oliveira, P., Ferreira, D., Pinto, F., Harris, D.J., Heidorn, T. & Lindblad, P. Cyanobacterial hydrogenases: diversity, regulation and applications. *FEMS Microbiol. Rev.* **31**, 692-720 (2007).

59. Horch, M., Lauterbach, L., Saggu, M., Hildebrandt, P., Lendzian, F., Bittl, R., Lenz, O. & Zebger, I. Probing the Active Site of an O_2-Tolerant NAD^+-Reducing [NiFe]-Hydrogenase from *Ralstonia eutropha* H16 by In Situ EPR and FTIR Spectroscopy. *Angew. Chem. Int. Edit.* **49**, 8026-8029 (2010).

60. Lauterbach, L., Liu, J.A., Horch, M., Hummel, P., Schwarze, A., Haumann, M., Vincent, K.A., Lenz, O. & Zebger, I. The Hydrogenase Subcomplex of the NAD^+-Reducing [NiFe] Hydrogenase from *Ralstonia eutropha* - Insights into Catalysis and Redox Interconversions. *Eur. J. Inorg. Chem.*, **7**, 1067-1079 (2011).

61. Thorgersen, M.P., Stirrett, K., Scott, R.A. & Adams, M.W.W. Mechanism of oxygen detoxification by the surprisingly oxygen-tolerant hyperthermophilic archaeon, *Pyrococcus furiosus*. *Proc. Natl. Acad. Sci. U.S.A.* **109**, 18547-18552 (2012).

62. Léger, C., Elliott, S.J., Hoke, K.R., Jeuken, L.J.C., Jones, A.K. & Armstrong, F.A. Enzyme electrokinetics: Using protein film voltammetry to investigate redox enzymes and their mechanisms. *Biochemistry* **42**, 8653-8662 (2003).

63. Armstrong, F.A., Belsey, N.A., Cracknell, J.A., Goldet, G., Parkin, A., Reisner, E., Vincent, K.A. & Wait, A.F. Dynamic electrochemical investigations of hydrogen oxidation and production by enzymes and implications for future technology. *Chem. Soc. Rev.* **38**, 36-51 (2009).

64. Vincent, K.A., Parkin, A. & Armstrong, F.A. Investigating and exploiting the electrocatalytic properties of hydrogenases. *Chem. Rev.* **107**, 4366-4413 (2007).

65. Fourmond, V., Infossi, P., Giudici-Orticoni, M.-T., Bertrand, P. & Léger, C. "Two-step" chronoamperometric method for studying the anaerobic inactivation of an oxygen tolerant NiFe hydrogenase. *J. Am. Chem. Soc.* **132**, 4848-4857 (2010).

66. Léger, C. & Bertrand, P. Direct electrochemistry of redox enzymes as a tool for mechanistic studies. *Chem. Rev.* **108**, 2379-2438 (2008).

67. McIntosh, C.L., Germer, F., Schulz, R.d., Appel, J. & Jones, A.K. The [NiFe]-Hydrogenase of the Cyanobacterium *Synechocystis* sp. PCC 6803 Works Bidirectionally with a Bias to H_2 Production. *J. Am. Chem. Soc.* **133**, 11308-11319 (2011).

68. Ma, K. & Adams, M.W. Hydrogenases I and II from *Pyrococcus furiosus*. *Methods Enzymol.* **331**, 208-216 (2001).

69. Fourmond, V., Hoke, K.R., Heering, H.A., Baffert, C., Leroux, F., Bertrand, P. & Léger, C. SOAS: A free program to analyze electrochemical data and other one-dimensional signals. *Bioelectrochemistry* **76**, 141-147 (2009).

70. Vincent, K.A., Cracknell, J.A., Lenz, O., Zebger, I., Friedrich, B. & Armstrong, F.A. Electrocatalytic hydrogen oxidation by an enzyme at high carbon monoxide or oxygen levels. *Proc. Natl. Acad. Sci. U.S.A.* **102**, 16951-16954 (2005).

71. Herr, N., Ratzka, J., Lauterbach, L., Lenz, O. & Ansorge-Schumacher, M.B. Stability enhancement of an O_2-tolerant NAD^+-reducing [NiFe]-hydrogenase by a combination of immobilisation and chemical modification. *J. Mol. Catal. B: Enzym.* **97**, 169-174 (2013).

72. Lauterbach, L., Lenz, O. & Vincent, K.A. H_2-driven cofactor regeneration with $NAD(P)^+$-reducing hydrogenases. *FEBS J.* **280**, 3058-3068 (2013).

73. Ratzka, J., Lauterbach, L., Lenz, O. & Ansorge-Schumacher, M.B. Stabilisation of the NAD^+-reducing soluble [NiFe]-hydrogenase from *Ralstonia eutropha* H16 through modification with methoxy-poly(ethylene) glycol. *J. Mol. Catal. B: Enzym.* **74**, 219-223 (2011).

74. van der Linden, E., Burgdorf, T., de Lacey, A.L., Buhrke, T., Scholte, M., Fernandez, V.M., Friedrich, B. & Albracht, S.P.J. An improved purification procedure for the soluble [NiFe]-hydrogenase of *Ralstonia eutropha*: new insights into its (in)stability and spectroscopic properties. *J. Biol. Inorg. Chem.* **11**, 247-260 (2006).

75. Burgdorf, T., van der Linden, E., Bernhard, M., Yin, Q.Y., Back, J.W., Hartog, A.F., Muijsers, A.O., de Koster, C.G., Albracht, S.P.J. & Friedrich, B. The soluble NAD^+-reducing [NiFe]-Hydrogenase from *Ralstonia eutropha* H16 consists of six subunits and can be specifically activated by NADPH. *J. Bacteriol.* **187**, 3122-3132 (2005).

76. van der Linden, E., Faber, B.W., Bleijlevens, B., Burgdorf, T., Bernhard, M., Friedrich, B. & Albracht, S.P.J. Selective release and function of one of the two FMN groups in the cytoplasmic NAD^+-reducing [NiFe]-hydrogenase from *Ralstonia eutropha*. *Eur. J. Biochem.* **271**, 801-808 (2004).

77. Porthun, A., Bernhard, M. & Friedrich, B. Expression of a functional NAD-reducing [NiFe] hydrogenase from the gram-positive *Rhodococcus opacus* in the gram-negative *Ralstonia eutropha*. *Arch. Microbiol.* **177**, 159-166 (2002).

78. Serebriakova, L.T. & Sheremet'eva, M.E. Characterization of catalytic properties of hydrogenase isolated from the unicellular cyanobacterium *Gloeocapsa alpicola* CALU 743. *Biochemistry (Mosc)* **71**, 1370-1376 (2006).

79. Sun, J.S., Hopkins, R.C., Jenney, F.E., McTernan, P.M. & Adams, M.W.W. Heterologous Expression and Maturation of an NADP-Dependent [NiFe]-Hydrogenase: A Key Enzyme in Biofuel Production. *PLOS One* **5**, e10526 (2010).

80. Dementin, S., Leroux, F., Cournac, L., de Lacey, A.L., Volbeda, A., Léger, C., Burlat, B., Martinez, N., Champ, S., Martin, L., Sanganas, O., Haumann, M., Fernandez, V.M., Guigliarelli, B., Fontecilla-Camps, J.C. & Rousset, M. Introduction of Methionines in the Gas Channel Makes [NiFe] Hydrogenase Aero-Tolerant. *J. Am. Chem. Soc.* **131**, 10156-10164 (2009).

81. Liebgott, P.P., Dementin, S., Léger, C. & Rousset, M. Towards engineering O_2-tolerance in [Ni-Fe] hydrogenases. *Energ. Environ. Sci.* **4**, 33-41 (2011).

82. Cracknell, J.A., Wait, A.F., Lenz, O., Friedrich, B. & Armstrong, F.A. A kinetic and thermodynamic understanding of O_2 tolerance in [NiFe]-hydrogenases. *Proc. Natl. Acad. Sci. U.S.A.* **106**, 20681-20686 (2009).

83. Fernandez, V.M., Hatchikian, E.C. & Cammack, R. Properties and reactivation of two different deactivated forms of *Desulfovibrio gigas* hydrogenase. *Biochim. Biophys. Acta* **832**, 69-79 (1985).

84. Fernandez, V.M., Hatchikian, E.C., Patil, D.S. & Cammack, R. ESR-detectable nickel and iron-sulphur centres in relation to the reversible activation of *Desulfovibrio gigas* hydrogenase. *Biochim. Biophys. Acta* **883**, 145-154 (1986).

85. Germer, F., Zebger, I., Saggu, M., Lendzian, F., Schulz, R. & Appel, J. Overexpression, Isolation, and Spectroscopic Characterization of the Bidirectional [NiFe] Hydrogenase from *Synechocystis* sp PCC 6803. *J. Biol. Chem.* **284**, 36462-36472 (2009).

BIBLIOGRAPHY

Abou Hamdan, A., Dementin, S., Liebgott, P.-P., Gutierrez-Sanz, O., Richaud, P., De Lacey, A.L., Rousset, M., Bertrand, P., Cournac, L. & Léger, C. Understanding and Tuning the Catalytic Bias of Hydrogenase. *J. Am. Chem. Soc.* **134**, 8368-8371 (2012).

Abou Hamdan, A., Burlat, B., Gutierrez-Sanz, O., Liebgott, P.P., Baffert, C., De Lacey, A.L., Rousset, M., Guigliarelli, B., Léger, C. & Dementin, S. O_2-independent formation of the inactive states of NiFe hydrogenase. *Nat. Chem. Biol.* **9**, 15-17 (2012).

Abou Hamdan, A., Liebgott, P.P., Fourmond, V., Gutierrez-Sanz, O., De Lacey, A.L., Infossi, P., Rousset, M., Dementin, S. & Léger, C. Relation between anaerobic inactivation and oxygen tolerance in a large series of NiFe hydrogenase mutants. *Proc. Natl. Acad. Sci. U.S.A.* **109**, 19916-19921 (2012).

Albracht, S.P.J., Kalkman, M.L. & Slater, E.C. Magnetic Interaction of Nickel(III) and the Iron-Sulfur Cluster in Hydrogenase from *Chromatium vinosum*. *Biochim. Biophys. Acta* **724**, 309-316 (1983).

Appel, J. & Schulz, R. Hydrogen metabolism in organisms with oxygenic photosynthesis: hydrogenases as important regulatory devices for a proper redox poising? *J. Photoch. Photobio. B* **47**, 1-11 (1998).

Appel, J., Phunpruch, S., Steinmuller, K. & Schulz, R. The bidirectional hydrogenase of *Synechocystis* sp PCC 6803 works as an electron valve during photosynthesis. *Arch. Microbiol.* **173**, 333-338 (2000).

Armstrong, F.A., Heering, H.A. & Hirst, J. Reactions of complex metalloproteins studied by protein-film voltammetry. *Chem. Soc. Rev.* **26**, 169-179 (1997).

Armstrong, F.A., Camba, R., Heering, H.A., Hirst, J., Jeuken, L.J.C., Jones, A.K., Léger, C. & McEvoy, J.P. Fast voltammetric studies of the kinetics and energetics of coupled electron-transfer reactions in proteins. *Farad. Discuss.* **116**, 191-203 (2000).

Armstrong, F.A., Belsey, N.A., Cracknell, J.A., Goldet, G., Parkin, A., Reisner, E., Vincent, K.A. & Wait, A.F. Dynamic electrochemical investigations of hydrogen oxidation and production by enzymes and implications for future technology. *Chem. Soc. Rev.* **38**, 36-51 (2009).

Asso, M., Guigliarelli, B., Yagi, T. & Bertrand, P. EPR and Redox Properties of *Desulfovibrio vulgaris* Miyazaki Hydrogenase - Comparison with the NiFe enzyme from *Desulfovibrio gigas*. *Biochim. Biophys. Acta.* **1122**, 50-56 (1992).

Bard, A.J. & Faulkner, L.R. Electrochemical Methods: Fundamentals and Applications (John Wiley & Sons, Inc., New York, 2001).

Barton, B.E., Olsen, M.T. & Rauchfuss, T.B. Artificial hydrogenases. *Curr. Opin. Biotech.* **21**, 292-297 (2010).

Bleijlevens, B., van Broekhuizen, F.A., De Lacey, A.L., Roseboom, W., Fernandez, V.M. & Albracht, S.P.J. The activation of the [NiFe]-hydrogenase from *Allochromatium vinosum*. An infrared spectro-electrochemical study. *J. Biol. Inorg. Chem.* **9**, 743-752 (2004).

Bryant, F.O. & Adams, M.W.W. Characterization of Hydrogenase from the Hyperthermophilic Archaebacterium, *Pyrococcus furiosus*. *J. Biol. Chem.* **264**, 5070-5079 (1989).

Buettner, G.R., Wagner, B.A. & Rodgers, V.G.J. Quantitative Redox Biology: An Approach to Understand the Role of Reactive Species in Defining the Cellular Redox Environment. *Cell Biochem. Biophys.* **67**, 477-483 (2013).

Buhrke, T., Lenz, O., Krauss, N. & Friedrich, B. Oxygen tolerance of the H_2-sensing [NiFe]-hydrogenase from *Ralstonia eutropha* H16 is based on limited access of oxygen to the active site. *J. Biol. Chem.* **280**, 23791-23796 (2005).

Burgdorf, T., De Lacey, A.L. & Friedrich, B. Functional analysis by site-directed mutagenesis of the NAD^+-reducing hydrogenase from *Ralstonia eutropha*. *J. Bacteriol.* **184**, 6280-6288 (2002).

Burgdorf, T., van der Linden, E., Bernhard, M., Yin, Q.Y., Back, J.W., Hartog, A.F., Muijsers, A.O., de Koster, C.G., Albracht, S.P.J. & Friedrich, B. The soluble NAD^+-reducing [NiFe]-Hydrogenase from *Ralstonia eutropha* H16 consists of six subunits and can be specifically activated by NADPH. *J. Bacteriol.* **187**, 3122-3132 (2005).

Cammack, R., Frey, M. & Robson, R. (eds.) Hydrogen as a fuel, learning from Nature (Taylor and Francis, London, 2001).

Choe, H., Joo, J.C., Cho, D.H., Kim, M.H., Lee, S.H., Jung, K.D. & Kim, Y.H. Efficient CO_2-Reducing Activity of NAD-Dependent Formate Dehydrogenase from *Thiobacillus* sp. KNK65MA for Formate Production from CO_2 Gas. *PLOS One* **9**, e103111 (2014).

Cipriani, G., Di Dio, V., Genduso, F., La Cascia, D., Liga, R., Miceli, R. & Galluzzo, G.R. Perspective on hydrogen energy carrier and its automotive applications. *Int. J. Hydrogen Energ.* **39**, 8482-8494 (2014).

Collinson, M. & Bowden, E.F. UV-Visible Spectroscopy of Adsorbed Cytochrome-*C* on Tin Oxide Electrodes. *Anal. Chem.* **64**, 1470-1476 (1992).

Collinson, M., Bowden, E.F. & Tarlov, M.J. Voltammetry of Covalently Immobilized Cytochrome-C on Self-Assembled Monolayer Electrodes. *Langmuir* **8**, 1247-1250 (1992).

Cournac, L., Mus, F., Bernard, L., Guedeney, G., Vignais, P. & Peltier, G. Limiting steps of hydrogen production in *Chlamydomonas reinhardtii* and *Synechocystis* PCC 6803 as analysed by light-induced gas exchange transients. *Int. J. Hydrogen Energ.* **27**, 1229-1237 (2002).

Cournac, L., Guedeney, G., Peltier, G. & Vignais, P.M. Sustained photoevolution of molecular hydrogen in a mutant of *Synechocystis* sp strain PCC 6803 deficient in the type I NADPH-dehydrogenase complex. *J. Bacteriol.* **186**, 1737-1746 (2004).

Cox, N., Pantazis, D.A., Neese, F. & Lubitz, W. Biological Water Oxidation. *Accounts Chem. Res.* **46**, 1588-1596 (2013).

Cracknell, J.A., Vincent, K.A. & Armstrong, F.A. Enzymes as working of inspirational electrocatalysts for fuel cells and electrolysis. *Chem. Rev.* **108**, 2439-2461 (2008).

Cracknell, J.A., Wait, A.F., Lenz, O., Friedrich, B. & Armstrong, F.A. A kinetic and thermodynamic understanding of O_2 tolerance in [NiFe]-hydrogenases. *Proc. Natl. Acad. Sci. U.S.A.* **106**, 20681-20686 (2009).

D'Adamo, S., Jinkerson, R.E., Boyd, E.S., Brown, S.L., Baxter, B.K., Peters, J.W. & Posewitz, M.C. Evolutionary and Biotechnological Implications of Robust Hydrogenase Activity in Halophilic Strains of *Tetraselmis*. *PLOS One* **9**, 1-13 (2014).

Dau, H., Zaharieva, I. & Haumann, M. Recent developments in research on water oxidation by photosystem II. *Curr. Opin. Chem. Biol.* **16**, 3-10 (2012).

Davis, K.L., Drews, B.J., Yue, H., Waldeck, D.H., Knorr, K. & Clark, R.A. Electron-transfer kinetics of covalently attached cytochrome c/SAM/Au electrode assemblies. *J. Phys. Chem. C* **112**, 6571-6576 (2008).

De Lacey, A.L., Fernandez, V.M., Rousset, M. & Cammack, R. Activation and inactivation of hydrogenase function and the catalytic cycle: Spectroelectrochemical studies. *Chem. Rev.* **107**, 4304-4330 (2007).

Dementin, S., Leroux, F., Cournac, L., de Lacey, A.L., Volbeda, A., Léger, C., Burlat, B., Martinez, N., Champ, S., Martin, L., Sanganas, O., Haumann, M., Fernandez, V.M., Guigliarelli, B., Fontecilla-Camps, J.C. & Rousset, M. Introduction of Methionines in the Gas Channel Makes [NiFe] Hydrogenase Aero-Tolerant. *J. Am. Chem. Soc.* **131**, 10156-10164 (2009).

El Kasmi, A., Leopold, M.C., Galligan, R., Robertson, R.T., Saavedra, S.S., El Kacemi, K. & Bowden, E.F. Adsorptive immobilization of cytochrome *c* on indium/tin

oxide (ITO): electrochemical evidence for electron transfer-induced conformation changes. *Electrochem. Commun.* **4**, 177-181 (2002).

Evans, R.M., Parkin, A., Roessler, M.M., Murphy, B.J., Adamson, H., Lukey, M.J., Sargent, F., Volbeda, A., Fontecilla-Camps, J.C. & Armstrong, F.A. Principles of Sustained Enzymatic Hydrogen Oxidation in the Presence of Oxygen - The Crucial Influence of High Potential Fe-S Clusters in the Electron Relay of [NiFe]-Hydrogenases. *J. Am. Chem. Soc.* **135**, 2694-2707 (2013).

Fernandez, V.M., Hatchikian, E.C. & Cammack, R. Properties and reactivation of two different deactivated forms of *Desulfovibrio gigas* hydrogenase. *Biochim. Biophys. Acta* **832**, 69-79 (1985).

Fernandez, V.M., Hatchikian, E.C., Patil, D.S. & Cammack, R. ESR-detectable nickel and iron-sulphur centres in relation to the reversible activation of *Desulfovibrio gigas* hydrogenase. *Biochim. Biophys. Acta* **883**, 145-154 (1986).

Fiala, G. & Stetter, K.O. *Pyrococcus furiosus* sp. nov. represents a novel genus of marine heterotrophic archaebacteria growing optimally at 100 degrees C. *Arch. Microbiol.* **145**, 56-61 (1986).

Fontecilla-Camps, J.C., Volbeda, A., Cavazza, C. & Nicolet, Y. Structure/Function Relationships of [NiFe]- and [FeFe]-hydrogenases. *Chem. Rev.* **107**, 4273-4303 (2007).

Fourmond, V., Hoke, K.R., Heering, H.A., Baffert, C., Leroux, F., Bertrand, P. & Léger, C. SOAS: A free program to analyze electrochemical data and other one-dimensional signals. *Bioelectrochemistry* **76**, 141-147 (2009).

Fourmond, V., Infossi, P., Giudici-Orticoni, M.-T., Bertrand, P. & Léger, C. "Two-step" chronoamperometric method for studying the anaerobic inactivation of an oxygen tolerant NiFe hydrogenase. *J. Am. Chem. Soc.* **132**, 4848-4857 (2010).

Fourmond, V., Baffert, C., Sybirna, K., Lautier, T., Abou Hamdan, A., Dementin, S., Soucaille, P., Meynial-Salles, I., Bottin, H. & Léger, C. Steady-State Catalytic Wave-Shapes for 2-Electron Reversible Electrocatalysts and Enzymes. *J. Am. Chem. Soc.* **135**, 3926-3938 (2013).

Frasca, S., von Graberg, T., Feng, J.J., Thomas, A., Smarsly, B.M., Weidinger, I.M., Scheller, F.W., Hildebrandt, P. & Wollenberger, U. Mesoporous Indium Tin Oxide as a Novel Platform for Bioelectronics. *Chemcatchem* **2**, 839-845 (2010).

Frasca, S., von Graberg, T., Feng, J.-J., Thomas, A., Smarsly, B.M., Weidinger, I.M., Scheller, F.W., Hildebrandt, P. & Wollenberger, U. Mesoporous indium tin oxide as a novel platform for bioelectronics. *ChemCatChem* **2**, 839-845 (2010).

Friedrich, B., Buhrke, T., Burgdorf, T. & Lenz, O. A hydrogen-sensing multiprotein complex controls aerobic hydrogen metabolism in *Ralstonia eutropha*. *Biochem. Soc. T.* **33**, 97-101 (2005).

Friedrich, B., Fritsch, J. & Lenz, O. Oxygen-tolerant hydrogenases in hydrogen-based technologies. *Curr. Opin. Biotech.* **22**, 358-364 (2011).

Frielingsdorf, S., Fritsch, J., Schmidt, A., Hammer, M., Lowenstein, J., Siebert, E., Pelmenschikov, V., Jaenicke, T., Kalms, J., Rippers, Y., Lendzian, F., Zebger, I., Teutloff, C., Kaupp, M., Bittl, R., Hildebrandt, P., Friedrich, B., Lenz, O. & Scheerer, P. Reversible [4Fe-3S] cluster morphing in an O_2-tolerant [NiFe] hydrogenase. *Nat. Chem. Biol.* **10**, 378-387 (2014).

Fritsch, J., Scheerer, P., Frielingsdorf, S., Kroschinsky, S., Friedrich, B., Lenz, O. & Spahn, C.M. The crystal structure of an oxygen-tolerant hydrogenase uncovers a novel iron-sulphur centre. *Nature* **479**, 249-252 (2011).

Fritsch, J., Lenz, O. & Friedrich, B. Structure, function and biosynthesis of O_2-tolerant hydrogenases. *Nat. Rev. Microbiol.* **11**, 106-114 (2013).

Gallon, J.R. The Oxygen Sensitivity of Nitrogenase - A Problem for Biochemists and Microorganisms. *Trends Biochem. Sci.* **6**, 19-23 (1981).

Germer, F., Zebger, I., Saggu, M., Lendzian, F., Schulz, R. & Appel, J. Overexpression, Isolation, and Spectroscopic Characterization of the Bidirectional [NiFe] Hydrogenase from *Synechocystis* sp PCC 6803. *J. Biol. Chem.* **284**, 36462-36472 (2009).

Ghirardi, M., Posewitz, M.C., Maness, P.-C., Dubini, A., Yu, J. & Seibert, M. Hydrogenases and hydrogen photoproduction in oxygenic photosynthetic organisms. *Annu. Rev. Plant Biol.* **58**, 71-91 (2007).

Ginley, D.S. & Bright, C. Transparent conducting oxides. *MRS Bull.* **25**, 15-18 (2000).

Goldet, G., Wait, A.F., Cracknell, J.A., Vincent, K.A., Ludwig, M., Lenz, O., Friedrich, B. & Armstrong, F.A. Hydrogen production under aerobic conditions by membrane-bound hydrogenases from *Ralstonia* species. *J. Am. Chem. Soc.* **130**, 11106-11113 (2008).

Goldet, G., Brandmayr, C., Stripp, S.T., Happe, T., Cavazza, C., Fontecilla-Camps, J.C. & Armstrong, F.A. Electrochemical kinetic investigations of the reactions of [FeFe]-hydrogenase with carbon monoxide and oxygen: comparing the importance of gas tunnels and active-site electronic/redox effects. *J. Am. Chem. Soc.* **131**, 14979-14989 (2009).

Gordon, J.C. & Kubas, G.J. Perspectives on How Nature Employs the Principles of Organometallic Chemistry in Dihydrogen Activation in Hydrogenases. *Organometallics* **29**, 4682-4701 (2010).

Gordon, R.G. Criteria for choosing transparent conductors. *MRS Bull.* **25**, 52-57 (2000).

Goris, T., Wait, A.F., Saggu, M., Fritsch, J., Heidary, N., Stein, M., Zebger, I., Lendzian, F., Armstrong, F.A., Friedrich, B. & Lenz, O. A unique iron-sulfur cluster is crucial for oxygen tolerance of a [NiFe]-hydrogenase. *Nat. Chem. Biol.* **7**, 310-318 (2011).

Green, D. & Perry, R. Perry's Chemical Engineers' Handbook, Eighth Edition (McGraw-Hill Education, 2007).

Gust, D., Moore, T.A. & Moore, A.L. Solar Fuels via Artificial Photosynthesis. *Accounts Chem. Res.* **42**, 1890-1898 (2009).

Haumann, M., Porthun, A., Buhrke, T., Liebisch, P., Meyer-Klaucke, W., Friedrich, B. & Dau, H. Hydrogen-induced structural changes at the nickel site of the regulatory [NiFe] hydrogenase from *Ralstonia eutropha* detected by X-ray absorption spectroscopy. *Biochemistry* **42**, 11004-11015 (2003).

Heineman, W.R. & Kuwana, T. Spectroelectrochemical Studies of Metal Deposition and Stripping and of Specific Adsorption on Mercury-Platinum Optically Transparent Electrodes. *Anal. Chem.* **44**, 1972-1978 (1972).

Herr, N., Ratzka, J., Lauterbach, L., Lenz, O. & Ansorge-Schumacher, M.B. Stability enhancement of an O_2-tolerant NAD^+-reducing [NiFe]-hydrogenase by a combination of immobilisation and chemical modification. *J. Mol. Catal. B: Enzym.* **97**, 169-174 (2013).

Herrero, C., Quaranta, A., Leibl, W., Rutherford, A.W. & Aukauloo, A. Artificial photosynthetic systems. Using light and water to provide electrons and protons for the synthesis of a fuel. *Energ. Environ. Sci.* **4**, 2353-2365 (2011).

Hildebrandt, P. & Stockburger, M. Cytochrome *c* at charged interfaces. 1. Conformation and redox equilibria at the electrode/electrolyte interface probed by surface-enhanced resonance raman spectroscopy. *Biochemistry* **28**, 6710-6721 (1989).

Hille, R., Hall, J. & Basu, P. The Mononuclear Molybdenum Enzymes. *Chem. Rev.* **114**, 3963-4038 (2014).

Hoffmann, M.C., Muller, A., Fehringer, M., Pfander, Y., Narberhaus, F. & Masepohl, B. Coordinated Expression of *fdxD* and Molybdenum Nitrogenase Genes Promotes Nitrogen Fixation by *Rhodobacter capsulatus* in the Presence of Oxygen. *J. Bacteriol.* **196**, 633-640 (2014).

Horch, M., Lauterbach, L., Saggu, M., Hildebrandt, P., Lendzian, F., Bittl, R., Lenz, O. & Zebger, I. Probing the Active Site of an O_2-Tolerant NAD^+-Reducing [NiFe]-Hydrogenase from *Ralstonia eutropha* H16 by In Situ EPR and FTIR Spectroscopy. *Angew. Chem. Int. Edit.* **49**, 8026-8029 (2010).

Hou, K., Puzzo, D., Helander, M.G., Lo, S.S., Bonifacio, L.D., Wang, W.D., Lu, Z.H., Scholes, G.D. & Ozin, G.A. Dye-Anchored Mesoporous Antimony-Doped Tin Oxide Electrochemiluminescence Cell. *Adv. Mater.* **21**, 2492-2496 (2009).

Hou, K., Puzzo, D., Helander, M.G., Lo, S.S., Bonifacio, D., Wang, W., Lu, Z.-H., Scholes, G.D. & Ozin, G.A. Dye-anchored mesoporous antimony-doped tin oxide electrochemiluminescence cell. *Adv. Mater.* **21**, 2492-2496 (2009).

Jenney, F.E., Jr. & Adams, M.W.W. Hydrogenases of the model hyperthermophiles. *Ann. NY Acad. Sci.* **1125**, 252-266 (2008).

Jeuken, L.J.C. http://www.mnp.leeds.ac.uk/ljcjeuken/Jellyfit.htm

Jeuken, L.J.C. & Armstrong, F.A. Electrochemical origin of hysteresis in the electron-transfer reactions of adsorbed proteins: Contrasting behavior of the "blue" copper protein, azurin, adsorbed on pyrolytic graphite and modified gold electrodes. *J. Phys. Chem. B* **105**, 5271-5282 (2001).

Jo, B.H., Hwang, B.H. & Cha, H.J. Draft genome sequence of *Hydrogenovibrio marinus* MH-110, a model organism for aerobic H_2 metabolism. *J. Biotechnol.* **185**, 37-38 (2014).

Jones, A.K., Lamle, S.E., Pershad, H.R., Vincent, K.A., Albracht, S.P.J. & Armstrong, F.A. Enzyme electrokinetics: electrochemical studies of the anaerobic interconversions between active and inactive states of *Allochromatium vinosum* [NiFe]-hydrogenase. *J. Am. Chem. Soc.* **125**, 8505-8514 (2003).

Jones, A.K., Dutta, A., Kwan, P., McIntosh, C.L., Roy, S. & Yang, S. in Enzymatic Fuel Cells 80-108 (John Wiley & Sons, Inc., 2014).

Kaim, W. & Fiedler, J. Spectroelectrochemistry: the best of two worlds. *Chem. Soc. Rev.* **38**, 3373-3382 (2009).

Kleihues, L., Lenz, O., Bernhard, M., Buhrke, T. & Friedrich, B. The H_2 sensor of *Ralstonia eutropha* is a member of the subclass of regulatory [NiFe] hydrogenases. *J. Bacteriol.* **182**, 2716-2724 (2000).

Kranich, A., Ly, H.K., Hildebrandt, P. & Murgida, D.H. Direct observation of the gating step in protein electron transfer: electric-field-controlled protein dynamics. *J. Am. Chem. Soc.* **130**, 9844-9848 (2008).

Kwan, P., Schmitt, D., Volosin, A.M., McIntosh, C.L., Seo, D.K. & Jones, A.K. Spectroelectrochemistry of cytochrome *c* and azurin immobilized in nanoporous antimony-doped tin oxide. *Chem. Commun.* **47**, 12367-12369 (2011).

Lamle, S.E., Albracht, S.P.J. & Armstrong, F.A. Electrochemical potential-step investigations of the aerobic interconversions of [NiFe]-hydrogenase from *Allochromatium vinosum*: Insights into the puzzling difference between unready and ready oxidized inactive states. *J. Am. Chem. Soc.* **126**, 14899-14909 (2004).

Lauterbach, L., Liu, J.A., Horch, M., Hummel, P., Schwarze, A., Haumann, M., Vincent, K.A., Lenz, O. & Zebger, I. The Hydrogenase Subcomplex of the NAD^+-Reducing [NiFe] Hydrogenase from *Ralstonia eutropha* - Insights into Catalysis and Redox Interconversions. *Eur. J. Inorg. Chem.* **7**, 1067-1079 (2011).

Lauterbach, L., Lenz, O. & Vincent, K.A. H_2-driven cofactor regeneration with $NAD(P)^+$-reducing hydrogenases. *FEBS J.* **280**, 3058-3068 (2013).

Lauterbach, L. & Lenz, O. Catalytic Production of Hydrogen Peroxide and Water by Oxygen-Tolerant [NiFe]-Hydrogenase during H_2 Cycling in the Presence of O_2. *J. Am. Chem. Soc.* **135**, 17897-17905 (2013).

Laviron, E. Voltammetric Methods For The Study Of Adsorbed Species. *Electroanal. Chem.* **12**, 53-157 (1982).

Léger, C., Heffron, K., Pershad, H.R., Maklashina, E., Luna-Chavez, C., Cecchini, G., Ackrell, B.A.C. & Armstrong, F.A. Enzyme electrokinetics: Energetics of succinate oxidation by fumarate reductase and succinate dehydrogenase. *Biochemistry* **40**, 11234-11245 (2001).

Léger, C., Elliott, S.J., Hoke, K.R., Jeuken, L.J.C., Jones, A.K. & Armstrong, F.A. Enzyme electrokinetics: Using protein film voltammetry to investigate redox enzymes and their mechanisms. *Biochemistry* **42**, 8653-8662 (2003).

Léger, C. & Bertrand, P. Direct electrochemistry of redox enzymes as a tool for mechanistic studies. *Chem. Rev.* **108**, 2379-2438 (2008).

Lenz, O., Bernhard, M., Buhrke, T., Schwartz, E. & Friedrich, B. The hydrogen-sensing apparatus in *Ralstonia eutropha*. *J. Mol. Microb. Biotech.* **4**, 255-262 (2002).

Lenz, O., Ludwig, M., Schubert, T., Bürstel, I., Ganskow, S., Goris, T., Schwarze, A. & Friedrich, B. H_2 Conversion in the Presence of O_2 as Performed by the Membrane-Bound [NiFe]-Hydrogenase of *Ralstonia eutropha*. *ChemPhysChem* **11**, 1107-1119 (2010).

Lewis, B.G. & Paine, D.C. Applications and processing of transparent conducting oxides. *MRS Bull.* **25**, 22-27 (2000).

Liebgott, P.-P., de Lacey, A.L., Burlat, B., Cournac, L., Richaud, P., Brugna, M., Fernandez, V.M., Guigliarelli, B., Rousset, M., Léger, C. & Dementin, S. Original design of an oxygen-tolerant [NiFe] hydrogenase: Major effect of a valine-to-cysteine mutation near the active site. *J. Am. Chem. Soc.* **133**, 986-997 (2011).

Liebgott, P.P., Leroux, F., Burlat, B., Dementin, S., Baffert, C., Lautier, T., Fourmond, V., Ceccaldi, P., Cavazza, C., Meynial-Salles, I., Soucaille, P., Fontecilla-Camps, J.C., Guigliarelli, B., Bertrand, P., Rousset, M. & Léger, C. Relating diffusion along the substrate tunnel and oxygen sensitivity in hydrogenase. *Nat. Chem. Biol.* **6**, 63-70 (2010).

Liebgott, P.P., Dementin, S., Léger, C. & Rousset, M. Towards engineering O_2-tolerance in [Ni-Fe] hydrogenases. *Energ. Environ. Sci.* **4**, 33-41 (2011).

Lu, Y., Berry, S.M. & Pfister, T.D. Engineering novel metalloproteins: design of metal-binding sites into native protein scaffolds. *Chem. Rev.* **101**, 3047-3080 (2001).

Lubitz, W., Ogata, H., Rudiger, O. & Reijerse, E. Hydrogenases. *Chem. Rev.* **114**, 4081-4148 (2014).

Lubner, C.E., Applegate, A.M., Knorzer, P., Ganago, A., Bryant, D.A., Happe, T. & Golbeck, J.H. Solar hydrogen-producing bionanodevice outperforms natural photosynthesis. *Proc. Natl. Acad. Sci. U.S.A.* **108**, 20988-20991 (2011).

Lukey, M.J., Parkin, A., Roessler, M.M., Murphy, B.J., Harmer, J., Palmer, T., Sargent, F. & Armstrong, F.A. How *Escherichia coli* is equipped to oxidize hydrogen under different redox conditions. *J. Biol. Chem.* **285**, 3928-3938 (2010).

Lukey, M.J., Roessler, M.M., Parkin, A., Evans, R.M., Davies, R.A., Lenz, O., Friedrich, B., Sargent, F. & Armstrong, F.A. Oxygen-Tolerant [NiFe]-Hydrogenases: The Individual and Collective Importance of Supernumerary Cysteines at the Proximal Fe-S Cluster. *J. Am. Chem. Soc.* **133**, 16881-16892 (2011).

Ma, K., Schicho, R.N., Kelly, R.M. & Adams, M.W.W. Hydrogenase of the hyperthermophile *Pyrococcus furiosus* is an elemental sulfur reductase or sulfhydrogenase: evidence for a sulfur-reducing hydrogenase ancestor. *Proc. Natl. Acad. Sci. U.S.A.* **90**, 5341-5344 (1993).

Ma, K., Hao, Z. & Adams, M.W.W. Hydrogen production from pyruvate by enzymes purified from the hyperthermophilic archaeon, *Pyrococcus furiosus*: A key role for NADPH. *FEMS Microbiol. Lett.* **122**, 245-250 (1994).

Ma, K. & Adams, M.W. Hydrogenases I and II from *Pyrococcus furiosus*. *Methods Enzymol.* **331**, 208-216 (2001).

Ma, K., Adams, M.W.W. & Kelly, R.M. in Methods in Enzymology 208-216 (Academic Press, 2001).

MacFarlane, S.L., Day, B.A., McEleney, K., Freund, M.S. & Lewis, N.S. Designing electronic/ionic conducting membranes for artificial photosynthesis. *Energ. Environ. Sci.* **4**, 1700-1703 (2011).

Manetto, G.D., Grasso, D.M., Milardi, D., Pappalardo, M., Guzzi, R., Sportelli, L., Verbeet, M.R., Canters, G.W. & Rosa, C. The role played by the cc-helix in the unfolding pathway and stability of azurin: Switching between hierarchic and nonhierarchic folding. *Chembiochem* **8**, 1941-1949 (2007).

Marshall, N.M., Garner, D.K., Wilson, T.D., Gao, Y.G., Robinson, H., Nilges, M.H. & Lu, Y. Rationally tuning the reduction potential of a single cupredoxin beyond the natural range. *Nature* **462**, 113-116 (2009).

McIntosh, C.L., Germer, F., Schulz, R.d., Appel, J. & Jones, A.K. The [NiFe]-Hydrogenase of the Cyanobacterium *Synechocystis* sp. PCC 6803 Works Bidirectionally with a Bias to H_2 Production. *J. Am. Chem. Soc.* **133**, 11308-11319 (2011).

McTernan, P.M., Chandrayan, S.K., Wu, C.H., Vaccaro, B.J., Lancaster, W.A., Yang, Q.Y., Fu, D., Hura, G.L., Tainer, J.A. & Adams, M.W.W. Intact Functional Fourteen-subunit Respiratory Membrane-bound [NiFe]-Hydrogenase Complex of the Hyperthermophilic Archaeon *Pyrococcus furiosus*. *J. Biol. Chem.* **289**, 19364-19372 (2014).

Melis, A. & Happe, T. Hydrogen production. Green algae as a source of energy. *Plant Physiol.* **127**, 740-748 (2001).

Mouesca, J.M., Fontecilla-Camps, J.C. & Amara, P. The Structural Plasticity of the Proximal [4Fe3S] Cluster is Responsible for the O_2 Tolerance of Membrane-Bound [NiFe] Hydrogenases. *Angew. Chem. Int. Edit.* **52**, 2002-2006 (2013).

Murray, J. & King, D. Climate policy: Oil's tipping point has passed. *Nature* **481**, 433-435 (2012).

Nishiyama, K., Ishida, H. & Taniguchi, I. Aminosilane modified indium oxide electrodes for direct electron transfer of ferredoxin. *J. Electroanal. Chem.* **373**, 255-258 (1994).

Ogata, H., Kellers, P. & Lubitz, W. The crystal structure of the [NiFe] hydrogenase from the photosynthetic bacterium *Allochromatium vinosum:* Characterization of the oxidized enzyme (Ni-A state). *J. Mol. Biol.* **402**, 428-444 (2010).

Ortega-Ramos, M., Jittawuttipoka, T., Saenkham, P., Czarnecka-Kwasiborski, A., Bottin, H., Cassier-Chauvat, C. & Chauvat, F. Engineering *Synechocystis* PCC6803 for hydrogen production: influence on the tolerance to oxidative and sugar stresses. *PLOS One* **9**, e89372 (2014).

Pandelia, M.-E., Fourmond, V., Tron-Infossi, P., Lojou, E., Bertrand, P., Léger, C., Giudici-Orticoni, M. & Lubitz, W. Membrane-bound hydrogenase I from the hyperthermophilic bacterium *Aquifex aelicus*: Enzyme activation, redox intermediates and oxygen tolerance. *J. Am. Chem. Soc.* **132**, 6991-7004 (2010).

Pandelia, M.-E., Nitschke, W., Infossi, P., Giudici-Orticoni, M.T., Bill, E. & Lubitz, W. Characterization of a unique [FeS] cluster in the electron transfer chain of the oxygen tolerant [NiFe] hydrogenase from *Aquifex aeolicus*. *Proc. Nat. Acad. Sci. U.S.A.* **108**, 6097-6102 (2011).

Pandelia, M.-E., Lubitz, W. & Nitschke, W. Evolution and diversification of Group 1 [NiFe] hydrogenases. Is there a phylogenetic marker for O_2-tolerance? *Biochim. Biophys. Acta* **1817**, 1565-1575 (2012).

Pandelia, M.-E., Bykov, D., Izsak, R., Infossi, P., Giudici-Orticoni, M.T., Bill, E., Neese, F. & Lubitz, W. Electronic structure of the unique [4Fe-3S] cluster in O_2-tolerant hydrogenases characterized by Fe-57 Mossbauer and EPR spectroscopy. *Proc. Natl. Acad. Sci. U.S.A.* **110**, 483-488 (2013).

Parkin, A., Goldet, G., Cavazza, C., Fontecilla-Camps, J.C. & Armstrong, F.A. The Difference a Se Makes? Oxygen-Tolerant Hydrogen Production by the [NiFeSe]-Hydrogenase from *Desulfomicrobium baculatum*. *J. Am. Chem. Soc.* **130**, 13410-13416 (2008).

Parkin, A. & Sargent, F. The hows and whys of aerobic H_2 metabolism. *Curr. Opin. Chem. Biol.* **16**, 26-34 (2012).

Pedroni, P., Della Volpe, A., Galli, G., Mura, G.M., Pratesi, C. & Grandi, G. Characterization of the locus encoding the [Ni-Fe] sulfhydrogenase from the archaeon *Pyrococcus furiosus*: evidence for a relationship to bacterial sulfite reductases. *Microbiology* **141**, 449-458 (1995).

Pelmenschikov, V. & Kaupp, M. Redox-Dependent Structural Transformations of the [4Fe-3S] Proximal Cluster in O_2-Tolerant Membrane-Bound [NiFe]-Hydrogenase: A DFT Study. *J. Am. Chem. Soc.* **135**, 11809-11823 (2013).

Pierik, A.J., Roseboom, W., Happe, R.P., Bagley, K.A. & Albracht, S.P.J. Carbon monoxide and cyanide as intrinsic ligands to iron in the active site of [NiFe]-hydrogenases - $NiFe(CN)_2CO$, biology's way to activate H_2. *J. Biol. Chem.* **274**, 3331-3337 (1999).

Pinske, C., Jaroschinsky, M., Sargent, F. & Sawers, G. Zymographic differentiation of [NiFe]-Hydrogenases 1, 2 and 3 of *Escherichia coli* K-12. *BMC Microbiol.* **12**, 134-145 (2012).

Popescu, C.V. & Munck, E. Electronic structure of the H cluster in [Fe]-hydrogenases. *J. Am. Chem. Soc.* **121**, 7877-7884 (1999).

Porthun, A., Bernhard, M. & Friedrich, B. Expression of a functional NAD-reducing [NiFe] hydrogenase from the gram-positive *Rhodococcus opacus* in the gram-negative *Ralstonia eutropha*. *Arch. Microbiol.* **177**, 159-166 (2002).

Ratzka, J., Lauterbach, L., Lenz, O. & Ansorge-Schumacher, M.B. Stabilisation of the NAD^+-reducing soluble [NiFe]-hydrogenase from *Ralstonia eutropha* H16 through modification with methoxy-poly(ethylene) glycol. *J. Mol. Catal. B: Enzym.* **74**, 219-223 (2011).

Reda, T., Plugge, C.M., Abram, N.J. & Hirst, J. Reversible interconversion of carbon dioxide and formate by an electroactive enzyme. *Proc. Natl. Acad. Sci. U.S.A.* **105**, 10654-10658 (2008).

Roessler, M.M., Evans, R.M., Davies, R.A., Harmer, J. & Armstrong, F.A. EPR spectroscopic studies of the Fe-S clusters in the O_2-tolerant [NiFe]-hydrogenase Hyd-1 from *Escherichia coli* and characterization of the unique [4Fe-3S] cluster by HYSCORE. *J. Am. Chem. Soc.* **137**, 15581-15594 (2012).

Sapra, R., Verhagen, M.F. & Adams, M.W.W. Purification and characterization of a membrane-bound hydrogenase from the hyperthermophilic archaeon *Pyrococcus furiosus*. *J. Bacteriol.* **182**, 3423-3428 (2000).

Schneider, K. & Schlegel, H.G. Purification and Properties of Soluble Hydrogenase from *Alcaligenes eutrophus* H16. *Biochim. Biophys. Acta* **452**, 66-80 (1976).

Schut, G.J., Bridger, S.L. & Adams, M.W.W. Insights into the metabolism of elemental sulfur by the hyperthermophilic archaeon *Pyrococcus furiosus*: Characterization of a coenzyme A-dependent NAD(P)H sulfur oxidoreductase. *J. Bacteriol.* **189**, 4431-4441 (2007).

Schut, G.J., Boyd, E.S., Peters, J.W. & Adams, M.W.W. The modular respiratory complexes involved in hydrogen and sulfur metabolism by heterotrophic hyperthermophilic archaea and their evolutionary implications. *FEMS Microbiol. Rev.* **37**, (2013).

Schut, G.J., Nixon, W.J., Lipscomb, G.L., Scott, R.A. & Adams, M.W.W. Mutational analyses of the enzymes involved in the metabolism of hydrogen by the hyperthermophilic archaeon *Pyrococcus furiosus*. *Front. Microbiol.* **3**, 1-6 (2013).

Serebriakova, L.T. & Sheremet'eva, M.E. Characterization of catalytic properties of hydrogenase isolated from the unicellular cyanobacterium *Gloeocapsa alpicola* CALU 743. *Biochemistry (Mosc)* **71**, 1370-1376 (2006).

Shafaat, H.S., Rudiger, O., Ogata, H. & Lubitz, W. [NiFe] hydrogenases: A common active site for hydrogen metabolism under diverse conditions. *Biochim. Biophys. Acta* **1827**, 986-1002 (2013).

Sharma, S., Volosin, A.M., Schmitt, D. & Seo, D.-K. Preparation and electrochemical properties of nanoporous transparent antimony-doped tin oxide (ATO) coatings. *J. Mater. Chem.* **1**, 699-706 (2013).

Shima, S., Pilak, O., Vogt, S., Schick, M., Stagni, M.S., Meyer-Klaucke, W., Warkentin, E., Thauer, R.K. & Ermler, U. The crystal structure of [Fe]-hydrogenase reveals the geometry of the active site. *Science* **321**, 572-575 (2008).

Shomura, Y., Yoon, K.S., Nishihara, H. & Higuchi, Y. Structural basis for a [4Fe-3S] cluster in the oxygen-tolerant membrane-bound [NiFe]-hydrogenase. *Nature* **479**, 253-256 (2011).

Simmons, C.R., Schmitt, D., Wei, X., Han, D., Volosin, A.M., Ladd, D.M., Seo, D.-K., Liu, Y. & Yan, H. Size selective incorporation of DNA nanocages into nanoporous antimony-doped tin oxide materials. *ACS Nano* **5**, 6060-6068 (2011).

Simmons, T.R., Berggren, G., Bacchi, M., Fontecave, M. & Artero, V. Mimicking hydrogenases: From biomimetics to artificial enzymes. *Coord. Chem. Rev.* **270**, 127-150 (2014).

Sun, J.S., Hopkins, R.C., Jenney, F.E., McTernan, P.M. & Adams, M.W.W. Heterologous Expression and Maturation of an NADP-Dependent [NiFe]-Hydrogenase: A Key Enzyme in Biofuel Production. *PLOS One* **5**, e10526 (2010).

Takano, T., Kallai, O.B., Swanson, R. & Dickerson, R.E. The structure of ferrocytochrome *c* at 2.45 A resolution. *J. Biol. Chem.* **248**, 5234-5255 (1973).

Tamagnini, P., Leitao, E., Oliveira, P., Ferreira, D., Pinto, F., Harris, D.J., Heidorn, T. & Lindblad, P. Cyanobacterial hydrogenases: diversity, regulation and applications. *FEMS Microbiol. Rev.* **31**, 692-720 (2007).

Teixeira, M., Moura, I., Xavier, A.V., Moura, J.J.G., Legall, J., Dervartanian, D.V., Peck, H.D. & Huynh, B.H. Redox Intermediates of *Desulfovibrio gigas* [NiFe] Hydrogenase Generated Under Hydrogenase - Mossbauer and EPR Characterization of the Metal Centers. *J. Biol. Chem.* **264**, 16435-16450 (1989).

Thorgersen, M.P., Stirrett, K., Scott, R.A. & Adams, M.W.W. Mechanism of oxygen detoxification by the surprisingly oxygen-tolerant hyperthermophilic archaeon, *Pyrococcus furiosus*. *Proc. Natl. Acad. Sci. U.S.A.* **109**, 18547-18552 (2012).

Topoglidis, E., Cass, A.E., Gilardi, G., Sadeghi, S., Beaumont, N. & Durrant, J.R. Protein Adsorption on Nanocrystalline TiO_2 Films: An Immobilization Strategy for Bioanalytical Devices. *Anal. Chem.* **70**, 5111-5113 (1998).

Topoglidis, E., Cass, A.E.G., O'Regan, B. & Durrant, J.R. Immobilisation and bioelectrochemistry of proteins on nanoporous TiO_2 and ZnO films. *J. Electroanal. Chem.* **517**, 20-27 (2001).

Topoglidis, E., Astuti, Y., Duriaux, F., Gratzel, M. & Durrant, J.R. Direct Electrochemistry and Nitric Oxide Interaction of Heme Proteins Adsorbed on Nanocrystalline Tin Oxide Electrodes. *Langmuir* **19**, 6894-6900 (2003).

van der Linden, E., Faber, B.W., Bleijlevens, B., Burgdorf, T., Bernhard, M., Friedrich, B. & Albracht, S.P.J. Selective release and function of one of the two FMN groups in the cytoplasmic NAD^+-reducing [NiFe]-hydrogenase from *Ralstonia eutropha*. *Eur. J. Biochem.* **271**, 801-808 (2004).

van der Linden, E., Burgdorf, T., de Lacey, A.L., Buhrke, T., Scholte, M., Fernandez, V.M., Friedrich, B. & Albracht, S.P.J. An improved purification procedure for the soluble [NiFe]-hydrogenase of *Ralstonia eutropha*: new insights into its (in)stability and spectroscopic properties. *J. Biol. Inorg. Chem.* **11**, 247-260 (2006).

Vignais, P.M., Billoud, B. & Meyer, J. Classification and phylogeny of hydrogenases. *FEMS Microbiol. Rev.* **25**, 455-501 (2001).

Vignais, P.M. & Billoud, B. Occurrence, classification, and biological function of hydrogenases: An overview. *Chem. Rev.* **107**, 4206-4272 (2007).

Vincent, K.A., Parkin, A., Lenz, O., Albracht, S.P.J., Fontecilla-Camps, J.C., Cammack, R., Friedrich, B. & Armstrong, F.A. Electrochemical definitions of O_2 sensitivity and oxidative inactivation in hydrogenases. *J. Am. Chem. Soc.* **127**, 18179-18189 (2005).

Vincent, K.A., Cracknell, J.A., Lenz, O., Zebger, I., Friedrich, B. & Armstrong, F.A. Electrocatalytic hydrogen oxidation by an enzyme at high carbon monoxide or oxygen levels. *Proc. Natl. Acad. Sci. U.S.A.* **102**, 16951-16954 (2005).

Vincent, K.A., Cracknell, J.A., Clark, J.R., Ludwig, M., Lenz, O., Friedrich, B. & Armstrong, F.A. Electricity from low-level H_2 in still air - an ultimate test for an oxygen tolerant hydrogenase. *Chem. Commun.* **48**, 5033-5035 (2006).

Vincent, K.A., Parkin, A. & Armstrong, F.A. Investigating and exploiting the electrocatalytic properties of hydrogenases. *Chem. Rev.* **107**, 4366-4413 (2007).

Volbeda, A., Martin, L., Cavazza, C., Matho, M., Faber, B.W., Roseboom, W., Albracht, S.P.J., Garcin, E., Rousset, M. & Fontecilla-Camps, J.C. Structural differences between the ready and unready oxidized states of [NiFe] hydrogenases. *J. Biol. Inorg. Chem.* **10**, 239-249 (2005).

Volbeda, A., Amara, P., Darnault, C., Mouesca, J.M., Parkin, A., Roessler, M.M., Armstrong, F.A. & Fontecilla-Camps, J.C. X-ray crystallographic and computational studies of the O_2-tolerant [NiFe]-hydrogenase 1 from *Escherichia coli*. *Proc. Natl. Acad. Sci. U.S.A.* **109**, 5305-5310 (2012).

Volosin, A.M., Sharma, S., Traverse, C., Newman, N. & Seo, D.-K. One-pot synthesis of highly mesoporous antimony-doped tin oxide from interpenetrating inorganic/organic networks. *J. Mater. Chem.* **21**, 13232-13240 (2011).

Wang, S.F., Xie, F. & Liu, G.D. Direct electrochemistry and electrocatalysis of heme proteins on SWCNTs-CTAB modified electrodes. *Talanta* **77**, 1343-1350 (2009).

Willit, J.L. & Bowden, E.F. Adsorption and redox thermodynamics of strongly adsorbed cytochrome *c* on tin oxide electrodes. *J. Phys. Chem.* **94**, 8241-8246 (1990).

Woolerton, T.W., Sheard, S., Pierce, E., Ragsdale, S.W. & Armstrong, F.A. CO_2 photoreduction at enzyme-modified metal oxide nanoparticles. *Energ. Environ. Sci.* **4**, 2393-2399 (2011).

Woolerton, T.W., Sheard, S., Chaudhary, Y.S. & Armstrong, F.A. Enzymes and bio-inspired electrocatalysts in solar fuel devices. *Energ. Environ. Sci.* **5**, 7470-7490 (2012).

Wulff, P., Day, C.C., Sargent, F. & Armstrong, F.A. How oxygen reacts with oxygen-tolerant respiratory [NiFe]-hydrogenases. *Proc. Natl. Acad. Sci. U.S.A.* **111**, 6606-6611 (2014).

Yang, K.Y., Haynes, C.A., Spatzal, T., Rees, D.C. & Howard, J.B. Turnover-Dependent Inactivation of the Nitrogenase MoFe-Protein at High pH. *Biochemistry* **53**, 333-343 (2014).

Zhang, X., Sherman, D.M. & Sherman, L.A. The uptake hydrogenase in the unicellular diazotrophic cyanobacterium *Cyanothece* sp. strain PCC 7822 protects nitrogenase from oxygen toxicity. *J. Bacteriol.* **196**, 840-849 (2014).

APPENDIX

PERMISSION TO REPRODUCE MATERIAL FROM PUBLISHED JOURNALS

Figure 1-4

As per the guidelines stipulated by the Nature Publishing Group, Figure 1-4 was modified from the following reference:

Reprinted by permission from Macmillan Publishers Ltd: Nature Chemical Biology from Abou Hamdan, A. *et al.* O_2-independent formation of the inactive states of NiFe hydrogenase. *Nature Chemical Biology* **9**, 15-17 (2012), Copyright 2012.

Proof of permission is provided on the following page:

NATURE PUBLISHING GROUP LICENSE
TERMS AND CONDITIONS

Aug 25, 2014

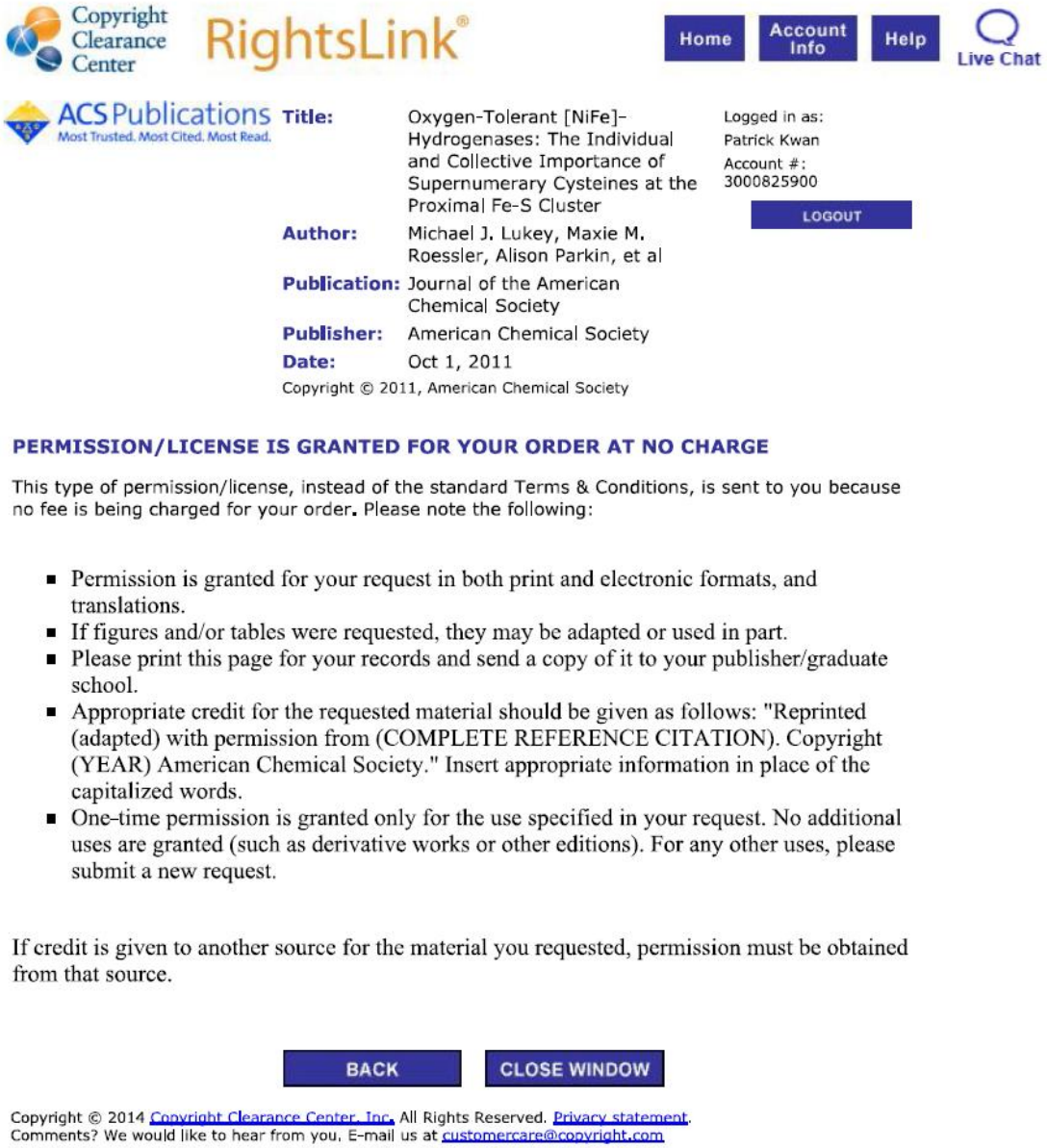
This is a License Agreement between Patrick Kwan ("You") and Nature Publishing Group ("Nature Publishing Group") provided by Copyright Clearance Center ("CCC"). The license consists of your order details, the terms and conditions provided by Nature Publishing Group, and the payment terms and conditions.

All payments must be made in full to CCC. For payment instructions, please see information listed at the bottom of this form.

License Number	3456071388856
License date	Aug 25, 2014
Licensed content publisher	Nature Publishing Group
Licensed content publication	Nature Chemical Biology
Licensed content title	O2-independent formation of the inactive states of NiFe hydrogenase
Licensed content author	Abbas Abou Hamdan, Bénédicte Burlat, Oscar Gutiérrez-Sanz, Pierre-Pol Liebgott, Carole Baffert, Antonio L De Lacey
Licensed content date	Nov 11, 2012
Volume number	9
Issue number	1
Type of Use	reuse in a dissertation / thesis
Requestor type	academic/educational
Format	print and electronic
Portion	figures/tables/illustrations
Number of figures/tables/illustrations	1
High-res required	no
Figures	Figure 1a
Author of this NPG article	no
Your reference number	None
Title of your thesis / dissertation	The Investigation and Characterization of Redox Enzymes Using Protein Film Electrochemistry
Expected completion date	Nov 2014
Estimated size (number of pages)	100
Total	0.00 USD

Figure 1-5

As per the guidelines stipulated by the American Chemical Society, Figure 1-5 was adapted with permission from Lukey, M.J. et al. Oxygen-Tolerant [NiFe]-Hydrogenases: The Individual and Collective Importance of Supernumerary Cysteines at the Proximal Fe-S Cluster. *Journal of the American Chemical Society* **133**, 16881-16892 (2011). Copyright (2011) American Chemical Society. Proof of permission is provided below:



Copyright Clearance Center RightsLink®

Home | Account Info | Help | Live Chat

ACS Publications
Most Trusted. Most Cited. Most Read.

Title: Oxygen-Tolerant [NiFe]-Hydrogenases: The Individual and Collective Importance of Supernumerary Cysteines at the Proximal Fe-S Cluster

Author: Michael J. Lukey, Maxie M. Roessler, Alison Parkin, et al

Publication: Journal of the American Chemical Society

Publisher: American Chemical Society

Date: Oct 1, 2011

Copyright © 2011, American Chemical Society

Logged in as: Patrick Kwan
Account #: 3000825900

LOGOUT

PERMISSION/LICENSE IS GRANTED FOR YOUR ORDER AT NO CHARGE

This type of permission/license, instead of the standard Terms & Conditions, is sent to you because no fee is being charged for your order. Please note the following:

- Permission is granted for your request in both print and electronic formats, and translations.
- If figures and/or tables were requested, they may be adapted or used in part.
- Please print this page for your records and send a copy of it to your publisher/graduate school.
- Appropriate credit for the requested material should be given as follows: "Reprinted (adapted) with permission from (COMPLETE REFERENCE CITATION). Copyright (YEAR) American Chemical Society." Insert appropriate information in place of the capitalized words.
- One-time permission is granted only for the use specified in your request. No additional uses are granted (such as derivative works or other editions). For any other uses, please submit a new request.

If credit is given to another source for the material you requested, permission must be obtained from that source.

BACK | CLOSE WINDOW

Copyright © 2014 Copyright Clearance Center, Inc. All Rights Reserved. Privacy statement.
Comments? We would like to hear from you. E-mail us at customercare@copyright.com

Chapter 2

As per the guidelines stipulated by the Royal Society of Chemistry, "Authors of RSC books and journal articles can reproduce material (for example a figure) from the RSC publication in a non-RSC publication, including theses, without formally requesting permission providing that the correct acknowledgement is given to the RSC publication. This permission extends to reproduction of large portions of text or the whole article or book chapter when being reproduced in a thesis." As such, Chapter 2 was reproduced in part from the following reference:

Kwan, P. et al. Spectroelectrochemistry of cytochrome c and azurin immobilized in nanoporous antimony-doped tin oxide. *Chemical Communications* **47**, 12367-12369 (2011) – Reproduced by permission of The Royal Society of Chemistry

Chapter 2-5

All authors have granted permission for use of the material in Chapters 2, 3, 4 and 5 for the purpose of this dissertation.